Metals and Ceramics Division

Heavy Vehicle Propulsion Materials Program
Quarterly Progress Report for
January through March 2001

D. R. Johnson
Technical Project Manager

Prepared for
U.S. Department of Energy
Assistant Secretary for Energy Efficiency and Renewable Energy
Office of Transportation Technologies
EE 07 01 00 0

Prepared by the
OAK RIDGE NATIONAL LABORATORY
Oak Ridge, Tennessee 37831-6066
Managed by
UT-Battelle, LLC
for the Department of Energy
Under contract DE-AC05-00OR22725

CONTENTS

Cost Effective High Performance Materials and Processing

Development of Low Cost Austenitic Stainless Diesel Engine Components with Enhanced High-Temperature Reliability (ORNL and Caterpillar, Inc.)

Cost-Effective Smart Materials for Diesel Engine Applications (ORNL)

Low-Cost Manufacturing Processes for Ceramic and Cermet Diesel Engine Components (SIU-C)

Low Cost High Toughness Ceramics (ORNL)

Advanced Manufacturing Technology

Intermetallic-Bonded Cermets (ORNL)

Low-Cost Manufacturing of Precision Diesel Engine Components (ORNL)

Cylindrical Wire Electrical Discharge Machining (EDM) and Temperature Measurement (North Carolina State University)

Testing and Characterization

NDE Technology for Heavy Duty Diesel Engines: Fuel Delivery and Insulating Materials (Argonne National Laboratory)

NDE Development for Ceramic Valves for Diesel Engines (Argonne National Laboratory)

Processing and Characterization of Structural and Functional Materials for Heavy Vehicle Applications (North Carolina A&T State University)

Life Prediction of Diesel Engine Components (ORNL)

Durability of Diesel Engine Component Materials (ORNL)

Materials and Testing Standards

Implementing Agreement for a Programme of Research and Development on Advanced Materials for Transportation Applications (ORNL)

Standards for Reliability Testing of Heavy Vehicle Propulsion Materials (NIST)

Mechanical Property Testing and Standards Development (NIST)

Development Of Low-Cost Austenitic Stainless Diesel Engine Components With Enhanced High-Temperature Reliability

P.J. Maziasz and R.W. Swindeman
Oak Ridge National Laboratory
and
M.T. Kiser, C.W. Siebenaler, and M.E. Frary
Caterpillar, Inc.

Objective/Scope

The objective of this work is to evaluate cast austenitic stainless steels as a high-performance alternative to SiMo ductile cast iron, which is currently the standard material used in most diesel engines for exhaust manifold and turbocharger housing components. The new material must be able to withstand prolonged exposure at temperatures of 750°C or above, as well to as survive the severe thermal cycling from near room temperature to such high temperatures without developing cracks. This project has tested commercially available cast alloys, as well as developed new, modified cast alloys with significantly enhanced performance. The ultimate project goal is to provide a high-performance, reliable material that is also cost-effective for such applications. This advanced diesel engine work is part of a broader CRADA (Cooperative Research and Development Agreement) project (ORNL99-0533) that began July 21,1999, and will last 2 years (ends in July 2001). The large CRADA project is blended to achieve similar objects for both advanced gas-turbine engines as well as advanced diesel engines. Any more detailed information on this project must be requested directly from Caterpillar, Inc.

Technical Highlights, 2nd Quarter, FY2001

Background

Advanced large diesel engine must have higher fuel efficiency as well as reduced exhaust emissions, with similar or greater durability and reliability. Therefore, exhaust manifold and turbocharger housing materials must withstand temperatures ranging from 70 to 750°C or higher in a normal duty cycle that includes prolonged, steady high-temperature exposure as well as more rapid and severe thermal cycling. New technology to reduce emissions like exhaust gas recirculation (EGR) will likely push temperatures in these critical components even higher. Current materials like SiMo ductile cast iron would be pushed beyond their current strength and corrosion limits, so new materials like cast austenitic stainless steels must be considered. Currently there is little industrial experience or appropriate high-temperature mechanical properties data available on cast austenitic stainless steels, like CN12, particularly for diesel engine applications. The purpose of this program is to focus on the exhaust manifold component and produce data on cast CN12, and to compare it to SiMo cast iron for such diesel component applications

Approach

Commercial cast CN12 austenitic stainless steel (Fe-25Cr-13Ni-1.8Nb, C, N, S) was chosen as the baseline alloy for evaluation relative to SiMo ductile cast iron. Materials were evaluated in the as-cast condition as well as after appropriate thermal aging at temperatures up to 850°C. Tensile and cyclic isothermal fatigue properties were evaluated selectively from room temperature up to 900°C, together with some high-temperature creep-rupture and oxidation/corrosion testing. Microstructure analysis was performed on some of the specimens to better understand mechanisms associated with the properties changes. In a parallel effort, new alloying element modifications were made to CN12 and studied to further enhance the high-temperature performance.

Technical Progress

To date, the commercial cast iron and baseline CN12 materials have been obtained, all mechanical properties specimens machined and all tensile and creep testing of unaged and aged specimens have been done. High-cycle isothermal fatigue up to 700°C has been completed, and similar fatigue testing at higher temperatures or thermal fatigue over this temperature range remain to be done. Microstructural analyses of selected specimens of as-cast or as-cast and aged materials have been completed or are in progress understand the properties behavior and to establish the effects of aging on the baseline CN12 material.

To date, eight smaller heats (15 lbs each) of modified CN12 austenitic stainless steels have been produced at ORNL and have been evaluated. Preliminary screening of as-cast or cast and aged material with tensile testing, and of as-cast material with creep-rupture testing at 850°C indicates that significant improvements have been achieved in high-temperature strength and aging resistance. The improvements of the best modified CN-12 alloys for creep-rupture testing at 850°C and 110 MPa relative to the standard commercial CN-12 alloy are shown in Figure 1. The best second-round modified CN-12 alloy is almost ten times better than the standard material.

In addition to the modified CN12 austenitic stainless steels, similar efforts were made to modify a less costly CF8C (Fe-19Cr-12Ni-Nb, C) cast austenitic stainless steel that is also considered as a candidate for diesel exhaust applications and does find use in some gas-turbine exhaust components at 650°C or below. Three smaller heats of modified CF8C were made at ORNL (one baseline unmodified alloy and two modified alloys) and screened using tensile tests and creep-rupture testing at 850°C. The dramatic improvements in creep-resistance of the modified CF8C alloys at 850°C relative to commercial material are shown in Figure 2. The two modified alloys may be several orders of magnitude better than the commercial steel, and are still in test. Comparison of the modified CF8C steels to standard, commercial CN12 steel will be done next quarter.

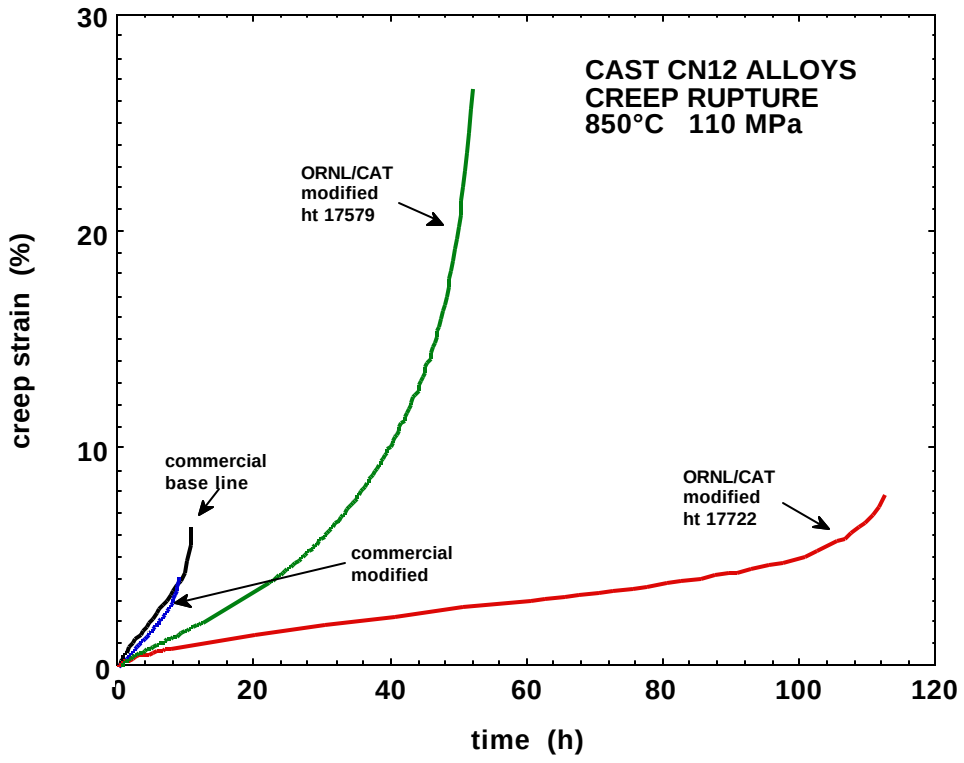

Figure 1 – Creep-rupture curves of creep-strain versus rupture time for a commercial standard (baseline) and modified heats of CN-12 cast austenitic stainless steel, and the two best laboratory heats from two rounds of alloy modifications of CN-12 steel developed by ORNL and Caterpillar.

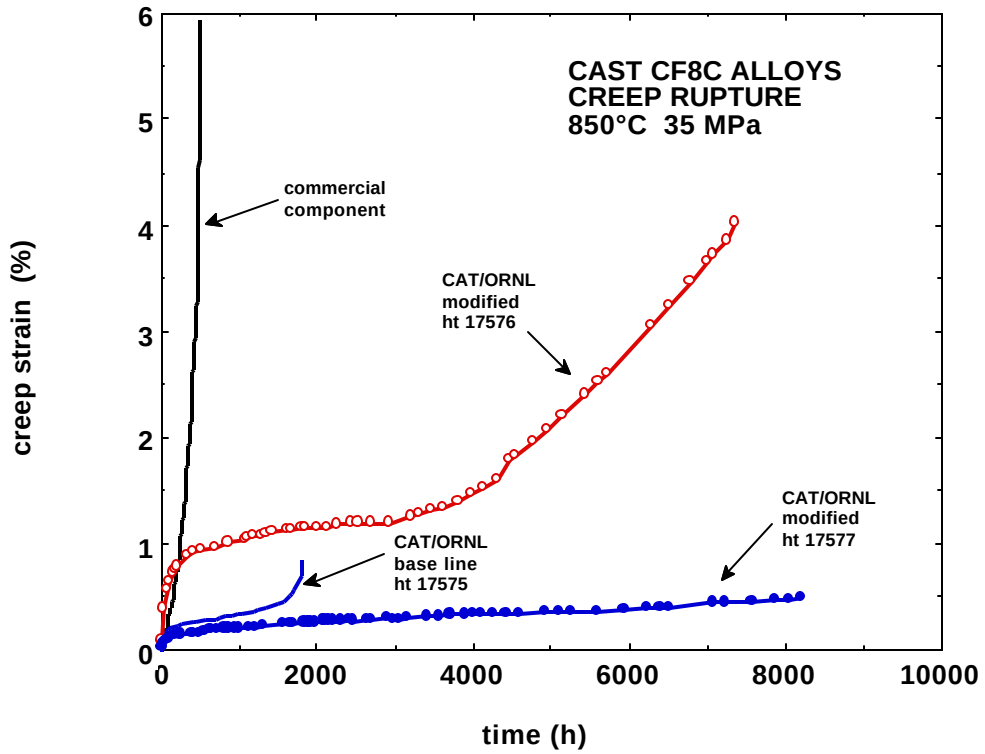

Figure 2 - Creep-rupture curves of creep-strain versus rupture time for a commercial standard CF8C cast austenitic stainless steel and several laboratory heats of baseline or modified CF8C cast austenitic stainless steel developed by ORNL and Caterpillar. Creep-rupture tests of the two best-modified CF8C steels are still on going.

Communications/Visits/Travel

Team communications between ORNL and Caterpillar occur on a regular basis. As part of the user-agreements imbedded in the CRADA, Mike Pollard of Caterpillar worked for one week at ORNL in January 2000, and Tim McGreevy (formerly at Caterpillar and now at Bradley University) worked for two weeks at ORNL in June 2000. Phil Maziasz of ORNL visited the Caterpillar Technical Center in Mossville, IL, for technical discussions and to summarize the progress of this project. Chad Siebenaler took over the project from Tim McGreevy and is summarizing the technical results of the project, but has moved to another area of the Caterpillar technical organization. Megan Frary, a new Caterpillar employee, is taking over this project.

An invention disclosure and patent application on cast austenitic stainless alloys with improved performance were completed by Caterpillar and filed with the U.S. Patent Office. It is entitled “Heat and Corrosion Resistant Cast Stainless Steels With Improved High Temperature Strength and

Ductility," by P. J. Maziasz (ORNL), T. McGreevy (U. of Bradley/CAT), M. J. Pollard (CAT), C. W. Siebenaler (CAT), and R. W. Swindeman (ORNL).

Status of Milestones

Formal milestones are imbedded in the CRADA and are not part of the HVPM Program FWP. However, all milestones have achieved on or significantly ahead of schedule.

Publications

None.

Cost-Effective Smart Materials for Diesel Engine Applications

J. O. Kiggans, Jr., T. N. Tiegs, F. C. Montgomery, and L. C. Maxey
Oak Ridge National Laboratory

Objective / Scope

There are two objectives for this project. The first is to evaluate the cost-effectiveness and maturity of various "Smart Materials Technologies," which are under consideration for diesel engine applications, such as fuel injection systems. The second is to develop "Smart Materials" to be incorporated into working actuators and sensors.

Task 1 - Multilayer Electroded Laminates
The purpose of this study is to find satisfactory methods for the preparation of PZT laminates with internal electrodes from tape cast materials. This task is in progress with no new results to share in this report.

Task 2 – Compositional Alteration of PZT-4
A second task of this project is the study of cost-effective alternative PZT compositions and processing methods, which will allow low temperature (<1125°C) sintering. Various sintering additives were selected for this study based on literature references.

Experimental Task 2 – Compositional Alteration of PZT-4

APC 840 powder (American Piezo Ceramics Inc.), also designated PZT-4, was used to make doped samples for this study. The APC 840 is a "hard" composition that we have used for several previous studies. Several compositions of APC 840 material with ceramic additives were fabricated for this study. Table 1 lists the additives that were used in this study. Table 1 also lists electrode materials used for this study. The final concentration of additives was 2 wt. % with the remainder being APC 840 powder. Figure 1 shows a schematic for sample preparation and characterization. Specific methods and techniques for sample preparation have been described in previous reports. Five-gram portions of PZT powder mixtures were pressed in a 2.85 cm steel die at 83 MPa pressure. Control samples of each sample type were heated to 700°C for 1 hour to remove binders prior to sintering. Bisque-fired densities of these samples were calculated. Control samples were sintered without electrodes, and then low-temperature Ag inks were fired on both surfaces to form electrodes. Final sintering temperatures for control samples were 825°C, 890°, 930°, or 960°C. Other samples were fabricated with alternative electrodes. Electrodes listed in Table 1, were first screen printed onto one side of the die-pressed green samples. These samples were sintered at 930°C. After sintering, the opposite non-electroded surface of the sintered samples was coated with low-temperature Ag electrode ink and reheated to 650°C for 10 min. to bake on this electrode. Weight changes during sintering were measured, and the final densities measured by the Archimedes method. The % theoretical densities were based on the reported value of 7.6 g/cm^3 for PZT-4. The samples were poled at 0.25 kV/mm, and the electromechanical properties measured. Some sample discs were cut into four pie-shaped sections using a diamond band saw. Two of the quarter parts from each sample were placed in plastic clips with the cut edges down towards the bottom of a Struers sample-mounting cup. The samples were then cast in Struers epoxy. The mounted samples were then

ground flat and polished using standard procedures. One of the cut sections (two per mount) was etched for 15 s at room temperature with a solution containing 2.3 wt. % hydrochloric acid and 0.12 wt. % hydrofluoric acid. Polished PZT samples were sputter coated with carbon prior to SEM analysis. SEM analysis was done on both the etched and non-etched sections of each sample type.

Results and Discussion

Figure 2 shows a plot of the densities for doped PZT samples bisque fired at 700°C, or sintered at 700°, 825°C, 890°, 930°, or 960°C. Note, that most doped samples reached 98 % T.D. at the 930° to 960° temperature points. Figure 3 shows that the d_{33} values for the sintered samples follow the same trend as the density plot, having increasing d_{33} values with increasing temperatures. This initial screening study indicated that the Bi_2O_3, Bi42Sr, and BiCuVOx had the highest d_{33} values following sintering. The Bi44Sr25Cu doped PZT samples densified well at both 930° and 960°C. However, these samples were difficult to pole and had low d_{33} values.

Figure 4 is a bar graph showing the d_{33} values for samples sintered at 930°C with and without the different electrodes applied onto the green samples. The purpose of this work was to determine if the electrode had an effect on the final electrical properties of the doped and sintered PZT. These results indicate that the PZT materials most immune to electrode interaction were those containing Bi_2O_3 and Bi42Sr, as indicated by the similar d_{33} values for samples sintered with or without electrodes. The BiFeVOx and BiCuVOx had the most severe interaction with the electrodes, since the d_{33} values were lower with samples sintered with all of the test electrodes. The Bi44Sr25Cu had low d_{33} values regardless of the presence or absence of electrodes, but had increased d_{33} values for all materials having co-fired electrodes. It is also possible that some differences in the d_{33} values between samples was due to poor bonding and poling capability for certain electrode–PZT combinations.

The next phase of the study involved the SEM examination of the microstructures of electroded control and doped PZT samples. Figure 5 shows the microstructure of an undoped PZT-4 disc sintered by APC Ceramics Inc. at approximately 1275°C. Note, that the grain size ranged between 2 and 5 µm in diameter. The Ag electrodes were applied and fired to the samples after sintering, and showed good bonding. However, even with this control sample, the etching step removes some material away from the Ag electrode, perhaps due to the type of flux used in the Ag electrodes. Figures 6 and 7 show SEM photos of the PZT-4 doped with Bi_2O_3, Bi42Sr, Bi44Sr25Cu, or BiCuVOx and sintered at 930° or 960°C. The grain sizes differ for each additive at both temperatures. The increase in temperature from 930° to 960°C resulted in a very large, unexpected increase in grain size for all of the compositions. The fact that the Bi44Sr25Cu materials had the smallest grain sizes for both temperatures may be due the lower Bi to PZT ratio (Table 1) of 1.94 versus values from 2.35 for BiCuVOx, to a high of 2.80 for Bi_2O_3. Figures 8 and 9 show SEM photos of the area adjacent to the electrodes and at the sample mid-point for Bi_2O_3, Bi42Sr, BiCuVOx, and BiFeVOx doped PZT-4 materials sintered at 930° for 3h with low temperature silver electrodes applied after sintering. No significant differences can be seen between the edge and the center or mid-plane area of these control samples, indicating the uniformity of the sintering. The uniform grain size between locations also shows that the post sintering application of low-fire Ag electrode material does not affect the grain growth or microstructures. Figures 10 and 11 show SEM photos of the area adjacent to the test

electrode and at the sample mid-point for Bi2O3, Bi42Sr, Bi44Sr25Cu, and BiFeVOx doped PZT-4 co-fired with "Ag/Pd with frit" electrodes at 930° for 3h. The results are similar to those for the controls indicating the "Ag/Pd with frit" electrodes do not affect the grain growth when co-fired with the PZT. Similar results to those shown in Figures 8 and 9 were observed for all of the combinations of the electrodes and samples. The depression or elevation of the d_{33} values shown in Figure 4 is also probably not due to differences in grain growth initiated by electrode interactions. Figures 12-15 show SEM photos of the cross-sections of non-etched doped PZT sections with the various electrodes types. Figure 12 shows that the "Ag/Pd no frit" and "Ag/Pd with frit" electrodes had poor bonding or thermal expansion mismatch with the Bi_2O_3 doped PZT. There was excellent bonding to the "Ag with frit" electrode material. Figure 13 shows that the Bi42Sr doped PZT did not bond well with the "Ag/Pd no frit" electrode. However, the "Ag/Pd with frit" and the "Ag with frit" electrodes showed good bonding. Figure 14 shows that the Bi44Sr25Cu did not have good bonding with the "Ag/Pd with frit" electrodes, but excellent bonding to the "Ag/Pd no frit" and the "Ag with frit" electrodes. Finally, figure 15 shows that all three electrode materials bonded to the BiFeVOx doped PZT, but there was some minor cracks in the material with the "Ag/Pd no frit" electrodes. These data indicate that the bonding and interaction of electrodes to PZTs sintered at low temperatures must be considered as critical to the success of making functional parts. The "Ag with frit" electrodes, the lowest cost electrode material, appeared to be compatible with bonding to most of the low temperature materials under consideration.

Status of Milestones

- Evaluate and characterize commercially -available PZT materials. Seek methods to improve the properties of these materials through alternative processing and forming methods. Fabricate new PZT compositions that allow sintering of the PZT materials at lower temperatures.
  Status: The evaluation of new commercial materials and low temperature PZT materials are in progress.
- Initiate studies on important variables in the fabrication of multilayer co-fired PZT stacks. Fabricate multilayer PZT stacks for testing.
  Status: Co-fire studies are presently in progress.
- Use ORNL expertise in motion amplifier devices to design and fabricate motion-amplifying fixtures for fuel injector assemblies.
  Status: An amplifier fixture has been designed at ORNL. The first amplifier has been fabricated.

Communications/Travel/Visits

None

Publications

None

Table 1. A) list of additives and B) electrode materials for for PZT-4 sintering and compatibility studies

A

Number	Sinter Aid	Amount Sinter Aid (wt %)	Bi:PZT Ratio (mole %)	Designation
1	Bi_2O_3	2.00%	2.80	Bi2O3
2	$58Bi_2O_3$-42SrO	2.01%	2.41	Bi42Sr
3	$Bi_2Fe_{0.35}V_{0.65}O_{5.15}$	2.00%	2.35	BiFeVOx
4	$Bi_2Cu_{0.1}V_{0.9}O_{5.35}$	2.00%	2.35	BiCuVOx
5	$31Bi_2O_3$-44SrO-25CuO	2.02%	1.94	Bi44Sr25Cu

B

Number	Electrode	Type	Frit	Temp °C
1	Metech* PCC11579	60 Ag / 40 Pd	No	950
2	Metech 3503	67Ag / 32 Pd	Yes	950
3	Metech 3571UF	Ag	No	925
4	Metech 3571	Ag	Yes	925
5	None			

* Metech Inc., Elverson, PA19520

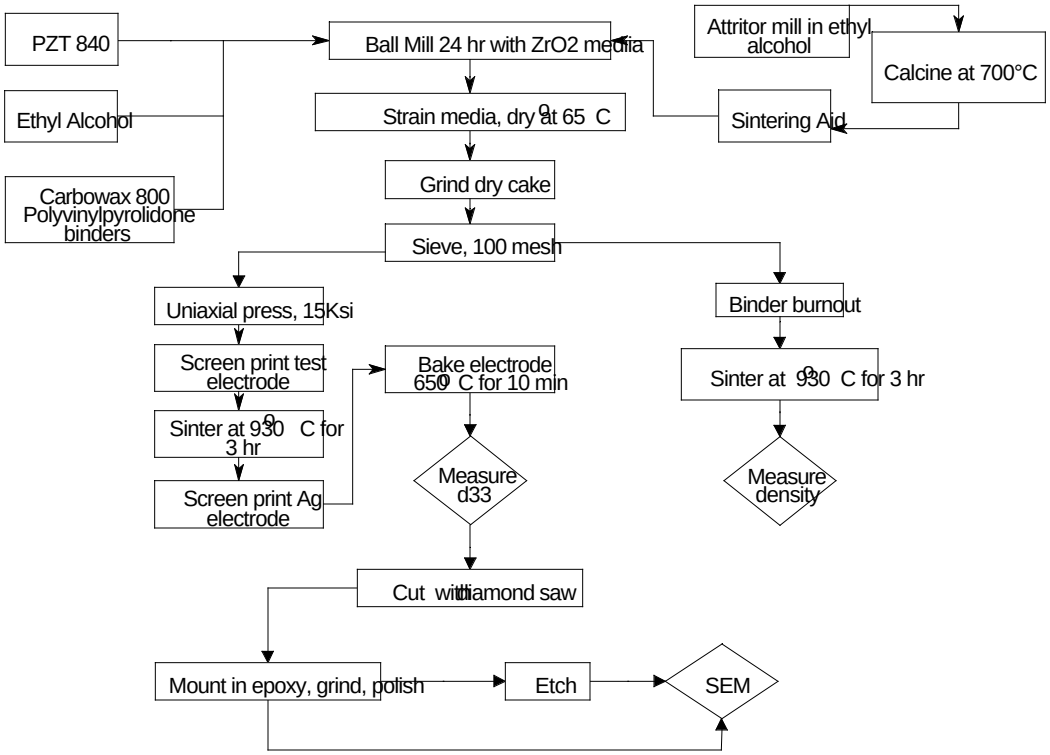

Figure 1. Schematic listing steps in PZT sample preparation and evaluation

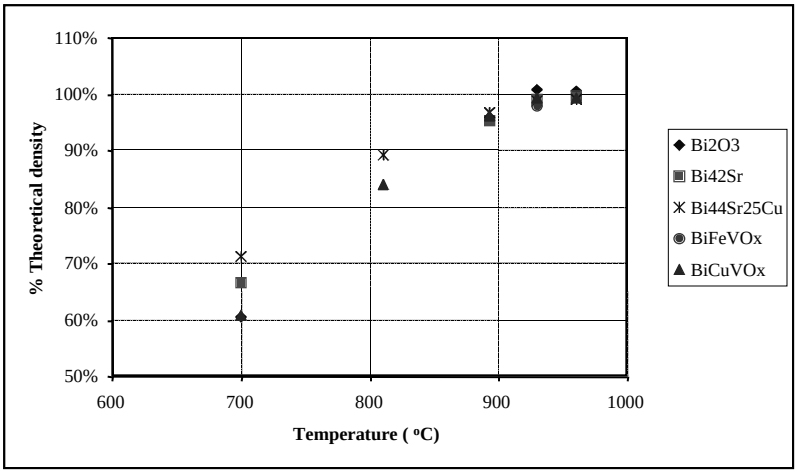

Figure 2. Plot of % theoretical density versus sintering temperature for PZT-4 with various additives

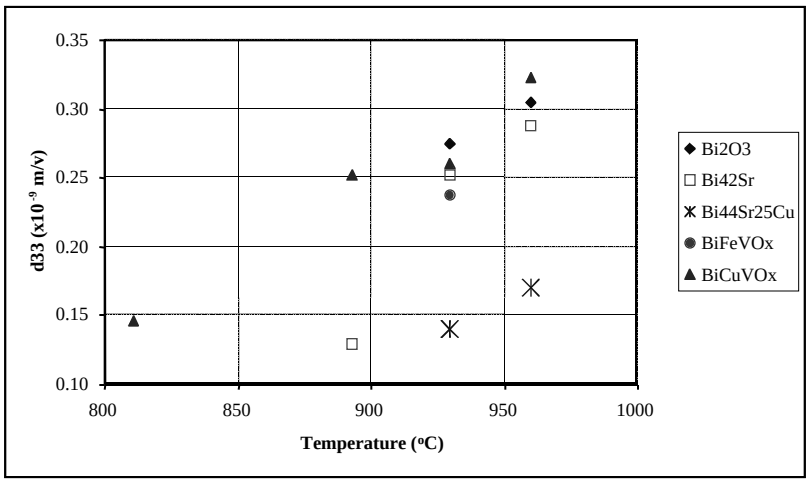

Figure 3. Plot of d_{33} values versus sintering temperature for PZT-4 with various additives

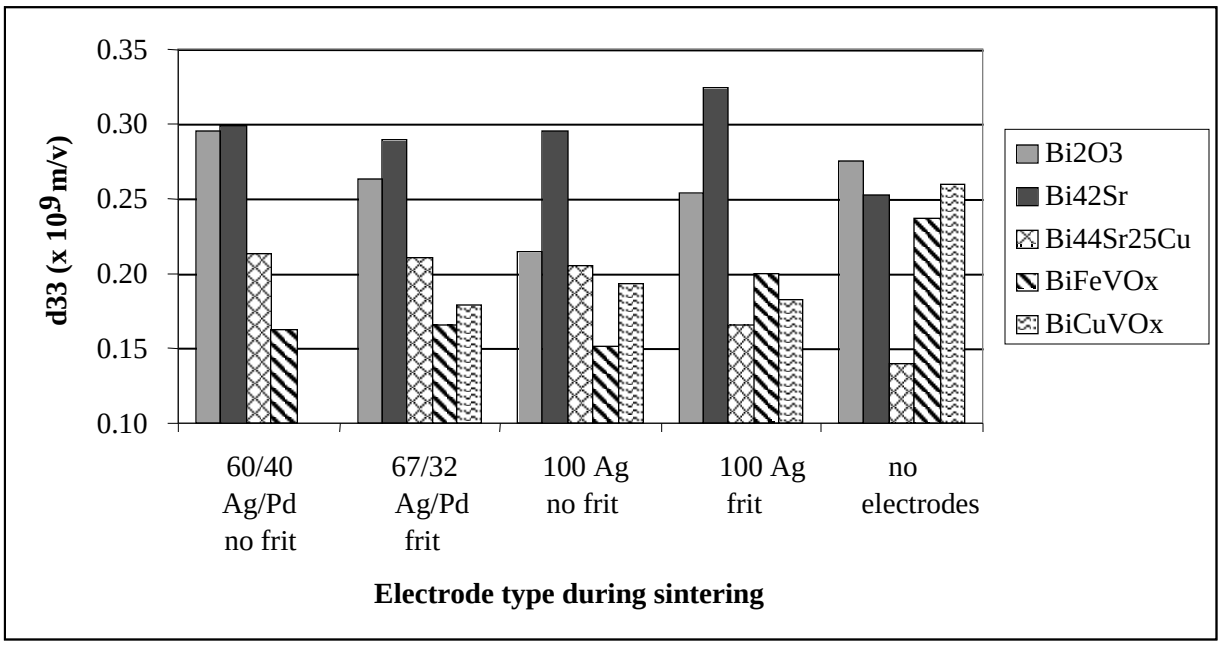

Figure 4. Plot of d_{33} values versus sintering temperature for doped PZT materials

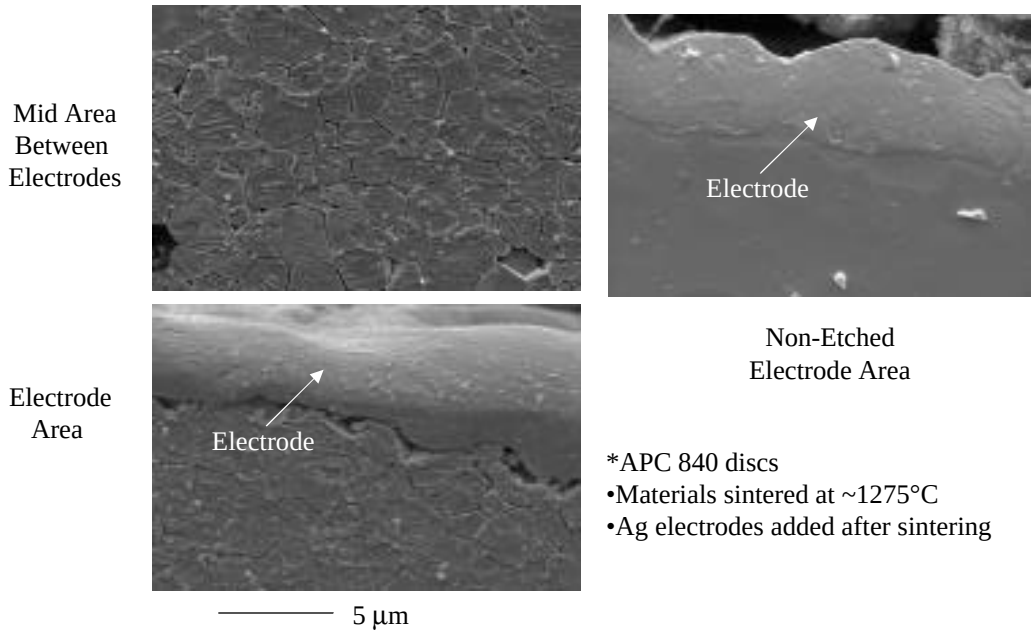

Figure 5. SEM photos of PZT-4 (APC 840) as sintered by APC Ceramics Inc.

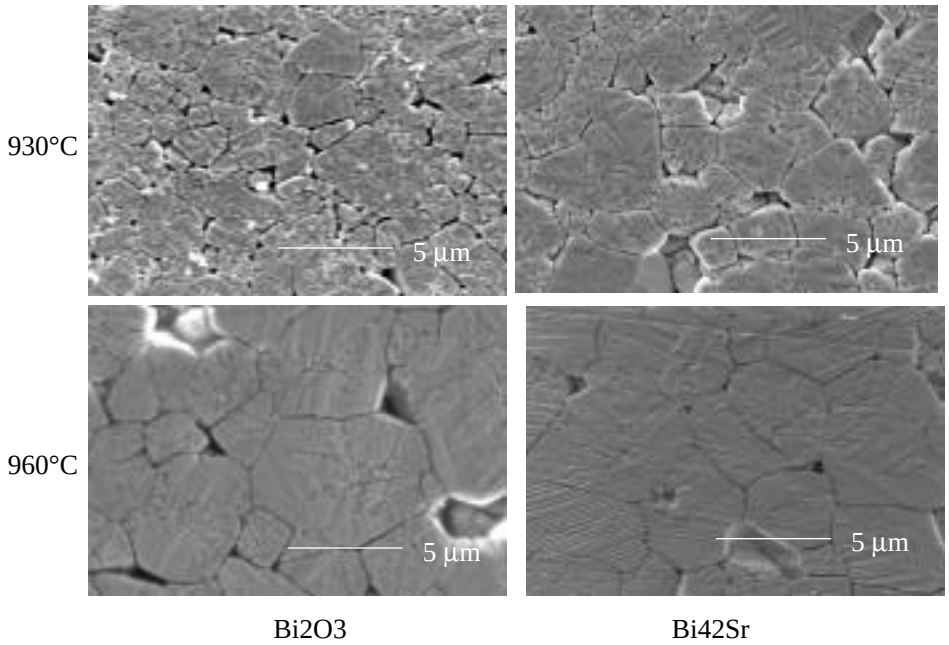

Figure 6. SEM photos of Bi_2O_3 and Bi42Sr doped PZT-4 materials sintered at 930° or 960°C for 3h in air.

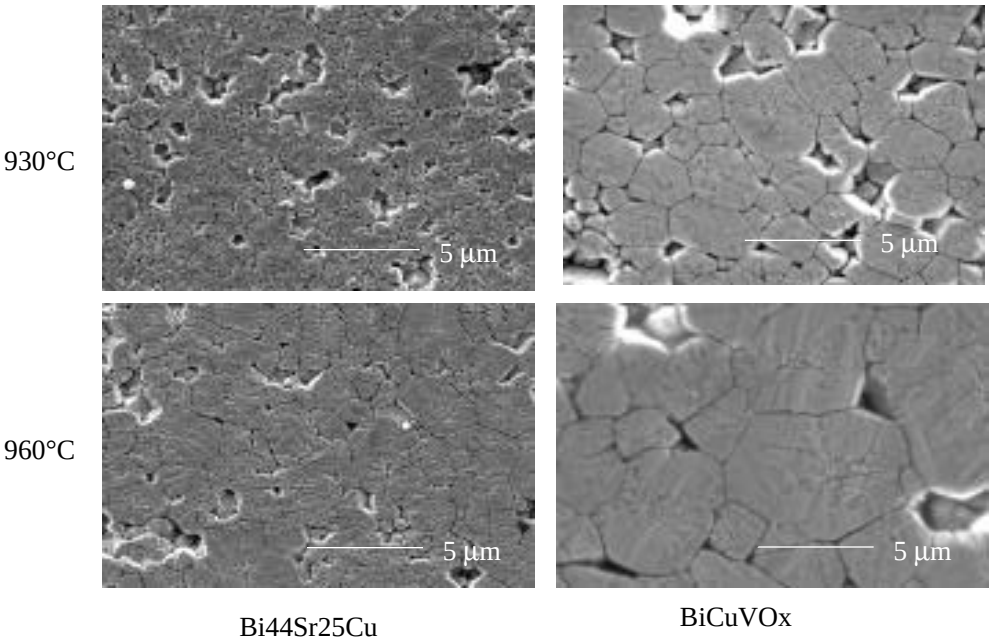

Figure 7. SEM photos of Bi44Sr25Cu and BiCuVOx doped PZT-4 materials sintered at 930° or 960°C for 3h in air.

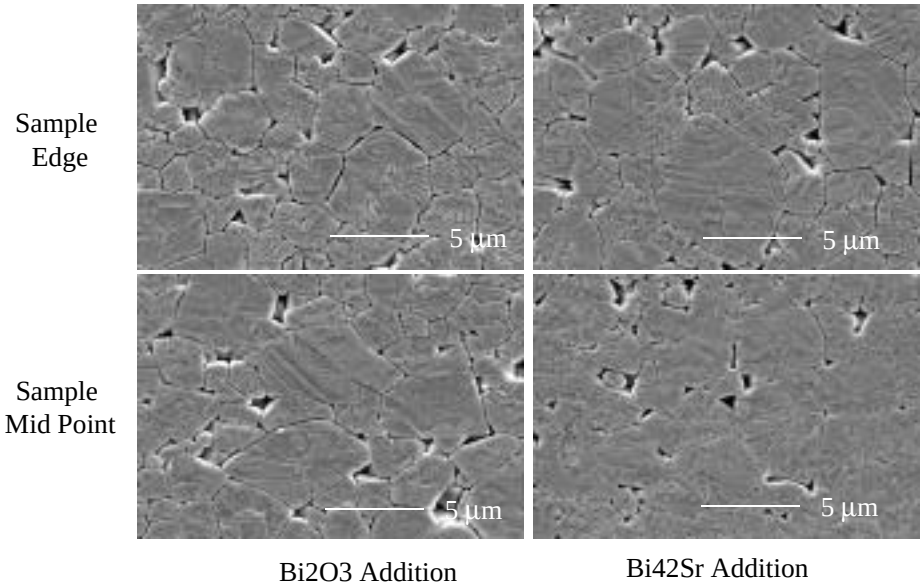

Figure 8. SEM photos of the area adjacent to the electrodes and at the sample mid-point for Bi_2O_3 and Bi42Sr doped PZT-4 materials sintered at 930° for 3h with low temperature silver electrodes applied after sintering.

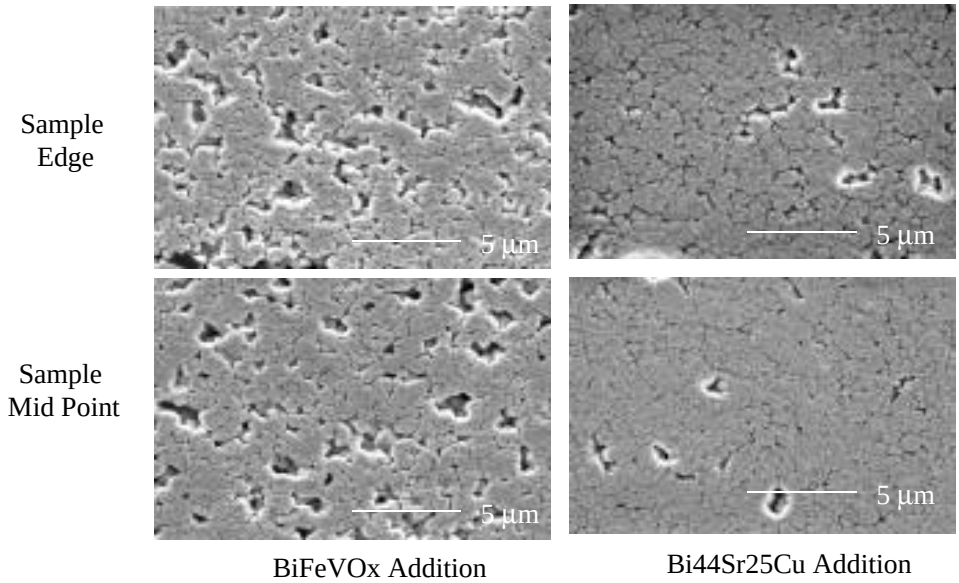

Figure 9. SEM photos of the area adjacent to the electrodes and at the sample mid point for BiFeVOx and BiFeVOx doped PZT-4 materials sintered at 930° for 3h with low temperature silver electrodes applied after sintering.

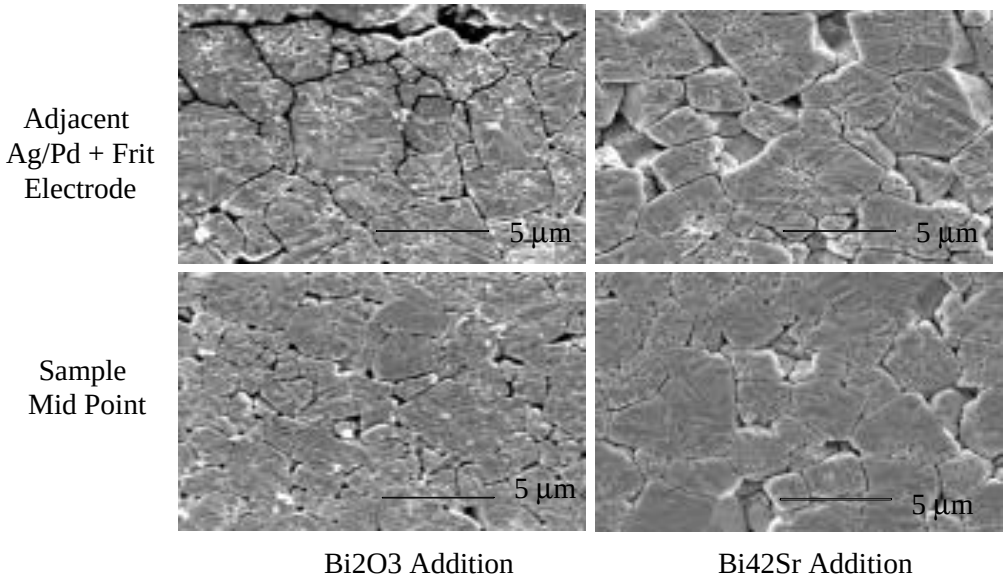

Figure 10. SEM photos of the area adjacent to the test electrode and at the sample mid-point for Bi_2O_3 and Bi42Sr doped PZT-4 materials co-fired with Ag/Pd + frit electrodes at 930° for 3h.

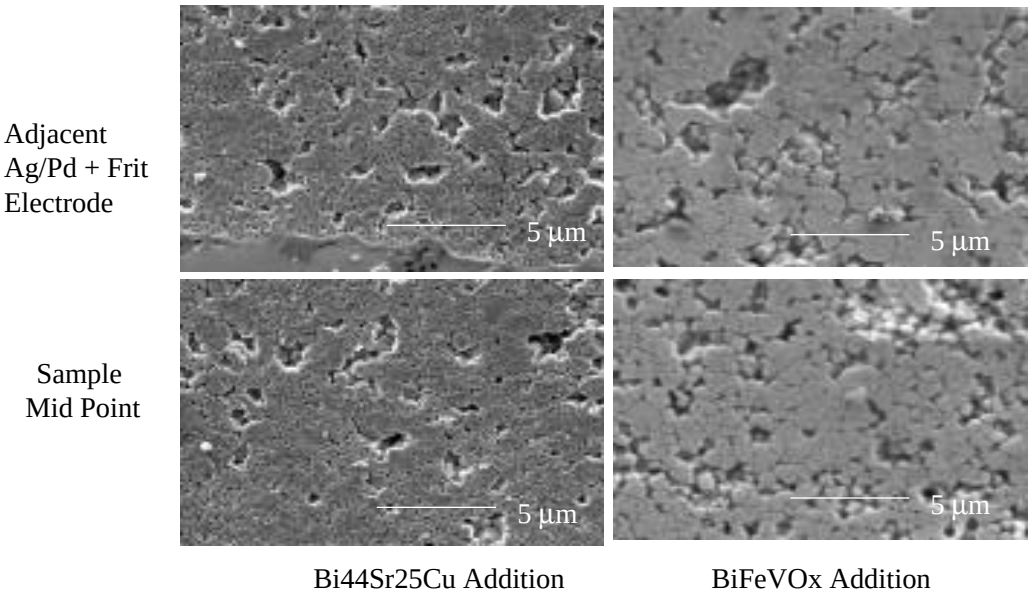

Figure 11. SEM photos of the area adjacent to the test electrode and at the sample mid-point for Bi44Sr25Cu and BiFeVOx doped PZT-4 materials co-fired with Ag/Pd + frit electrodes at 930° for 3h.

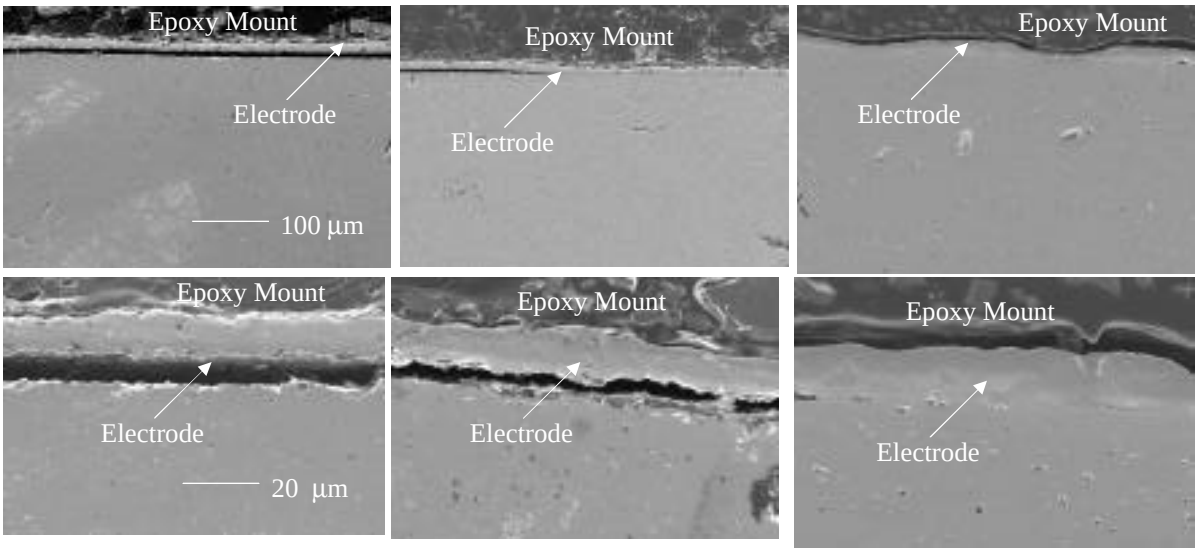

Ag/Pd No Frit Electrode Ag/Pd With Frit Electrode Ag With Frit Electrode

Figure 12. SEM photos showing the cross-section of non-etched Bi_2O_3 doped PZT-4 which was co-fired at 930° for 3h with various electrode materials

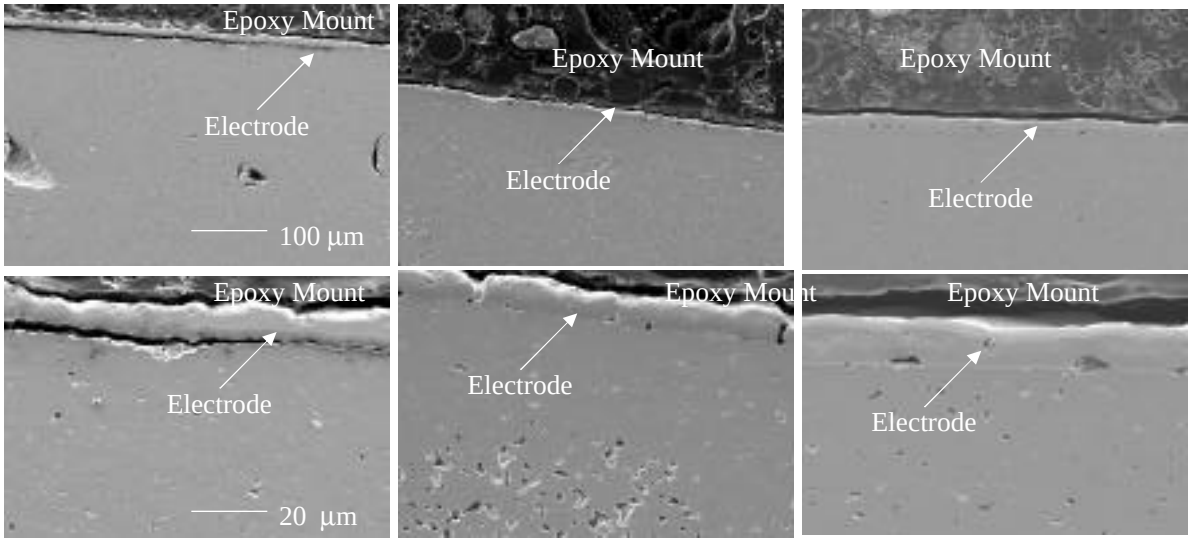

Ag/Pd No Frit Electrode Ag/Pd With Frit Electrode Ag With Frit Electrode

Figure 13. SEM photos showing the cross-section of non-etched Bi42Sr doped PZT-4 which was co-fired at 930° for 3h with various electrode materials

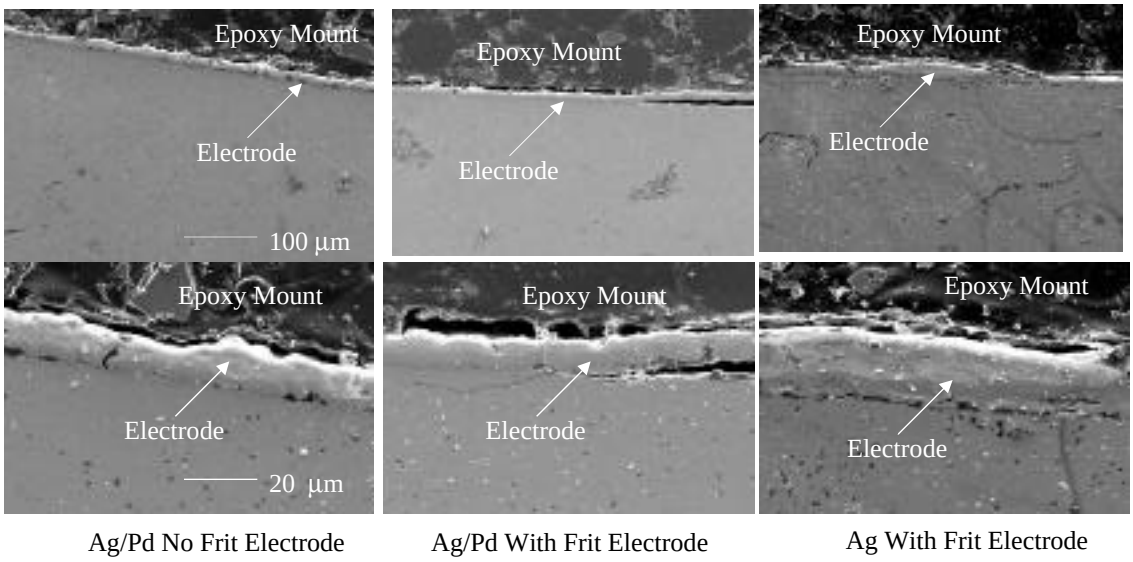

Figure 14. SEM photos showing the cross-section of non-etched Bi44Sr25Cu doped PZT-4 which was co-fired at 930° for 3h with various electrode materials

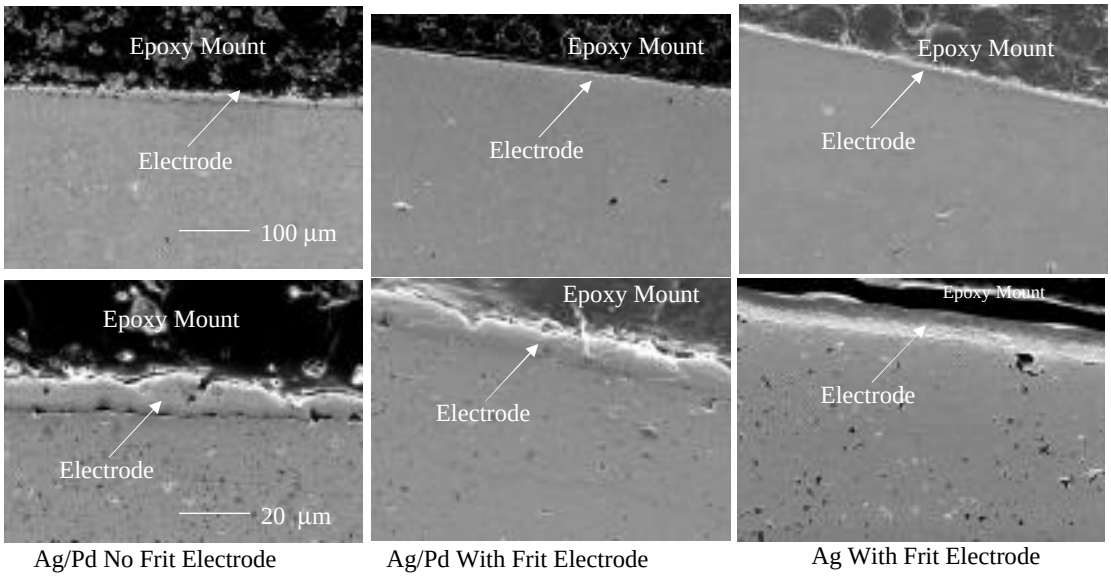

Figure 15. SEM photos showing the cross-section of non-etched BiFeVOx doped PZT-4 which was co-fired at 930° for 3h with various electrode materials

Low-Cost Manufacturing Processes for Ceramic and Cermet Diesel Engine Components

D. E. Wittmer
Department of Mechanical Engineering
and Energy Processes
Southern Illinois University
Carbondale, IL 62901

Objective/Scope

The purpose of this work is to investigate the potential of low-cost manufacturing processed for ceramic and cermet diesel engine components. The primary task is to develop cost effective processing, forming and sintering methodologies for cermet and ceramic formulations, used by industrial diesel engine manufacturers.

Technical Highlights

Task 1. Collaboration with Industrial Partner(s).

This task involves the collaboration with industrial partners to assist them in processing and sintering of their diesel engine components. Our goal is provide assistance in processing which reduces surface reactions and warpage and provide an alternative sintering process that may allow them to improve the throughput efficiency of their manufacturing processes. Due to the proprietary nature of this task, any research data generated from this task is normally controlled by the terms of each specific confidentiality agreement. The reporting of this data and any results are the responsibility of the industrial partner(s).

During this reporting period, several samples of 40 vol% NiCr, NiCrFe, and Ni3Al-20%Fe bonded TiC were processed and sent out for preliminary evaluation. All of the test materials were processed by either low-pressure injection molding/isopress/ continuous sinter or by isopress/continuous sinter. Although all of the materials delivered were >96% of theoretical density. All of the materials were returned as having large voids or other processing defects which made them unsuitable for further testing by the industrial partner. We have screen these materials and have sent several of them out for machining into test bars to try to determine the source of the defects. It is believed at the present time that the excess oxygen from the Starck TiC is the main source of the porosity observed. Addition runs are planned using the Kennametal TiC, which is known to have a lower oxygen content.

Task 2. Cost Effective Processing and Sintering

During this reporting period, concentration was primarily on the binder removal phase of our processing. It was believed that some of our distortion and low density results were created by insufficient removal of the organic binders from the low-pressure injection molded cermets. For this reason, a commercial grade of spherical zirconia (Quackenbush QBZ-95) was used for the burn-out packing material and compared with results obtained from using no packing or from using our standard silica sand packing.

The reason that the packing has been used is to keep the part geometry stable during the binder removal and during sintering. Since the packing materials chosen are stable to temperatures above the melting point of the intermetallics being investigated, these powders are being used for binder burn-out and for sintering. Several different combinations of processes are concurrently being investigated. Isopressing has been found to improve or impede densification, depending on the intermetallic system being studied. Because of this, all low-pressure injection molding trials have included both isopressed and non-isopressed billets in the process investigations.

Figure 1 shows the densification results for a 40 vol% Ni3Al-20%Fe-TiC cermet where the cylinders were not isopressed, following the binder removal stage. As seen in these results, using no setter material was nearly as effective as using the QBZ-95 setter at the lower sintering belt speed (lower heating rate and longer sintering time). The poorest results were obtained for the silica sand setter. Also, increasing the belt speed (higher heating rate and loss sintering time) produced a negative effect on density.

Figure 2 shows the densification results for the same cermet where the cylinders were isopressed to 20 Ksi, following the binder removal stage. As seen in these results, the overall density was higher when isopressing was used, except in the case where no setter was used and sintering was at the lower belt speed. Also, the use of the higher belt speed produced slightly higher densities.

These trials will be repeated during the next reporting cycle using the NiCr and NiCrFe formulations. Also, vacuum-low pressure hot isostatic pressing (V-LPHIP) will be conducted at ORNL on these same formulations.

Status of Milestones

Collaboration with Industrial Partners	On Schedule
Cost Effective Processing and Sintering	On Schedule

Communications/Visits/Travel

D. E. Wittmer to Detroit, MI to discuss possible collaboration with SiNeramics, Inc.

D. E. Wittmer discussed program objectives and new initiatives with D. Ray Johnson and Terry Tiegs.

Problems Encountered

Major isopress pump failure caused delay in isopressing studies. Unit fixed and operating.

Publications and Presentations

D. E. Wittmer, A. Woods, F. Goransson, T. Tiegs, and P. Menchhofer, "Continuous Sintering of NiCr and NiCrFe-TiC Intermetallics," Metal Powder Industries Federation, Princeton, NJ (to be published in 2001)

Aaron Woods, NiCr and NiCrFe as Alternative Binders for Intermetallic Bonded TiC,
MS Thesis, Southern Illinois University, Carbondale, IL 62901, April 2001

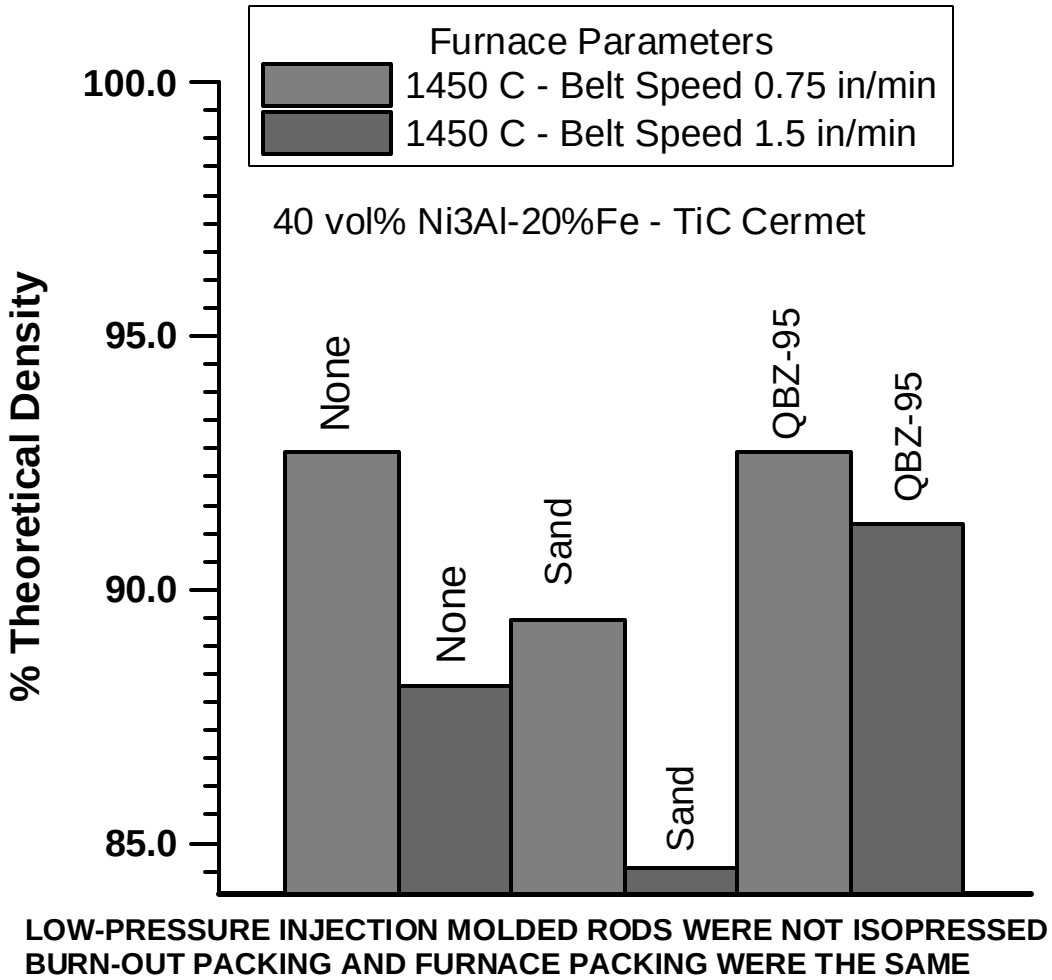

Figure 1. Comparison of density results as a function of packing material type for cermet cylinders that were not isopressed following binder burn-out.

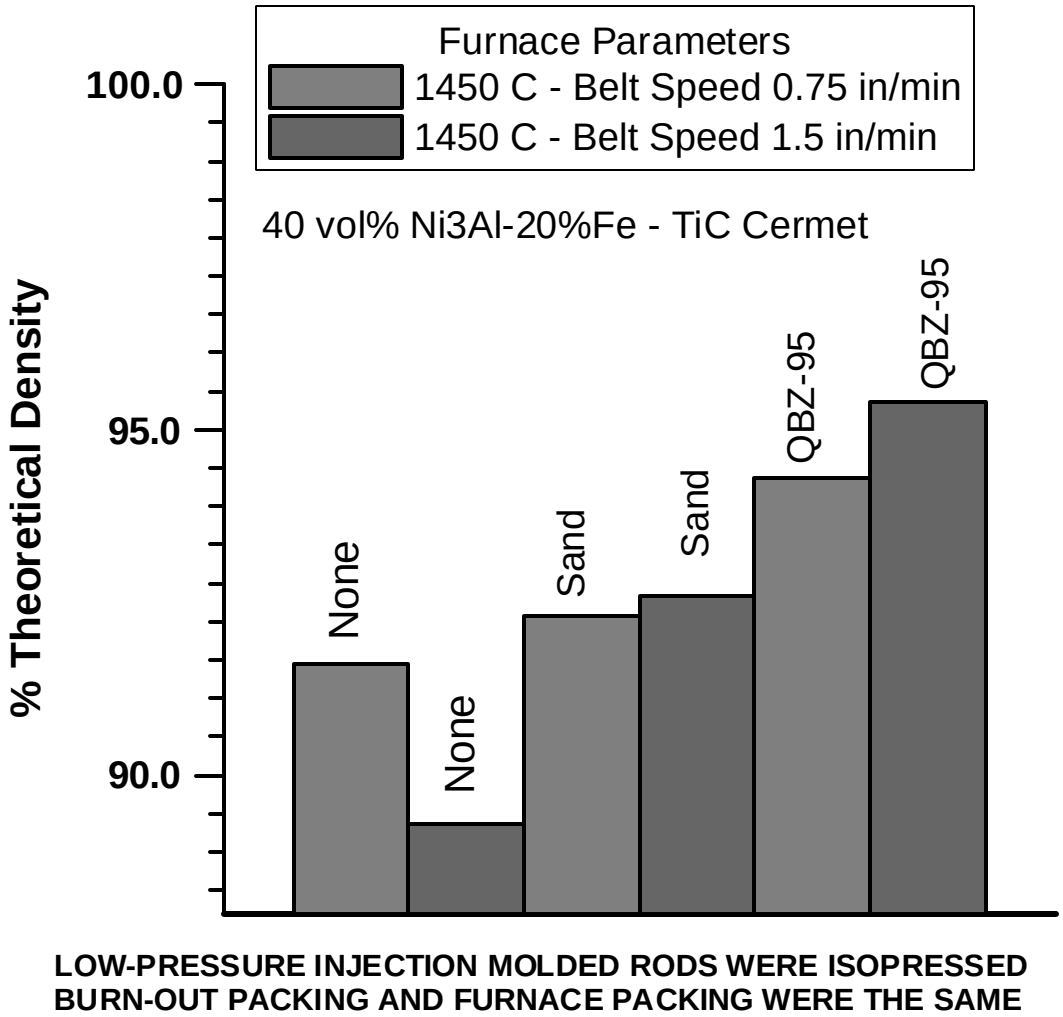

Figure 2. Comparison of density results as a function of packing material type for cermet cylinders that were isopressed following binder burn-out.

Low Cost-High Toughness Ceramics

T. N. Tiegs, F. C. Montgomery, P. A. Menchhofer, and J. O. Kiggans
Oak Ridge National Laboratory

Objective/Scope

Significant improvement in the reliability of structural ceramics for advanced diesel engine applications could be attained if the critical fracture toughness (K_{Ic}) were increased without strength degradation. Currently, the project is examining toughening of ceramics by two methods: microstructure development in oxide-based ceramics, and incorporation of ductile intermetallic phases.

Technical Highlights

Previous studies have shown that the properties of the aluminide-bonded ceramics (ABC) are attractive for diesel engine applications and consequently, development of these materials was started. At the present time, TiC-40 vol. % Ni_3Al composites are being developed because they have expansion characteristics very close to those for steel. Preliminary wear testing indicated that improved wear resistance could be achieved by decreasing the grain size of the TiC. Achieving fine grain size with the high binder contents is difficult because of the large inter-grain distances. In addition, it was thought that changing the TiC grain shape from a highly faceted one to a more rounded equiaxed grain would reduce localized stress at sharp corners. This, in turn, would improve abrasion resistance from any wear debris. Consequently, grain size refinement is presently being studied. Several approaches can be used to control the final TiC grain size. The methods studied in the present report include: (1) use of additives to change the interface behavior of the growing TiC grains, and (2) reduction of the initial TiC particle size.

Microwave Sintering of TiC-Ni_3Al Composites

Prior research has indicated that microwave sintering of powder metals and cermets offers some advantages compared to conventional heating.[1-3] Consequently, several batches of TiC-40 vol. % Ni_3Al composites were pressed into discs and heated in a 2.45 GHz microwave cavity. This is the same frequency that is used in home appliances and readily available commercially. Sintering was done by placing two samples in packaging arrangements as shown in Fig. 1. The packing is necessary as insulation to allow the samples to achieve high temperatures. The different packing arrangements and experimental conditions used for each of the various tests are given in Table 1.

Initially, heating of the samples by only using microwave energy was attempted. It is well known that dense metal parts do not absorb microwave energy, however as mentioned, previous studies have shown that discreet metal particles will heat in a microwave furnace. The insulation and BN spacer used have low dielectric losses at room temperature, so heating was principally by microwave absorption by the samples themselves. Heating proceeded adequately at low temperatures, however, at temperatures >500°C, the microwave power levels required to heat the samples at the desired rate of 5°C/min increased to =2000 watts. In the first test, a plasma was produced spontaneously in the microwave cavity because of the high electric fields and the run was aborted. In the next test, the power was intentionally limited (to prevent plasma generation) and the result was that the heating rate of 5°C/min could not be maintained and the run was terminated when the temperature deviation reached >50°C as shown in Fig. 2. It may be

possible to attain high temperatures by heating at a slower rate, but those experiments are beyond the scope of the current study.

As described, the initial attempts to sinter the composites where the microwave energy coupled directly with the parts were unsuccessful. Heating was adequate up to temperatures of 700-1000°C, however the runs were aborted after that because of poor heating even at relatively high power levels. Prior to heating, the approximate electrical resistivity of the pressed green parts was = 4 ? •cm due to limited particle-particle contact in the powder compact and the presence of some residual oxides on the surfaces of the TiC and metal particles. After heating to intermediate temperatures (~1000°C in Test MW-1-1,2), the approximate electrical resistivity of the non-densified parts was measured at 0.5 ? •cm. Sintered dense samples typically exhibited resistivities of 0.2 ? •cm. These results insinuate that the pressed green powdered compacts heat adequately up to intermediate temperatures, however, once the powdered metal part develops sufficient electrical conductivity, direct heating of the parts by microwaves is diminished or non-existent. While the prior research on the metal parts has shown the use of secondary microwave absorbing materials (often referred to as hybrid heating), there have been some recent claims that no additional microwave absorbing material is necessary. The present results do not support those observations and confirm the need for secondary heating materials.

In an attempt to achieve uniform heating to the sintering temperature, the packaging arrangement was modified by placing ZrO_2 fiber around the crucible holding the samples. It is well known that the dielectric properties of ZrO_2 change significantly at temperatures around 600-700°C and it starts to couple strongly with microwave energy.[1] It was thought that the samples would heat adequately up to temperatures of 500-700°C, and at that point, the ZrO_2 would begin to heat and allow uniform heating up to the sintering temperature. The third run (MW-2-1a,2a) showed erratic heating behavior at low temperature and two rapid temperature excursions (commonly referred to as thermal runaway) occurred at ~110 and ~130 minutes in the run (Fig. 3). High temperatures were attained and the samples achieved high densities. However, the erratic heating behavior and non-uniform heating resulted in cracking of one of the samples. Cracking is less of problem with small samples just because the size decreases the actual temperature gradients observed. This may have contributed to the cracking observed because the samples in the present study were relatively large and are about the size limit for reported powder metallurgy samples sintered by microwave heating.

To generate more uniform heating and thus stop cracking, the packaging arrangement was further modified. A second insulation barrier was added to reduce the thermal loss from the ZrO_2 fiber (which, in effect, is acting as the heating element). In addition, a BN spacer was used to act as a heat distributor (because of its high thermal conductivity) that is adjacent to the samples. Both techniques have been used previously with microwave heated silicon nitride samples to prevent macroscopic cracking. The effects these modifications have on the heating/microwave power profile are shown in Fig. 4. While the control was obviously improved compared to the previous tests, it was still inadequate to prevent sample cracking. As before, high densities were achieved for the specimens.

---

[1] As a comparison, Al_2O_3 starts to couple strongly at temperatures of 1100-1300°C [4].

From prior experience, it was believed that the cracking was predominantly caused by poor heating uniformity at low temperatures. Therefore, in place of the ZrO_2 fiber, B_4C grit was used as the microwave absorption medium because it couples well with microwave energy even at ambient temperatures. This packaging arrangement is most similar to previous microwave heating of powder metallurgy parts, which relied on either SiC or $MoSi_2$ to act as the microwave absorption medium. The effect of the B_4C grit on the heating/microwave power profile is shown in Fig. 5. As can be seen, the heating profile is extremely consistent and total power required to heat the samples up to 1400°C was moderate (= 1300 watts). Most importantly, no sample cracking was observed. Because of the clearly better heating uniformity with the B_4C grit, samples were also sintered at significantly higher heating rates (20°C/min). As shown in Fig. 6, the heating profile appeared uniform even at the higher rate and no sample cracking was evident. High densities were achieved in all cases.

Microstructural characterization showed there was very little difference between the samples sintered by microwaves and by conventional heating. Examples are shown in Figs. 7 and 8. As shown, the grain sizes and microstructural features were similar for both. Typical of these microstructures are the core-rim features that are developed during liquid phase sintering.

A comparison of the flexural strength of sintered samples from conventional sintering and the various microwave-heated samples is shown in Fig. 9. As can be seen, within the experimental standard deviation, no significant differences between the conventional and microwave-heated materials are observed.

The results of the study show that microwave heating can be used to sinter TiC-Ni_3Al cermets to high density. Initially, the TiC-Ni_3Al powder compacts can be heated directly by the microwave radiation. This is because a continuous conductive network does not exist due to the small amount of surface oxides on the TiC and metal particles. However, as the samples heat up, these surface films disappear rapidly (especially in the Ar-4% H_2 gas atmosphere) and the compacts become quite conductive. At that stage, direct heating of the TiC-Ni_3Al compacts is limited. Earlier work on microwave sintering of hardmetals, such as WC-Co, reported that they could be sintered to high density. These materials probably heat well (at least prior to liquid phase sintering) because the metal constituent is small and is commonly less than the percolation limit to form a continuous network of conductive phase. This limit is typically in the range of 20-30 vol. %. In the case of the TiC-40 vol. % Ni_3Al cermets in the present study (or powdered metal compacts, in general), the volume content of the metal phase is sufficient to form a continuous conductive network. Thus, to reach temperatures sufficient for liquid phase sintering to occur, a secondary microwave-absorbing medium is needed. In the present tests, ZrO_2 or B_4C were used; however, other materials, such as SiC or $MoSi_2$ would probably have been effective also.

Because the heating was primarily from the secondary microwave absorbing medium, the microstructures and flexural strength properties of the TiC-Ni_3Al cermets were similar to those densified by conventional heating.

Status of Milestones

On schedule.

Communications/Visits/Travel
None.

Problems Encountered
None.

Publications
None.

References
1. R. Roy, et al, "Full Sintering of Powdered Metal Bodies in a Microwave Field," Nature, Vol. 399, 668-670 (1999).

2. S. Gedevanishvili, et al, "Microwave Combustion Synthesis and Sintering of Intermetallics and Alloys," J. Mater. Sci. Lett., 18, 665-668 (1999).

3. D. Agrawal, "Metal Parts from Microwaves," Mater. World, 17 [11] 672-673 (1999).

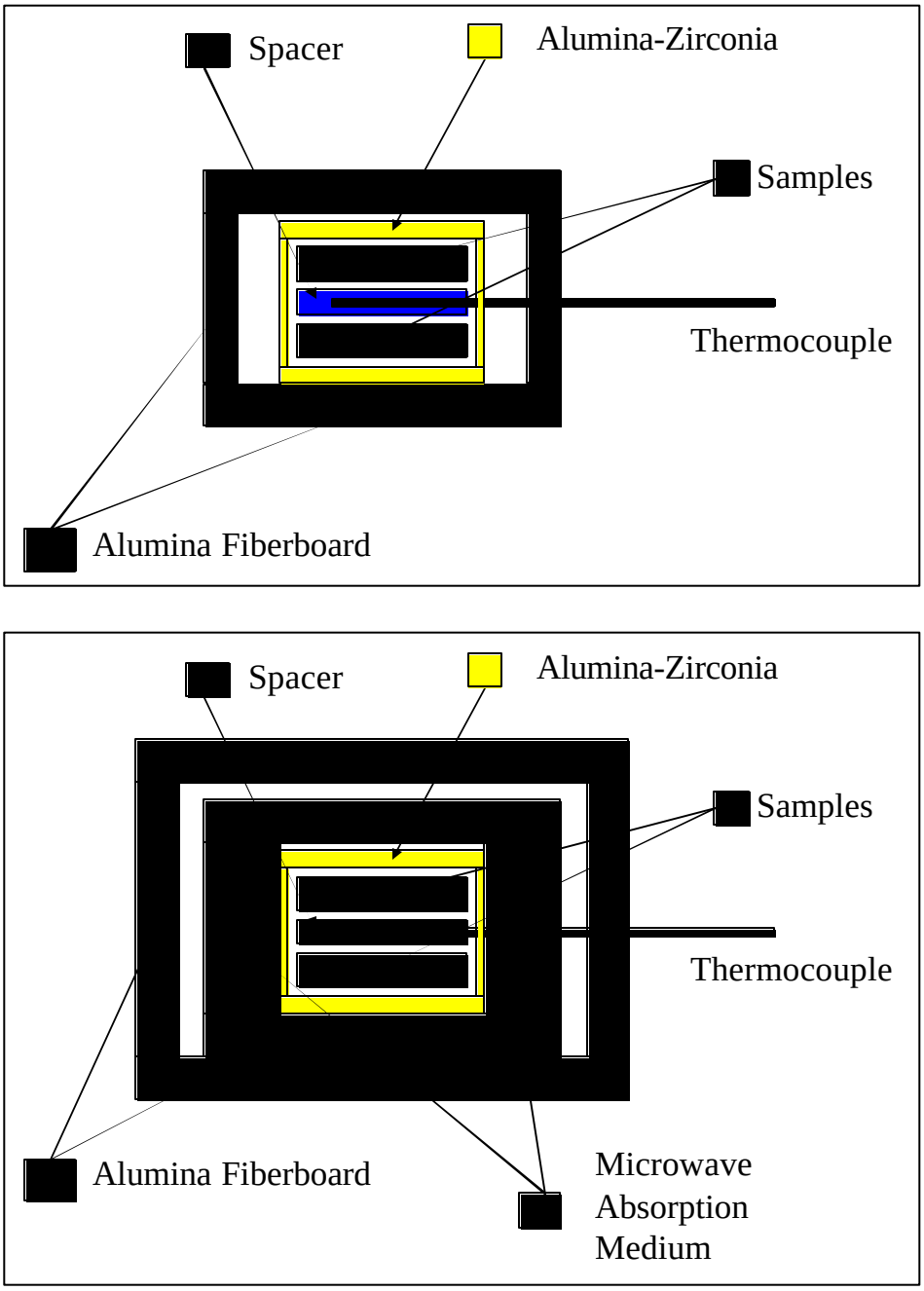

Fig. 1. Packaging arrangement for microwave sintering of TiC-Ni_3Al composites. (a) Single-wall arrangement, and (2) double-wall arrangement.

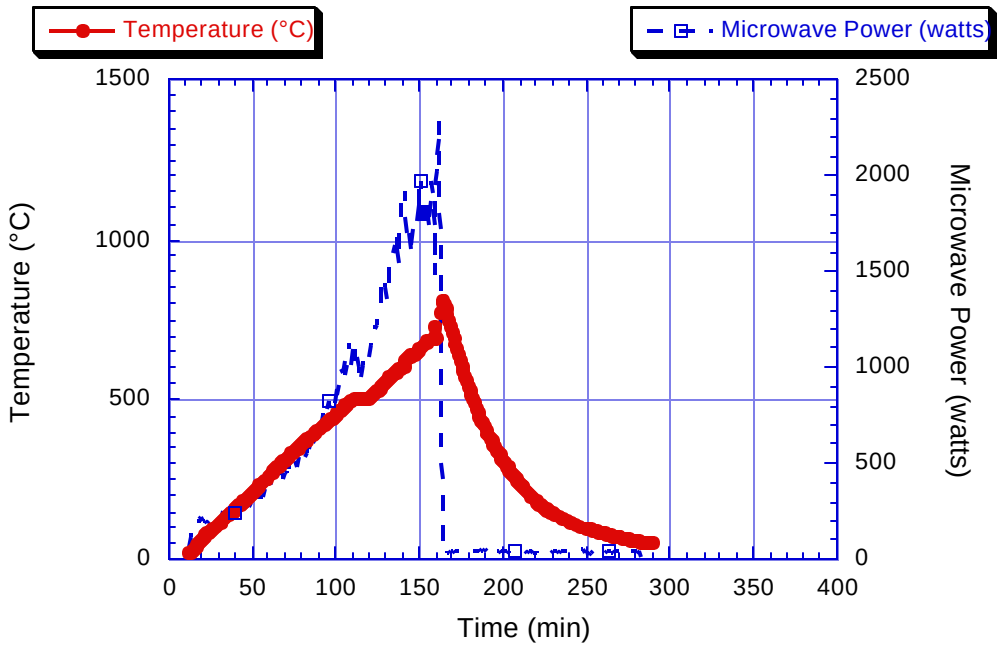

Fig. 2. Temperature and microwave power profile for MW-2-1,2.

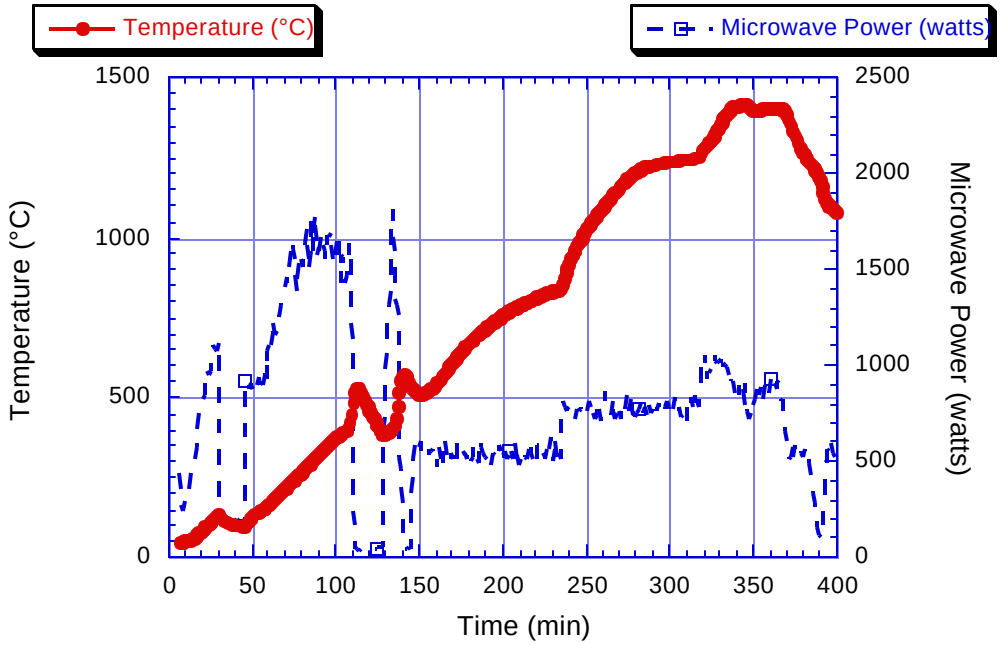

Fig. 3. Temperature and microwave power profile for MW-2-1a,2a.

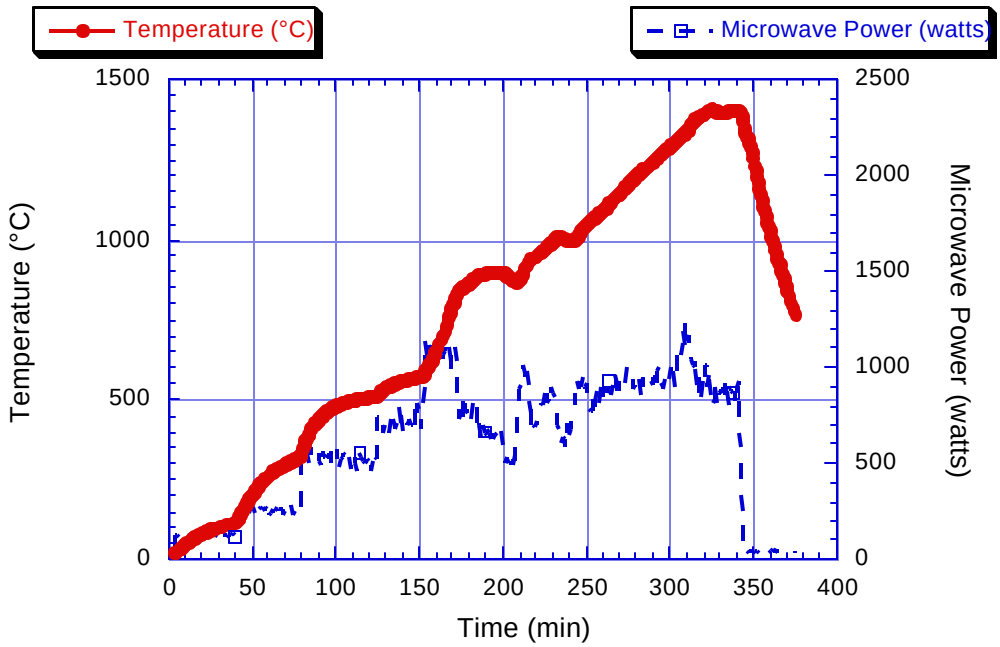

Fig. 4. Temperature and microwave power profile for MW-2A-1,2.

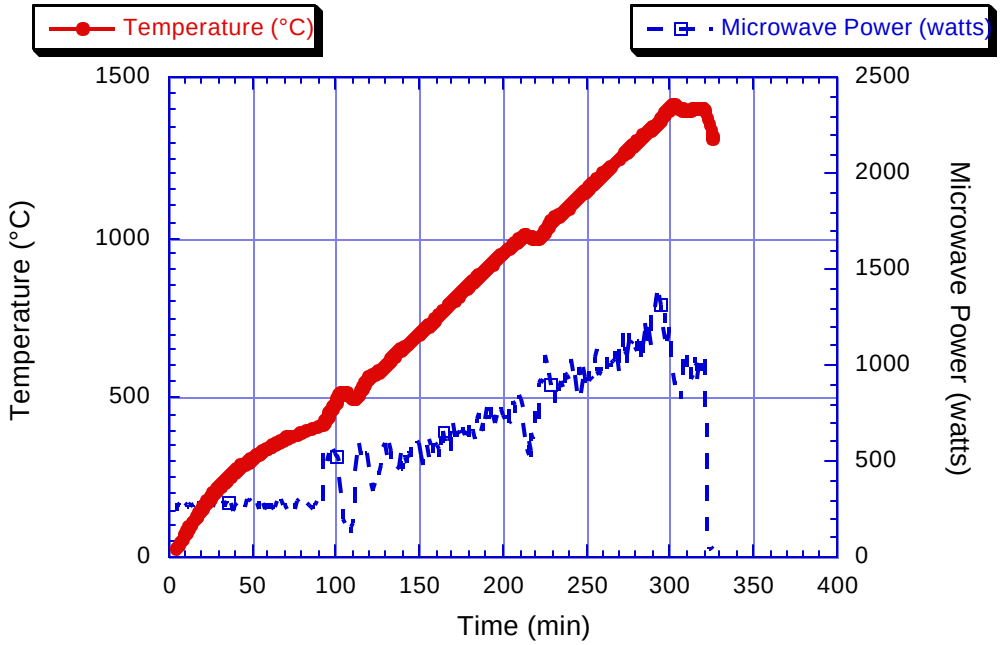

Fig. 5. Temperature and microwave power profile for MW-2A-3,4.

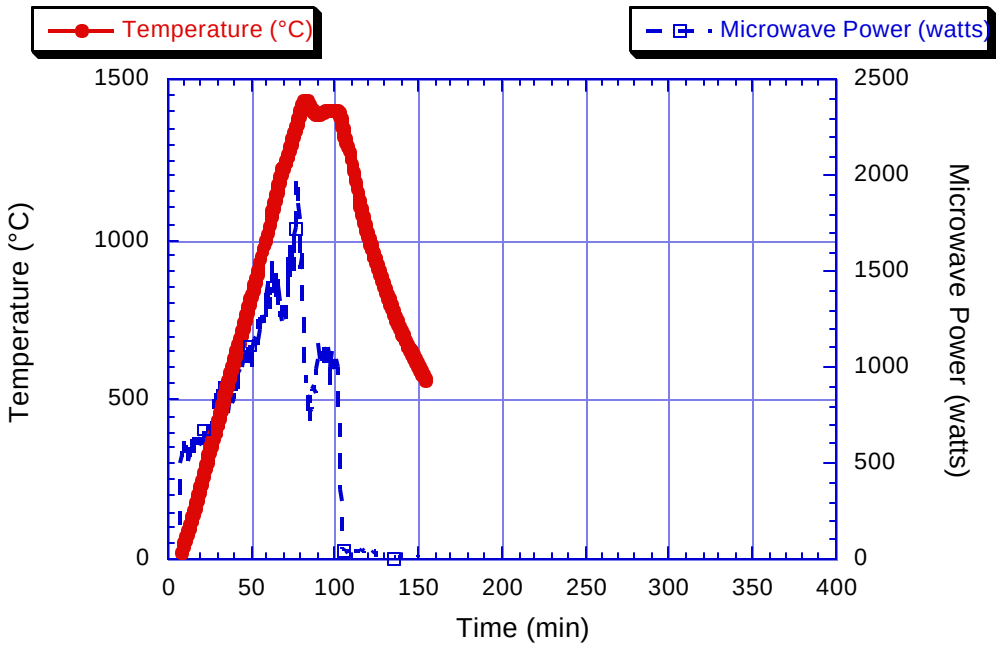

Fig. 6. Temperature and microwave power profile for MW-2A-5,6.

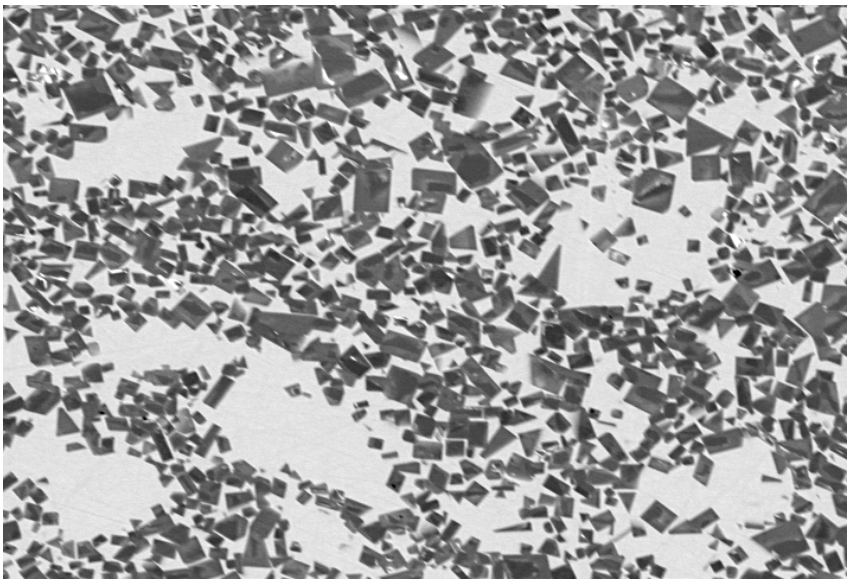

Fig. 7. Microstructure of conventionally sintered TiC-Ni_3Al cermet.

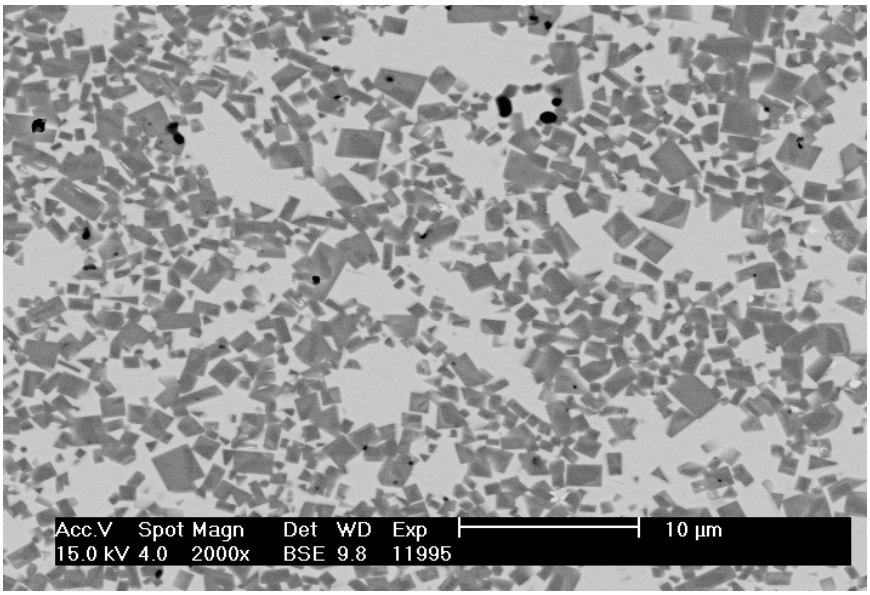

Fig. 8. Microstructure of microwave sintered TiC-Ni_3Al cermet from test MW-2-5,6.

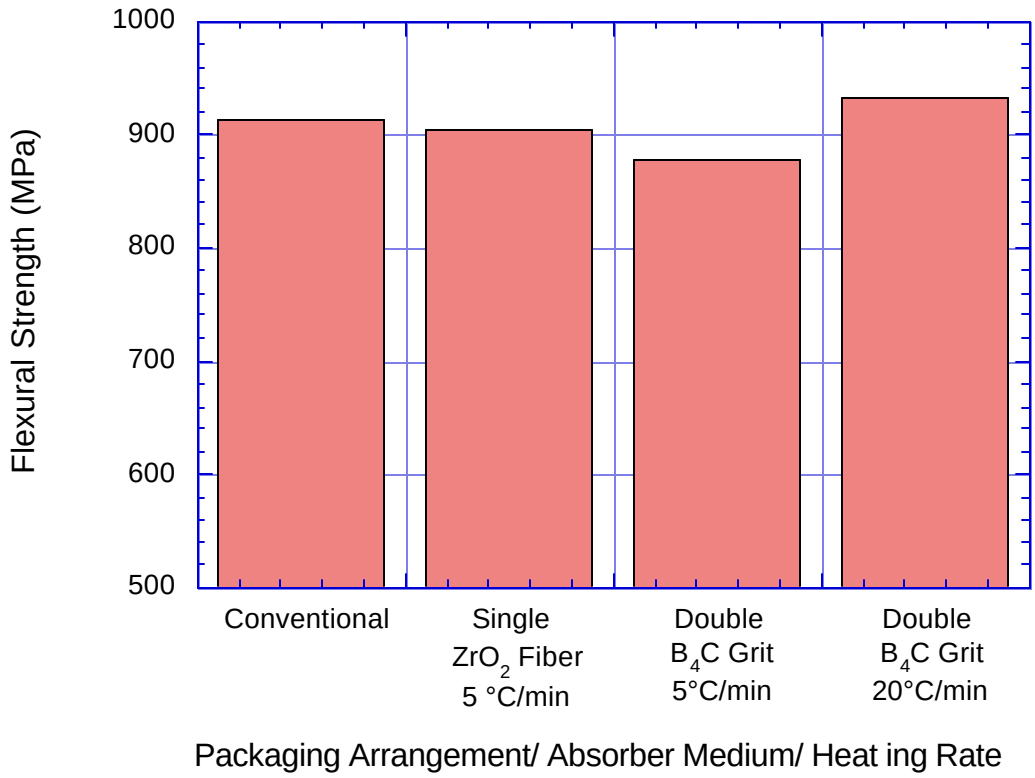

Fig. 9. Comparison of flexural strength of conventional and microwave sintered TiC-40 vol. % Ni_3Al cermets.

able 1. Summary of results on microwave sintering of TiC-Ni_3Al composites. Sintering was done under an argon-4% hydrogen atmosphere at 1400°C for 20 inutes.

ample o.*	Microwave Absorption Medium	Spacer Type**	Insulation Scheme	Heating Rate†† (°C/min)	Initial Electrical Resistivity (Ohm-cm)	Final Electrical Resistivity (Ohm-cm)	Sintered Density (% T.D.)	Comments
IW-1-2	None	BN	Single Wall	5	N. D.	0.5	N.A.	Run aborted. Plasma at ~1000°C.
IW-2-2	None	ZTA	Single Wall	5	5.3	---	N.A.	Run aborted. Temp. deviation >50°C at ~700°C.
IW-2-a,2a†	ZrO_2 fiber	ZTA	Single Wall	5	---	0.4	99.6, 99.6	Sample 2a cracked.. Erratic temperature control
IW-A-1,2	ZrO_2 fiber	BN	Double Wall	5	4.0	0.2	99.2, 99.3	Sample 1 cracked. Inadequate temperature control.
IW-2-4	B_4C grit	BN	Double Wall	5	5.4	0.2	98.7, 98.3	Samples looked good.
IW-A-3,4	B_4C grit	BN	Double Wall	5	4.2	0.2	99.4, 99.2	Samples looked good.
IW-2-6	B_4C grit	BN	Double Wall	20	6.8	0.2	98.0, 96.8	Samples looked good.
IW-A-5,6	B_4C grit	BN	Double Wall	20	4.4	0.2	99.7, 99.7	Samples looked good.
onven ional	N. A.	N. A.	N. A.	10	N. D.	N. D.	99.5	Conventional heating.

Two samples (~85 g each) were fired at the same time.
* ZTA - alumina/30 % zirconia; BN - boron nitride.
Refire of the previous samples MW-2-1 and -2.
Rate from room temperature to 1400°C. Heating schedule included 10 minute holds at 500°C and 1000°C, with the exception of runs MW-2-5,6 and MW-2A-6.

Intermetallic-Bonded Cermets

P. F. Becher and S. B. Waters
Oak Ridge National Laboratory

Objective /Scope

The goal of this task is to develop materials for diesel engine applications, specifically for fuel delivery systems and wear components (e.g., valve seats and turbocharger components). This will require materials which have a minimum hardness of 11 GPa and a thermal expansion coefficient of between 10 to 15 x 10^{-6}/°C. The material should also have excellent corrosion resistance in a diesel engine environment, flexure strength in excess of 700 MPa, and fracture toughness greater than 10 MPavm to ensure long-term reliability. The material should also be compatible with steels and not cause excessive wear of the steel counter face. The upper temperature limit for fuel delivery systems applications is 540° C, and for the other wear applications, the limit is 815° C. Finally, the total material processing costs for these advanced materials should be competitive with competing technologies such as TiN or other ceramic coatings on high-speed tool steels.

Technical Highlights

The ability to tailor the physical properties of cermets such as the TiC-Ni_3Al system can be a very important added benefit, over and above the capacity to develop high fracture strength and toughness. For example, increasing the Ni_3Al content leads to an increase in the linear thermal expansion coefficient (Figure 1), which allows one to match those of metallic alloys. Note that fracture toughness of the cermets also increases as the Ni_3Al content is raised so that one can obtain a toughened cermet whose thermal expansion matches that of adjacent metallic components. At the same time, the addition of the Ni_3Al binder phase results in a decrease in the Young's modulus of the cermet, as seen in Figure 1. The observed Young's modulus-Ni_3Al content trend is similar to that predicted by a simple rule-of-mixtures.

Status of Milestones

On schedule

Communication/Visits/Travel

Discussions held with Jim Stephan of AMT/CoorsTek on our thermal expansion measurements of cermets prepared in collaboration with T. N. Tiegs of ORNL.

Publications

K.P. Plucknett and P.F. Becher, "TiC/Ni_3Al Composites Prepared by Melt-infiltration Sintering: Processing and Microstructure Development," *J. Am. Ceram. Soc.*, 84(1) 55-61 (2001).

References

None

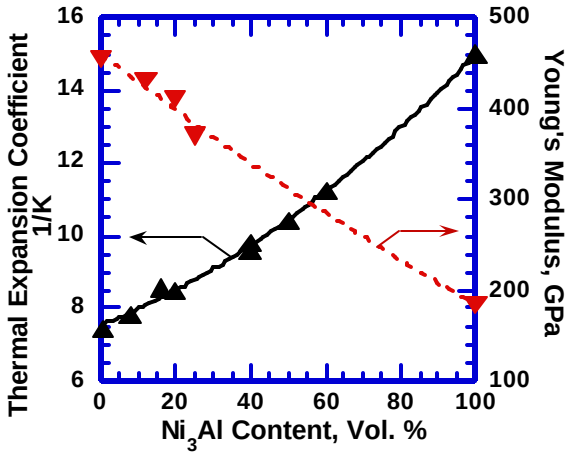

Figure 1. An increase in the Ni_3Al content of the TiC-based cermets results in an increase in the linear thermal expansion coefficient, which are shown here for the temperature range of 22° to 622°C. At the same time, the room temperature Young's modulus of the cermets will decrease with the addition of Ni_3Al .

Low-Cost Manufacturing of Precision Diesel Engine Components

S.B. McSpadden, Jr.
Oak Ridge National Laboratory

Objective/Scope

To develop and demonstrate optimized, cost-effective fabrication processes for the production of precision components for use in diesel engines. To develop and demonstrate optimized, cost-effective, non-destructive testing methods for the detection and prevention of machining-induced damage in engine components.

Technical Highlights

Caterpillar CRADA – A draft CRADA report has been prepared and transmitted to Mr. Jeff Thiele at Caterpillar for review and identification of any CRADA-protected information. The report will be issued in its final version as soon as the review is complete. This will bring to a close a multi-year, multi-task effort to address the manufacturing issues associated with the use of ceramic materials for diesel engine components. Discussions were held at Caterpillar to discuss lessons learned from the recent CRADA and to determine future areas of collaboration. Although the CRADA was generally successful, it was hampered by unforeseen personnel changes in both organizations, which had a negative effect on project continuity. The following consensus was reached regarding future CRADAs:

- The duration should be no more than 12 to 18 months.
- The work should be broken down into short-term tasks with well-defined goals, specific completion dates and easily measured milestones.
- Principal investigators at both organizations should be actively involved in the day-to-day research and should communicate on a frequent basis.

State Partnership Program Proposal for the Investigation of Non-Destructive Detection of Flaws in Ceramic Diesel Engine Fuel System Components Receives Funding – The subject proposal, which was prepared jointly by ORNL, Cummins Engine, CoorsTek, and the Indiana and Colorado state energy offices, has received $50K of ORNL (DOE) funding with in-kind contributions from the other participants. The objective of the project is to investigate non-destructive measurement techniques that are capable of detecting sub-surface machining damage in ceramic components. This is an area of great interest to Cummins. Although some laboratory techniques show promising results, the challenge is to find a relatively inexpensive, robust method that can be used in a production environment. Scanning acoustic microscopy, resonant ultrasound, x-ray and laser-based techniques are among those being considered. Since this work is well within the stated objective/scope of the *Low-Cost Manufacturing of Precision Diesel Engine Components* task, the work will be augmented with available funds from OHVT should initial technical efforts prove successful.

A review of existing literature on damage detection using scanning acoustic microscopy is in progress. Groups of zirconia test parts containing machining-induced subsurface damage will be prepared and evaluated using an existing high-frequency scanning acoustic microscope at ORNL. Although the microscope is currently not operational, complete service manuals have

been obtained and the repair should be straightforward. Other non-destructive inspection techniques will also be evaluated.

Collaborations with North Carolina State University Continuing – Dr. Albert Shih, Associate Professor of the N.C. State University Materials Science and Engineering Department, is currently involved with numerous collaborative efforts with the HTML Machining and Inspection Research Group, most of which involve the cost-effective machining of ceramic engine components. Messrs. Curry and Rhoney, two of Dr. Shih's graduate students, recently completed their thesis work and have been awarded Masters of Science degrees. Both the abstracts and full thesis text are available online at the N.C. State web site at the following locations:
http://www.lib.ncsu.edu/etd/public/etd-495511531014941/etd-title.html, "Methods of Measuring Flash Temperatures in the Grinding of MgO-Doped PSZ," Curry, Adam Craig.

http://www.lib.ncsu.edu/etd/public/etd-543213431013931/etd-title.html, "Cylindrical Wire Electrical Discharge Truing of Metal Bond Diamond Grinding Wheels," Rhoney, Brian Keith.

Mr. Curry's work on the measurement of temperature at the grinding wheel/workpiece interface is important enough that it is being continued by another student who will work at the HTML this summer.

Communications/Visits/Travel

Sam McSpadden visited Caterpillar's Peoria facility to discuss short-term and strategic areas of mutual interest that should be supported by the HTML Machining and Inspection Research Group. This information will be used to better focus the group's ceramic machining/inspection/tribology activities.

Cylindrical Wire Electrical Discharge Machining (EDM) and Temperature Measurement

Albert Shih
North Carolina State University

Objective/Scope

To develop precise, efficient, and cost-effective cylindrical Wire Electrical Discharge Machining (WEDM) process for cermet and other electrically conductive advanced engineering materials, and temperature measurement methods for grinding and diesel exhaust aftertreatment devices.

Technical Highlights

Two highlights in this quarter are the roundness improvement of cylindrical wire EDM parts and analyzing the runout of underwater spindle. The roundness, as low as 1.7 μm, for carbide was achieved.

1. Roundness

For the cylindrical wire EDM process, most of the potential applications, such as diesel engine injector plunger or micro-shaft, require tight roundness tolerance. In this study, effects of different process parameters on roundness were investigated.

Two types of materials, brass and carbide, were used. The carbide material is tungsten carbide with 10% cobalt bond. This material has hardness of 92 Rc, transverse rupture stress of 3.4 MPa, and specific density of 14.5. Two sets of experiments were conducted. In experiment I, the goal was to achieve high Material Removal Rate (MRR) and long electrical spark on-time was applied. In experiment II, the goal was to achieve good roundness and surface finish and short electrical spark on-time was applied. The machine setup and process parameters for the cylindrical wire EDM experiment are listed in Table 1.

Table 1. Machine setup for the cylindrical wire EDM experiments.

Wire EDM machine	Brother HS-5100	
Wire manufacturer	Charmilles Technologies, BercoCut	
Wire material	Brass	
Wire diameter (mm)	0.25	
Workpiece material	Brass	Carbide
Spark cycle (μs)	20	28
On-time (μs) in Experiment I	14	14
On-time (μs) in Experiment II	2~5	2~5
(Percentage of on-time in Experiment I)	(70%)	(50%)
(Percentage of on-time in Experiment II)	(10~25%)	(7~18%)
Axial direction wire speed (mm/s)	15	18
Wire tension (g) in Experiment I	1500	1500
Wire tension (g) in Experiment II	1800	1800
Gap voltage (V)	45	35

1.1. Experiment I – High Material Removal Rate

A set of 12 parts was produced using the cylindrical wire EDM at four part rotational speeds (w) and three wire traverse speeds (v_f) for two work-materials, brass and carbide, respectively. The test configuration is illustrated in Figure 1 with a=0, R=3.175 mm, and r=2.54 mm.

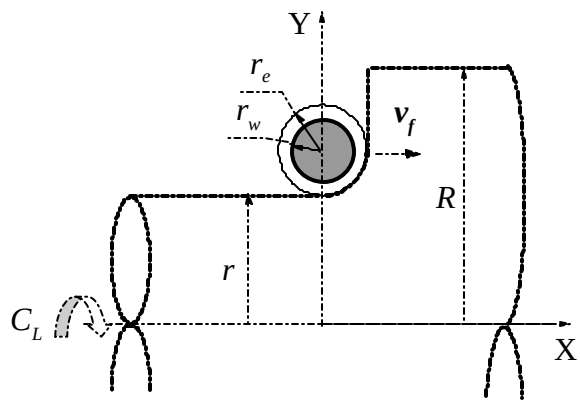

Figure 1. The configuration of roundness experiment.

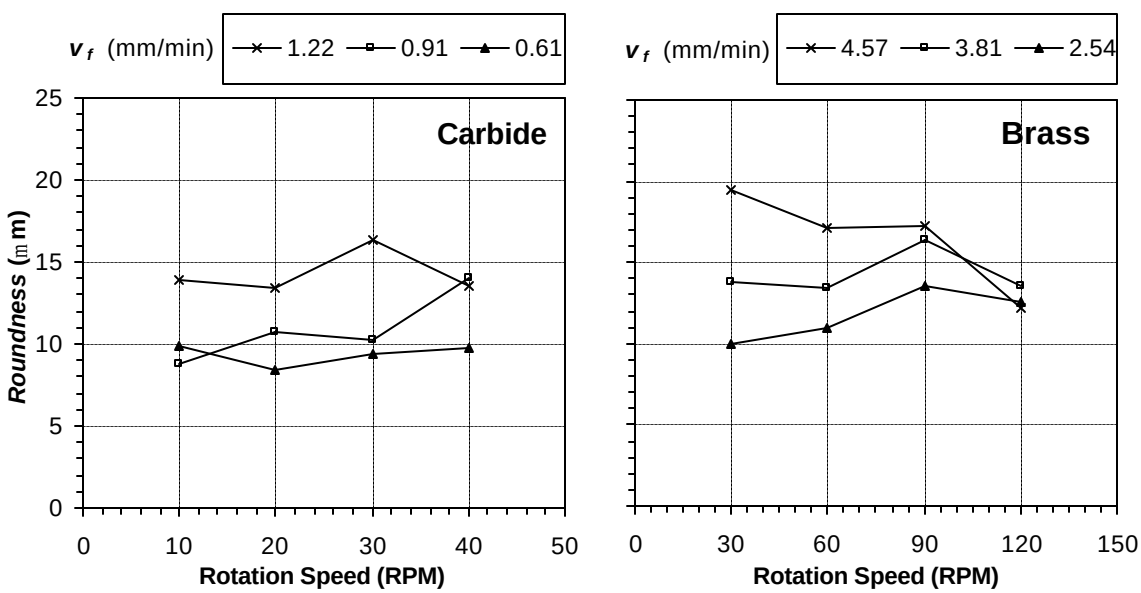

Figure 2. The roundness of cylindrical wire EDM parts in experiment I.

The roundness results are shown in Figure 2. Most of the roundness traces are oval. The spindle runout, to be discussed in Section 2, is the major source of the error in the part roundness.

Results in Figure 2 also indicate that better roundness can be achieved at lower v_f, possibly due to less wire vibration. The effect of part rotational speed on roundness is not obvious.

1.2. Experiment II – Fine surface finish and roundness

The goal of Experiment II was to improve the surface finish and roundness. To achieve this goal, the electrical spark on-time and wire traverse speed was reduced and a thin, 50 μm layer of material was removed during the cylindrical wire EDM. The cutting configuration, as shown in Figure 1, was with a=0, R=2.59 mm, and r=2.54 mm. Preliminary experiments have identified two parameters, wire traverse speeds, v_f, and spark on-times, t_{on}, to have significant effect on roundness. Figure 3 shows the roundness results by cylindrical wire EDM carbide and brass at three v_f and four t_{on} values. By comparing the roundness results in Figure 2 and Figure 3, it can be seen that the roundness errors in Experiment II are much smaller than those in Experiment I. The shorter on-time and lower wire traverse speed generated better roundness. When t_{on}=2 μs, the roundness drops to 1.7 μm for carbide and 2.9 μm for brass, respectively. This has opened the possibility to apply the cylindrical wire EDM for machining precision parts.

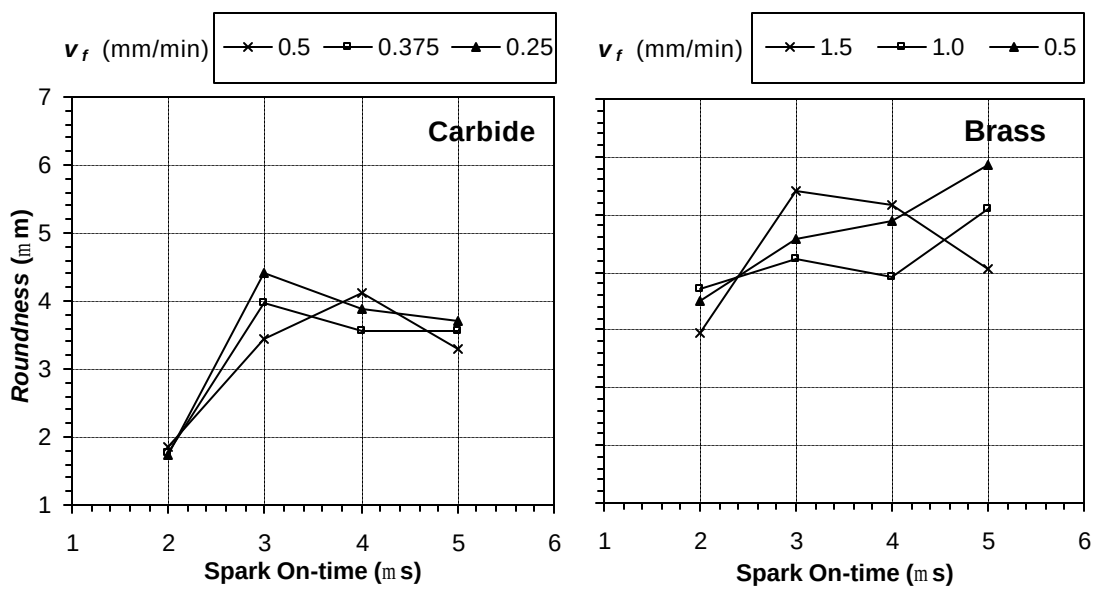

Figure 3. The roundness of cylindrical wire EDM parts in experiment II.

2. Spindle Runout

The runout is an important parameter of a precision spindle and can affect the roundness and surface finish of the cylindrical wire EDM parts. The Donaldson's method [Slocum, 1992] was used to measure the spindle runout. A 6.35-mm-diameter silicon nitride bar was held by the R8 collet in the spindle. An electronic indicator with 0.1 μm resolution was used to measure two spindle runout traces on opposite sides of the bar. The spindle runout was calculated from these two traces. A sample spindle runout trace at 20 rpm is shown in Figure 4. The maximum runout at 10 spindle speeds are shown in Figure 5. Fourier transformation was applied to analyze the spindle runout data to identify the source of error. Figure 6 shows the amplitude of runout vs

frequency for two spindle rotational speeds at 20 and 30 rpm. Four major peaks can be identified.

(i) f_o: This is the major peak and is equal to the rotational speed of the spindle.
(ii) f_1: This is always equal to five times the rotational speed of the spindle, possibly caused by the form error on bearing races.
(iii) f_3 and f_4: These two frequencies at 30 and 120 Hz remain unchanged for different motor rotational speeds. These two frequency peaks are possibly caused by the electrical motor.

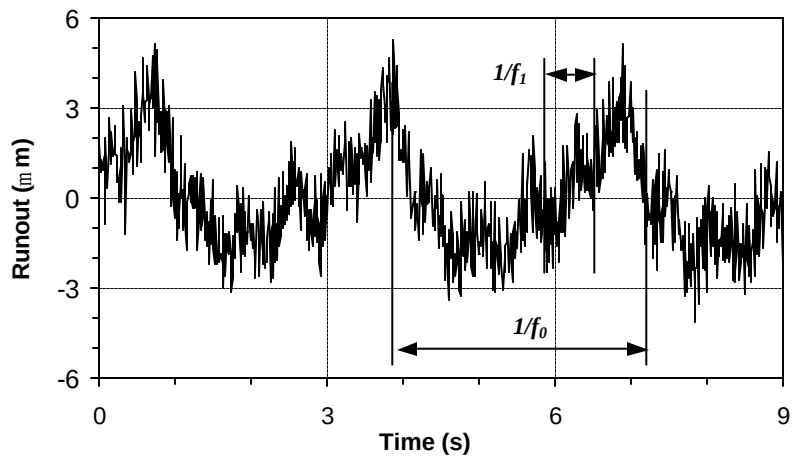

Figure 4. Spindle runout at rotation speed of 20 RPM.

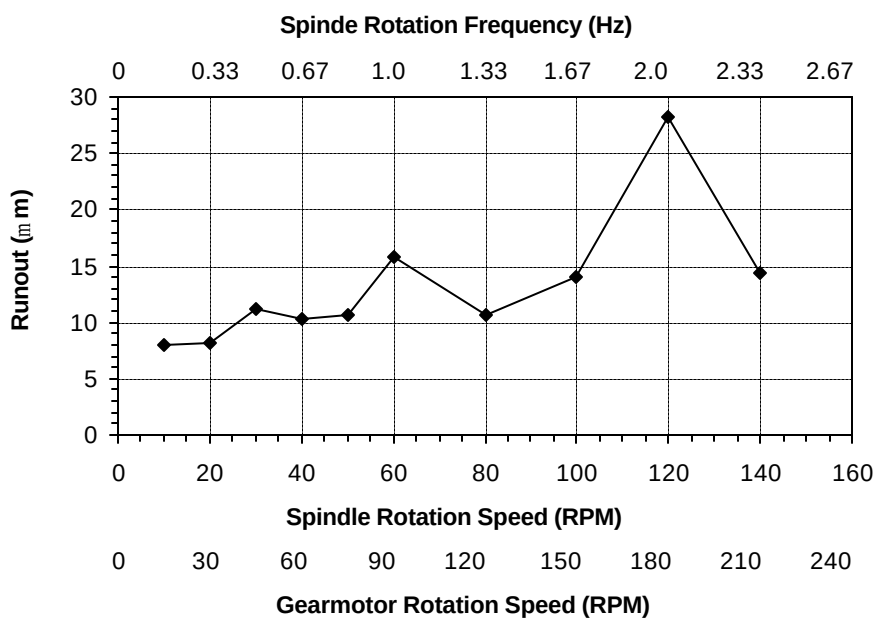

Figure 5. Spindle runout *vs* rotation speed.

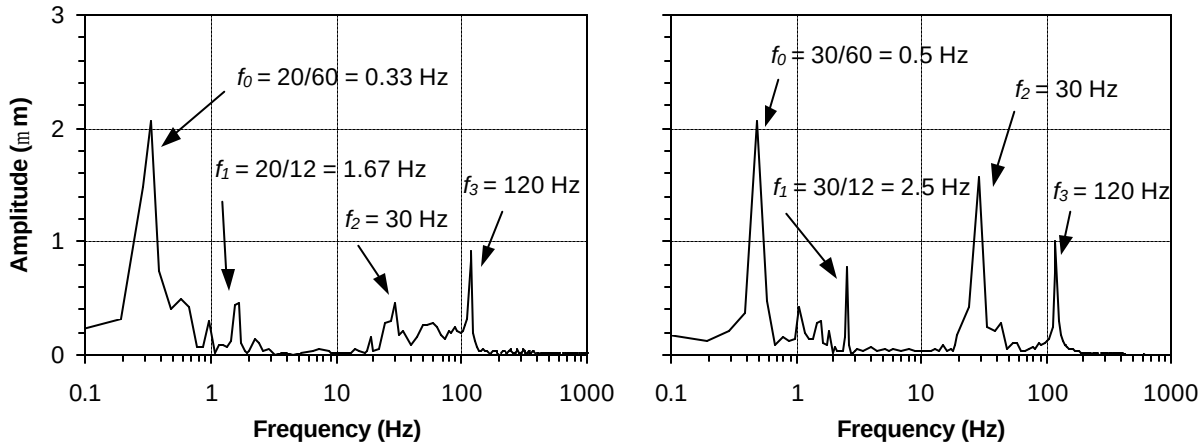

(a). Spindle rotation speed of 20 RPM. (b). Spindle rotation speed of 30 RPM.

Figure 6. Frequency spectrum by FFT of the spindle runout.

Status of Milestones

Milestone 1: Develop process technology to achieve high material removal rate in cylindrical WEDM of advanced engineering materials.

Status: Nothing to report. Experiments have been conducted to quantify the maximum material removal rate. Results showed the maximum material removal rate in cylindrical wire EDM is higher than the conventional 2D wire EDM.

Milestone 2: Determine the level of form tolerances and surface finish achievable by the cylindrical WEDM.

Status: Experiments was conducted at High Temperature Materials Lab at Oak Ridge National Lab to measure the roundness and surface finish. The cylindrical wire EDM parts with roundness as low as 1.7 μm for carbide and 2.9 μm for brass were achieved. Analysis of the spindle runout helped to understand and improve the roundness of parts. The surface finish was as low as 0.6 mm Ra, comparable to rough grinding, for the carbide materials.

Milestone 3: Prototype needles, armature pins, and plungers for diesel engine fuel injectors.

Status: Several prototype diesel injector plungers were manufactured. Exploratory experiments to machine miniature shafts in the size under 0.1 mm diameter were conducted.

Milestone 4: Develop mathematical models for material removal rate and surface finish of the cylindrical WEDM.

Status: Noting to report. The mathematical models for material removal rate and surface finish have been derived. These results have been summarized in a technical paper.

Milestone 5: Characteristics of the recast layer after WEDM and cylindrical WEDM and the surface condition after abrasive blasting.

Status: Experiments was conducted at High Temperature Materials Lab at Oak Ridge National Lab to use the SEM to observe the surface and cross-section of cylindrical wire EDMed brass and carbide parts.

Milestone 6: Development of optical fiber based temperature measurement method, with applications for grinding process and diesel exhaust aftertreatment filters.

Status: Adam Curry finished his MS thesis defense and is summarizing his research results in two technical papers, planning to be submitted to the Journal of ACS.

Communications/Visit/Travel

Adam Curry, Brian Rhoney, and Jun Qu, visited Oak Ridge National Lab. January 29 to February 2, 2001, to do experiments on grinding temperature measurement and roundness and surface finish measurement of cylindrical wire EDM parts.

Brian Rhoney, and Jun Qu, visited Oak Ridge National Lab. from February 5 to February 10, 2001, to analyze wire EDMed surfaces using the stereo SEM.

Jun Qu, Monika Garrell, and John Kong, visited Oak Ridge National Lab. from March 12 to Mar. 15, 2001 to run more roundness measurement and analyze of wire EDM surfaces using SEM.

Publications

A technical paper entitled "Development of the Cylindrical Wire Electrical Discharging Process" by J. Qu, A. J. Shih, and R. O. Scattergood was submitted to the Symposium on Nontraditional Manufacturing Research and Applications in 2001 American Society of Mechanical Engineers International Mechanical Engineering Congress and Exposition.

References

A. H. Slocum, 1992, *Precision Machine Design*, Prentice Hall.

NDE Technology for Fuel Delivery and Insulating Materials

W. A. Ellingson
Argonne National Laboratory

Objective/Scope

The objective of the work in this task, part of the Testing and Characterization research area of the Heavy Vehicle Propulsion System Materials Program, is to develop enabling nondestructive evaluation/characterization (NDE/C) technology for lower cost and high performance materials. Specifically, this project addresses development of advanced NDE/C technology for; a)-advanced fuel delivery systems (including injector nozzles) and b)-insulating materials for reducing heat losses in the combustion zone. Fuel delivery systems for heavy-duty diesel engines are complex, very expensive and represent a significant portion of the cost of a heavy vehicle diesel engine. High pressures inside these fuel delivery systems contribute to poor fuel delivery and hence poor emissions. Materials development is part of Goal 3 of the heavy vehicle propulsion materials program. Insulating materials are also a significant materials development area because of the improvement in engine efficiency if reduced heat losses can be obtained. NDE/C technology that can provide information for reliable cost production and engine component surveillance would be of benefit to reaching the goals.

Technical Highlights

The highlight this period is that we have improved the experimental set up for the polarized back-scattered laser light for detection of subsurface machining-induced or operational-induced cracking on ceramic fuel metering plungers. Should the developments continue to be favorable, more consideration might be given to the idea of using the laser technology for an on-line tool for component manufacturing reliability.

Technical Progress

Work this period again focused on the ceramic fuel metering plungers under development by Cummins Engine Company of Columbus, IN.

Fuel Delivery Systems

Fuel delivery systems are critical and impact many engine performance parameters. Higher pressures required for advanced fuel systems are driving new designs and as with any design, material trade-offs become an area for evaluation. Ceramic materials provide many advantages but only if there is a reduced cost with the same or better reliability of a metal component. High pressures and potential for erosion inside fuel metering systems usually call for hard tool steels in the design and thus costs immediately become a factor. Ceramics offer a desirable option because they offer high hardness and erosion resistance. As noted last period, Cummins Engine Company has optioned in their CELECT™ fuel injector system to use MgO materials in the metering plunger.

The efforts we have been undertaking on MgO plungers have been to study the potential of non-contact polarized back-scattered laser light methods to detect subsurface machining damage in these plungers. Figure 1 shows the primary locations on the plungers, which have been of interest.

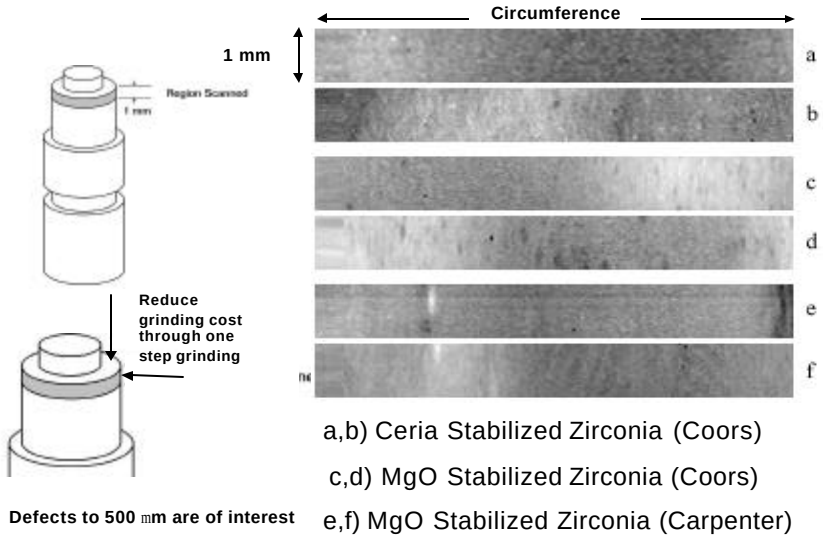

(A) (B)

Figure 1. Schematic diagram showing locations on the plunders where subsurface cracking is of interest from a detection point of view

This period we received from Cummins Engine Company four new MgO plungers of an advanced design, which had been run in a test cylinder for between 75 and 145 hours. Because of certain internal engine conditions, some of the plungers sustained slight damage that is visible on the surface but the depth of damage is unknown. Work next period will provide information and confirmation of the depth of the damage.

NDE for Insulating Materials

We continue work on developing this aspect of this effort.

Meetings, Trips, Communications

Meetings

A project review of this project was held February 1, 2001, at Argonne National Laboratory. Present at the review were Dr. Sid Diamond, Heavy Vehicle Program Manager for DOE, and Dr. Ray Johnson, ORNL program manager for Heavy Vehicle/Propulsion Materials.

Trips
None

Communications
Discussions were held with staff of Cummins Engine in Columbus, IN.
Discussions were held with staff of Enceratec of Columbus, IN

NDE Development for Ceramic Valves for Diesel Engines

J. G. Sun, A. A. Parikh, W. A. Ellingson
Argonne National Laboratory
and
S. K. Lee
Caterpillar, Inc.

Objective/Scope

Emission reduction in diesel engines designated to burn fuels from several sources has lead to the need to assess ceramic valves to reduce corrosion and emission. The objective of this work is to evaluate several nondestructive evaluation (NDE) methods to detect defect/damage in structural ceramics valves for diesel engines. There are four tasks to be carried out in this work: (1) Establish correlation of NDE data with mechanical properties for fatigue/wear damaged samples. These include rotary fatigue, dynamic fatigue, impact/sliding wear, and possible thermal shock testing. The induced damage will be assessed using various NDE methods including dye penetrant, optical scatter, impact acoustic resonance (IAR), X-ray CT, thermal imaging, and others. NDE data will be correlated with those from characterization tests including mechanical strength, SEM, and others. (2) Develop NDE techniques for ceramic-metal joints. Effort will be focused on developing new methods as well as evaluating existing NDE techniques to characterize quality of ceramic-metal joints. NDE data will be correlated with mechanical data. (3) Conduct NDE studies of full-size engine valves. In this part of the work, full sized ceramic valves will be produced for testing in a single cylinder test engine. These valves will be examined using NDE techniques developed at Argonne. (4) Finalize correlation of NDE to machining damage. This limited effort will conclude the earlier work to correlate NDE data with mechanical properties of machining-damaged Si_3N_4 ceramics. Elastic optical scatter method will be used to examine these specimens and the NDE data will be correlated with flexural strength.

Technical Highlights

Work during this period (January - March 2001) focused on developing filtering schemes for statistical evaluation of laser scatter data and on conducting water-coupled ultrasonic NDE study for detection of interface cracks in ceramic-metal joints.

1. Elastic Optical Scattering NDE for Machining Damage

We have developed two filtering schemes for calculation of statistical parameters from laser scatter data. The filtering schemes are based on moving-window averaging or median filtering to determine the local mean intensity instead of using a constant mean intensity value for the entire image. Statistical parameters are then calculated using the local deviation from the mean intensity image. Because laser scatter intensity is affected by the local color variation that may vary considerably for large sample surfaces, these filtering schemes can effectively remove the effects of specimen color change or presence of surface contamination.

Figure 1a shows the laser scatter sum image for silicon nitride flexure-bar specimen AS800 #6. This specimen has a significant color variation on its surface, from yellowish white at the upper portion to dark gray at the lower portion. The sum image shows clearly the strong back-scattered light from the

white surface at the top. The moving-window averaged sum image for this specimen surface is shown in Figure 1b, with the averaging window size of 101 x 101-pixels (or 1 mm x 1 mm area averaging) at each pixel. It is seen that the averaged sum image resembles closely to the original sum image, but with the detailed local variations being smoothed out. In Figure 2, the statistical parameter C_v is plotted for all AS800 specimens. The "old data" refer to those calculated with a single mean value for the entire image (C_v = standard deviation / mean) while the "new data" to those with the mean at each pixel represented by the moving-window averaged image (e.g., Figure 1b). It is seen that the C_v has appreciable change only for specimens #6, #9, and #15 because there is large color variation on the surface of these specimens. Work is continued to correlate the "new" statistical laser scatter data with the strength of Caterpillar GS44, AS800, CFI, and SN235 flexure-bar specimens and results will be presented in the next quarterly report.

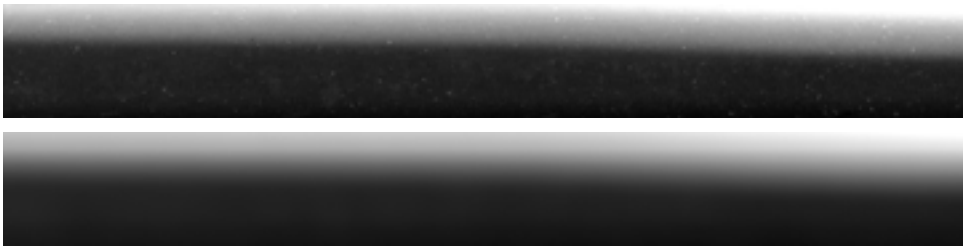

Figure 1. (a) Laser scatter sum image data for flexure-bar specimen AS800 #6; (b) image obtained by applying moving-window averaging for the image in (a).

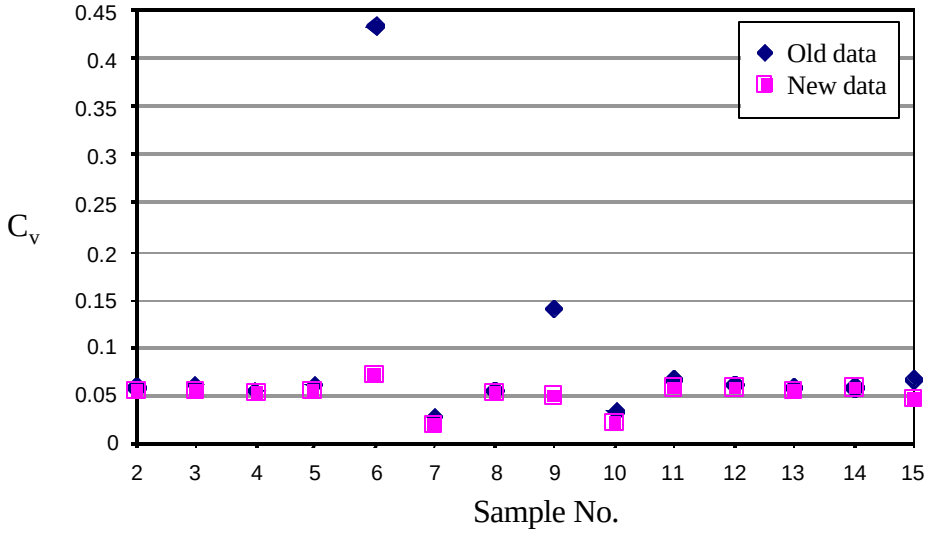

Figure 2. Comparison of statistical parameter C_v for fourteen AS800 flexure-bar specimens calculated using single mean value (old data) and moving-window averaged mean images (new data).

2. NDE Development for Ceramic-Steel Joints

During this period we conducted water-coupled ultrasonic NDE study of the 10 large ceramic-steel joint samples for detection of interface cracks. The experimental setup is illustrated in Figure 3, with a machined (an EDM cut) steel rod simulating a joint having an interfacing crack. The transducers are arranged in a pitch-catch setup at 5° angle from the normal direction of the rod axis. The transducer frequency is 5MHz. The EDM cut on the steel rod extends a length of 90° along the circumference and has a depth of one quarter of the rod diameter. Figure 4 shows the ultrasonic C-scan image of the machined steel rod. The EDM cut is clearly detected in the image as a horizontal line with reduced intensity. It is also shown twice in the image, once when it is facing the transmitter and once when facing the receiver.

Typical water-coupled ultrasonic scan images of a ceramic-steel-joint sample are shown in Figure 5. As illustrated in Figure 5c, each sample contains two joint regions. Two scans were performed for each sample with the sample at upward and at downward setup. It was found that the ultrasonic intensity data are more sensitivity for the upper joint (see intensity difference between Joint 2 in Figure 5a and Joint 1 in Figure 5b), while the data are less sensitive for the lower joint (see intensity difference between Joint 1 in Figure 5a and Joint 2 in Figure 5b). By comparing the images in Figures 5a and 5b, it is apparent that the ultrasonic intensity through Joint 2 has more reduction than that through Joint 1, indicating possible defects in the interfaces of Joint 2. This reduction of ultrasonic intensity occurs only in a few joints.

Further investigations and calibrations are needed before this ultrasonic NDE technique can be used to reliably predict interface qualities in a joint. The data shown in Figures 5a and 5b represent the intensity of the first peak in the receiver signal, which is likely coming from the beams as illustrated in Figure 3. However, there are many mode-converted beams within the sample, and some of them may be more sensitive to interface abnormalities. In addition, the angle of the ultrasonic beam to the surface and the ultrasound frequency may also affect the detection sensitivity. These issues will be studied in the next period.

Status of Milestones

Current ANL milestones are on or ahead of schedule.

Communications/Visits/Travel

W. A. Ellingson and J. G. Sun attended the American Ceramic Society's 25th Annual International Conf. on Advanced Ceramics & Composites, Cocoa Beach, FL, Jan. 21-26, 2001.

W. A. Ellingson and J. G. Sun made a presentation at the Heavy Vehicle Propulsion Materials Project Review Meeting held at Argonne National Laboratory on Feb. 1, 2001.

Problems Encountered

None this period.

Publications

None this period.

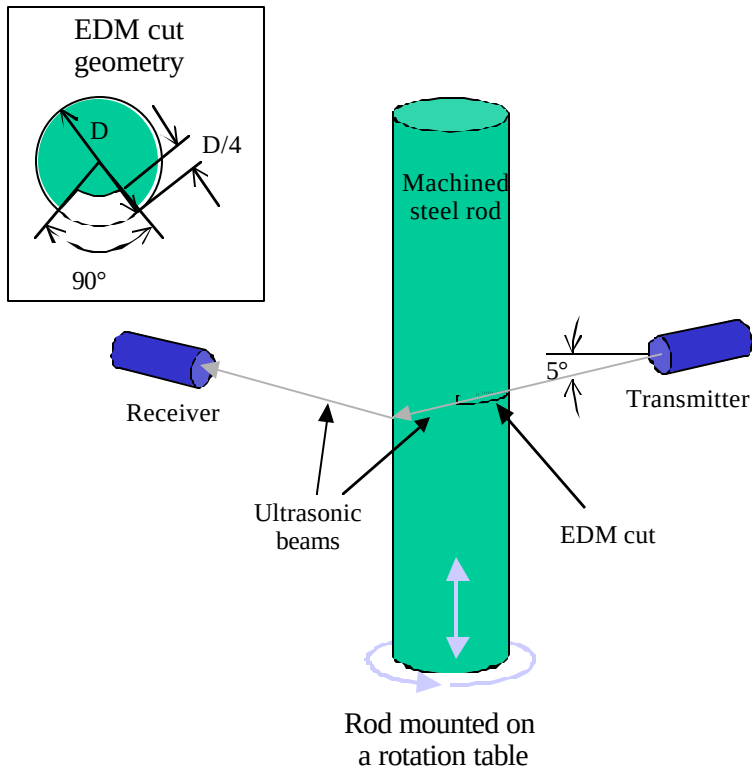

Figure 3. Water-coupled ultrasonic scanning setup for detecting cracks in the interfaces of cylindrical joints.

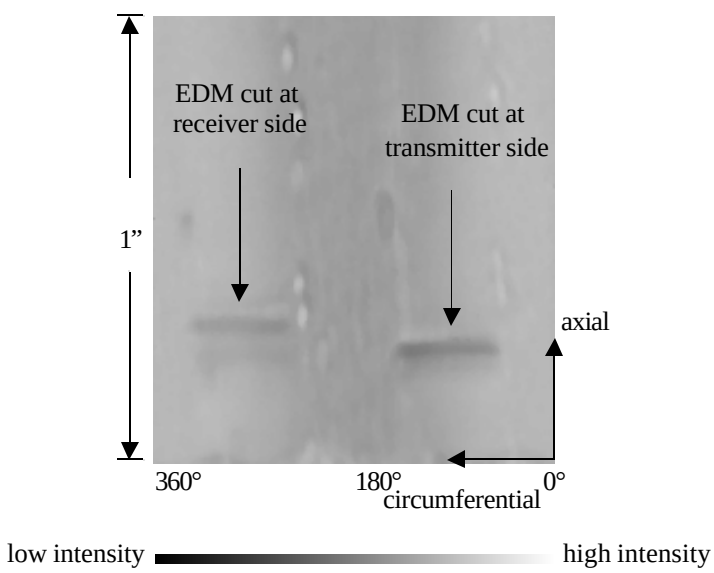

Figure 4. Ultrasonic scan image of a steel rod with an EDM machined cut of 90° circumferential length and 1/4 of rod diameter depth.

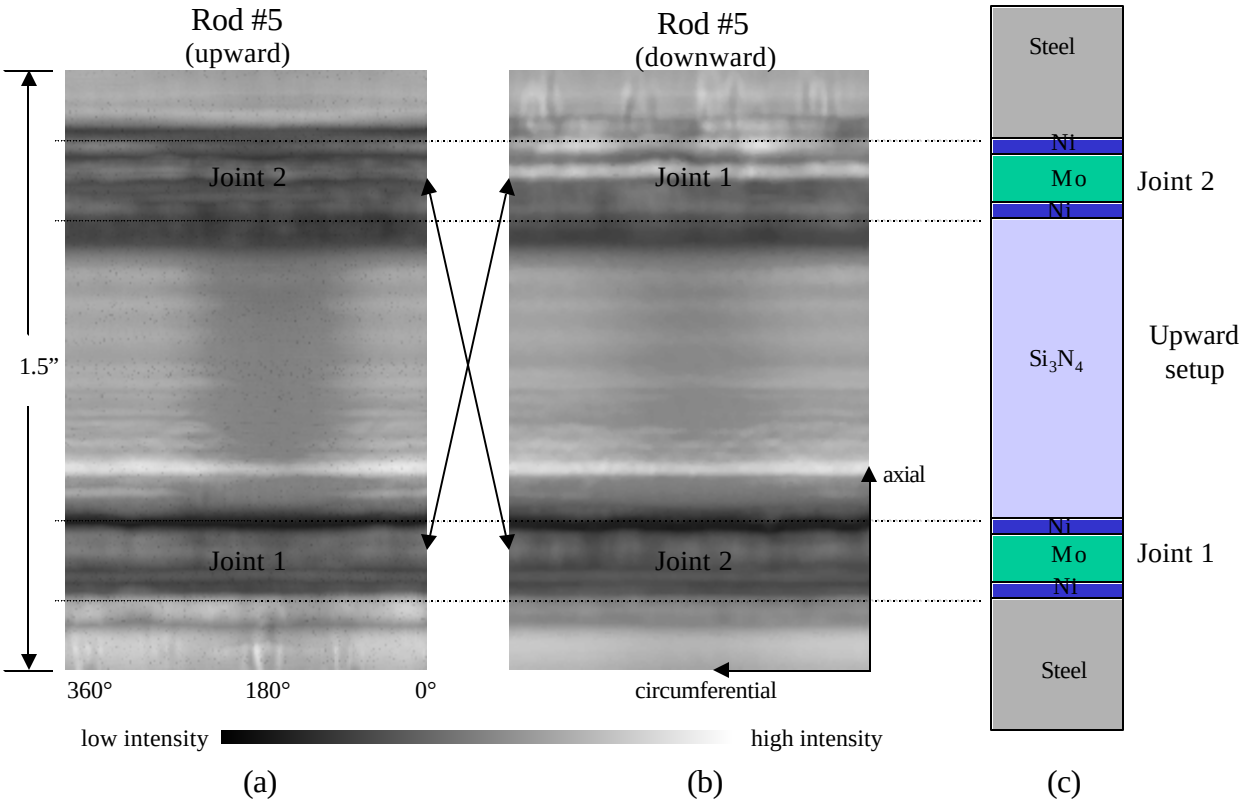

Figure 5. Ultrasonic scan images of cylindrical joint sample #5 at (a) upward setup and (b) downward setup; (c) schematic diagram of the joint sample.

Processing and Characterization of Structural and Functional Materials for Heavy Vehicle Applications

J. Sankar, D. E. Klett, A.D. Kelkar, J. Muchai, and S. Yarmolenko
North Carolina A & T State University

Objective/Scope

(The following reports the activities related to one of the tasks of the research program.)

To investigate the effect of yttria partially stabilized zirconia (PSZ) thermal barrier coating on diesel engine performance.

The required research includes three (3) major tasks:

Task 1. Diesel Engine Piston Modification

Engine piston modification has to be performed because the cost of individual pistons prohibits application of thermal barrier coating on each piston.

Task 2. Plasma Sprayed Thermal Barrier Coating

Eight custom made pistons for the Ricardo Hydra single cylinder DI diesel engine have been machined and ready for coating with plasma sprayed PSZ for evaluation of the coating thickness on diesel engine performance and emissions.

Task 3. Analytical Model Development

Finite element model for each piston/coating combination has been developed for evaluation of thermal and structural effect of the coating thickness on the piston.

Technical Highlights

Zirconium oxide has been extensively used in thermal barrier coatings for many years. Yttria stabilized zirconia (YSZ) has very low thermal conductivity. Therefore, it can be used to reduce heat transferred from engine combustion gases to the combustion chamber walls (cylinder head, piston face and cylinder liners).

Finite element model of the piston has been done for coating thickness ranging from 0.1 to 2.0 mm. The thermal barrier coat was modeled as plasma sprayed yttria stabilized zirconia (PYSZ) applied on the piston face.

Results and Discussion

Analytical

Finite Element Analysis (FEA) using ANSYS was used to systematically evaluate thermal and structural effect of the coating thickness on the piston. Although a number of researchers have investigated the temperature distribution in piston [1,2,3,4] the innovation of this analysis is that the coating thickness is varied systematically from 0.5 to 2.0 mm, with detailed boundary

conditions. To reduce computational time, a 2-d axisymmetric model was used. The AL alloy piston, with oil splash cooling, has a thermal conductivity k=153 W/m^{2}K, and a heat capacity ρc=1.6x10^6 J/m^3 K. The low heat rejection piston has 0.5-2.0 mm yttria stabilized zirconia coating applied on the top. The coating has thermal conductivity k=2.2 W/m^{2}K, and a heat capacity ρc=3.2x10^6 J/m^{3}K. Figure 1 shows the axisymmetric piston model used for the FE analysis. 1-D engine thermodynamic cycle analysis was done for a Ricardo single cylinder diesel engine to obtain the piston thermal boundary conditions. The heat transfer coefficient H_{gas} was calculated according to

$$H_{gas} = C_1 V_c^{-0.06} P^{0.8} T^{-0.4} \left(v_p + C_2\right)^{0.8}$$

where C_1, C_2 are constants and V_c, P, T and v_p are cylinder volume, pressure, temperature and piston velocity respectively.[5]

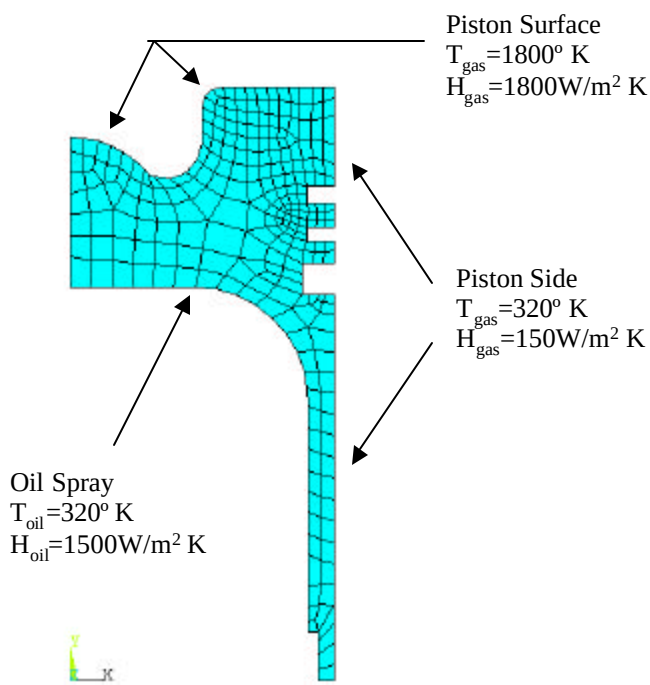

Figure 1. FEA Piston model for the Ricardo Hydra single cylinder DI diesel engine

Figure 2 shows a 1.0 mm thick YSZ thermal barrier coating applied on the piston. The piston and coating model have a total of 730 nodes and 210 elements.

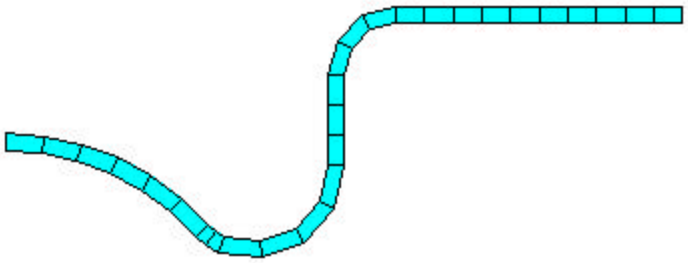

Figure 2. 1.0mm thick FEA Thermal Barrier Coating model

Figure3 shows the piston face (#6) and bowl center (#7) locations. The temperature for these locations is shown in Table 1 for each coat.

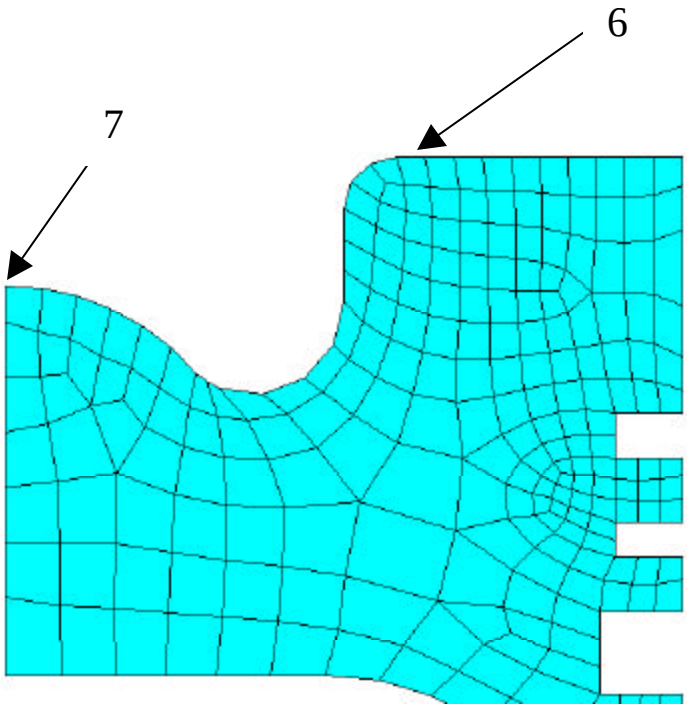

Figure 3: Piston temperature fields

Table 1. Temperature Fields (K)

Location		Coating thickness (mm)				
		0	0.5	1.0	1.5	2.0
Crown Center	***7***	480	594	644	695	760
Top surface	***6***	493	600	642	682	736
Max Temp		500	610	660	712	768

Status of Milestones
On Schedule

Communications/Visitors/Travel
None

Problems Encountered
None

Status of Milestones
Work on piston temperature distribution, heat transfer and thermal stress analysis is in progress.

Publications

1. Jesse Muchai, Ajit Kelkar, David Klett and Jag Sankar**,** "Analytical Study On The Effects Of Thermal Barrier Coatings On Diesel Engine Piston Conference," The American Ceramic Society 103rd annual meeting and Exposition, Indianapolis, Indiana**,** April 22-25, 2001
2. D. Pai, Y. Acharya, S. Yarmolenko, J. Sankar, J. Lua, and L. Zawada, "Single Fiber Testing and Creep Modeling," 25th Annual Conference on Composites, Advanced Ceramics, Materials and Structures, Cocoa Beach, FL, Jan 2001 (full paper under review).

References

1. D.N. Assanis and E. Badillo, SAE Paper 910460, 1991
2. Y. Zhang, B. Gao, and B. Zhang, SAE Paper 981488
3. A. Gorel, K. Voss and G. Austell, SAE Paper 1999-01-3666
4. R.C. Nova et. al., Materials &Manufacturing Processes, 7(1) 15-30 (1992)
5. G. F. Hohenburg, SAE Paper 790825

Life Prediction of Diesel Engine Components

H. T. Lin, T. P. Kirkland, M. K. Ferber
Oak Ridge National Laboratory
and
M. J. Andrews
Caterpillar Inc.

Objective/Scope

The valid prediction of mechanical reliability and service life is a prerequisite for the successful implementation of structural ceramics as internal combustion engine components. There are three primary goals of this research project which contribute toward that implementation: the generation of mechanical engineering data from ambient to high temperatures of candidate structural ceramics; the microstructural characterization of failure phenomena in these ceramics and components fabricated from them; and the application and verification of probabilistic life prediction methods using diesel engine components as test cases. For all three stages, results are provided to both the material suppliers and component end-users.

The systematic study of candidate structural ceramics (primarily silicon nitride) for internal combustion engine components is undertaken as a function of temperature (< 900°C), environment, time, and machining conditions. Properties such as strength and fatigue will be characterized via flexure and rotary bend testing.

The second goal of the program is to characterize the evolution and role of damage mechanisms, and changes in microstructure linked to the ceramic's mechanical performance, at representative engine component service conditions. These will be examined using several analytical techniques including optical and scanning electron microscopy. Specifically, several microstructural aspects of failure will be characterized:

(1) strength-limiting flaw-type identification;
(2) edge, surface, and volume effects on strength and fatigue size-scaling
(3) changes in failure mechanism as a function of temperature;
(4) the nature of slow crack growth; and
(5) what role residual stresses may have in these processes.

Lastly, numerical probabilistic models (*i.e.*, life prediction codes) will be used in conjunction with the generated strength and fatigue data to predict the failure probability and reliability of complex-shaped components subjected to mechanical loading, such as a silicon nitride diesel engine valve. The predicted results will then be compared to actual component performance measured experimentally or from field service data. As a consequence of these efforts, the data generated in this program will not only provide a critically needed base for component utilization in internal combustion engines, but will also facilitate the maturation of candidate ceramic materials and a design algorithm for ceramic components subjected to mechanical loading in general.

Technical Highlights

Studies of dynamic fatigue test in four-point bending on Kyocera SN237 silicon nitride materials at 850 and 1000°C at stressing rates of 30 and 0.003 MPa/s was added to the test matrix reported previously and completed during this reporting period. The SN237 silicon nitride, presumably a more cost-effective material, was sintered with oxide additives similar to those employed for SN235 and SN235P tested earlier in the program. The objective of the incorporation of SN237 silicon nitride into the test matrix is to generate the database for life prediction of exhaust valve components and compare with those previously generated for SN235 and SN235P. The SN237 silicon nitride bend bars were transversely machined per ASTM C116 standard. Dynamic fatigue test results showed that SN237 silicon nitride exhibited a comparable (and/or higher) characteristic strength to those obtained for SN235 and SN235P under the same test condition, as shown in Table 1 and Figure 1. Test results also showed that SN237 exhibited 9% and 17% decrease in strength when tested at 850 and 1000°C at 0.003 MPa/s in air, respectively. On the other hand, both of SN235 and SN235P silicon nitride revealed a minor decrease (~5%) in strength when tested at 850°C at 0.003 MPa/s. However, they both showed a substantial loss in characteristic strength (44-46%) when tested at 1000°C at 0.003 MPa/s in air, as shown in Table 1. The observed significant strength degradation of SN235 and SN235P at 1000°C at 0.003 MPa/s was attributed to the onset of slow crack growth and/or creep processes. The SN237 exhibits a relative low fatigue exponent (N=26) at 850°C as compared with the exponents obtained for SN235 (N=164) and SN235P (N=140). The fatigue exponent of SN237 at 1000°C (N=30), however, is higher than the exponents obtained for SN235 (N=14) and SN235P (N=13). The cause of the low fatigue exponent of SN237 at 850°C is still not clear, but it may be associated with the instability of secondary phase, as evident by the change of color on tensile surface, resulting in lower mechanical strength. Detailed SEM examinations will be conducted on SN237 bend bars tested at 850°C to provide insight into the low fatigue exponent obtained. Dynamic fatigue testing at room temperature is in progress and will be reported in next quarterly report.

Element mapping of Kyocera SN235 silicon nitride after 1000h exposure to an oil ash environment at 850°C in air was completed during this reporting period. The objective of the element mapping is to understand the effect of long-term oil ash exposure on the chemical composition of secondary phase(s) and the depth of silicon nitride materials influenced by the environment. The analysis showed that the elements of Zn, Ca, P, Na, S, and Mg present in the engine oil was only detected in the subsurface region of 2-3 microns. The analysis, thus, suggests that SN235 silicon nitride exhibits an excellent corrosion resistance to oil engine environment, consistent with the measured strength results reported previously, as shown in Table1.

Studies of stress rupture test on Honeywell GS44 silicon nitride was carried out at 850°C in air during this reporting period to determine the effect of applied stress on the lifetime response as well as the life limiting processes. The results showed that the GS44 silicon nitride exhibited a stress-dependent lifetime at applied stress greater than the fatigue limit with lifetimes decreasing as applied stress level increasing, Figure 2. The apparent fatigue limit of GS44 at 850°C is ~ 400 MPa, below which the GS44 did not fracture after 1000 h of testing time. Fatigue results also showed that the lifetime of GS44 was not sensitive the testing environments (air versus nitrogen) employed in the present study. SEM examinations on the surfaces of

fractured bend bars showed that similar features of liquid-like glassy ligaments were observed on specimens tested in air and nitrogen environment (Figure 3). The observed glassy skeletons suggested the softening of secondary phase occurred at test temperature. Note that the analysis of thermal expansion coefficient indicated that the softening point of GS44 is about 760°C. The independence of lifetime upon the testing environment suggests that the lifetime of GS44 may mainly be governed by the softening of the secondary phase at 850°C. The incorporation of oxygen into the glassy phase could cause a further decrease in the softening and viscosity of glassy phase, thus shortening the lifetime. Nonetheless, the oxidation effect is not apparent under the stress levels employed in the present study.

Status of Milestones

All milestones are on schedule.

Communications / Visitors / Travel

- Results of dynamic fatigue tests of SN237 at 850 and 1000°C and element mapping on SN235 after 1000h oil ash exposure were communicated with M. J. Andrews at Caterpillar.
- Communication was made with M. J. Andrews at Caterpillar regarding the evaluation of other brittle components employed in advanced diesel engines.
- Communication with Dave Carruthers at Kyocera regarding the acquisition of additional SN237 silicon nitride for mechanical properties database generation.

Problems Encountered

None.

Publications

"Strength and Dynamic Fatigue of Silicon Nitride at Intermediate Temperatures," A. A. Wereszczak, H. - T. Lin, T. P. Kirkland, M. J. Andrews, and S. K. Lee, in preparation.

"Silicon Nitride Ceramics for Valve Train Applications in Advanced Diesel Engines," S. K. Lee, P. H. McCluskey, M. J. Readey, H. T. Lin, and A. A. Wereszczak, to be published in *Ceramic Engineering and Science Proceedings* (2001).

References

[1] A. A. Wereszczak, M. J. Andrews, M. K. Ferber, and T. P. Kirkland, "Life Prediction Verification," *Heavy Vehicle Propulsion System Materials Program Semiannual Technical Progress Report to DOE Office of Transportation Technologies*, Apr. 1997 - Sep. 1997.
[2] A. A. Wereszczak, and T. P. Kirkland, M. J. Andrews, M. K. Ferber, and R. Tandonl, "Life Prediction of Ceramic Diesel Engine Components," *Heavy Vehicle Propulsion System Materials Program Semiannual Technical Progress Report to DOE Office of Transportation Technologies*, Oct. 1998 - Mar. 1999.
[3] C. R. Brinkman, T. P. Kirkland, H. - T. Lin, R. A. Ott, S. K. Lee, and J. Thiele, "Life Prediction of Ceramic Diesel Engine Components," *Heavy Vehicle Propulsion System Materials Program Bimonthly Technical Progress Report to DOE Office of Transportation Technologies*, Apr. 2000 - May 2000.

[4] J. C. Cuccio, P. Brehm, H. T. Fang, J. Hartman, W. Meade, M. N. Menon, A. Peralta, J. Z. Song, T. Strangman, J. Wade, J. Wimmer, and D. C. Wu, *Life Prediction Methodology for Ceramic Components of Advanced Heat Engines, Phase 1*, DOE Report ORNL/Sub/89-SC674/1/V2, 1995.

Table 1. Summary of uncensored Weibull and strength distributions for Kyocera SN235 and SN235P silicon nitride specimens transversely machined per ASTM C1161.

Material	# of Spmns. Tested	Stressing Rate (MPa/s)	Temp. (°C)	Uncens. Weibull Modulus	± 95% Uncens. Weibull Modulus	Uncens. Chrctstic Strength (MPa)	± 95% Uncens. Chrctstic Strength (MPa)
SN235	15	30	20	23.8	15.4, 33.9	901	879, 923
SN235P	15	30	20	38.1	24.0 55.8	666	656, 676
SN235**	10	30	20	15.9	10.2, 25.2	891	863, 926
SN235	15	30	850	26.7	18.0, 36.7	777	760, 793
SN235P	15	30	850	19.3	12.5, 27.6	631	612, 649
SN237	15	30	850	19.4	13.5 28.3	849	831, 872
SN235	14	0.003	850	18.5	11.8, 26.8	744	720, 767
SN235P	15	0.003	850	18.2	11.5, 26.8	594	575, 612
SN235**	10	0.003	850	6	4.0, 10.0	801	737, 879
SN237	15	0.003	850	6.0	4.2, 8.6	778	723, 841
SN235	15	30	1000	12	8.5, 17.2	711	686, 740
SN235P	11	30	1000	11	7.3, 17.1	560	536, 590
SN237	15	30	1000	11	7.8, 15.9	796	767, 832
SN235	15	0.003	1000	20.6	14.5, 29.5	395	387, 405
SN235P	10	0.003	1000	22.8	14.7, 36.1	301	295, 309
SN237	15	0.003	1000	17.2	12.1, 24.7	661	645, 680
SN235	9	30	1200	22.4	12.6, 34.8	442	427, 457
SN235	9	30	1200	61.3	34.5, 96.2	338	334, 342
SN235	6	0.003	1200	10.3	5.6, 16.7	247*	229*, 266*
SN235P	6	0.003	1200	18.5	9.0, 31.5	137*	130*, 145*

* Specimens crept-Shown rates/strengths uncorrected.

** Specimens after 1000 h exposure to an oil ash environment at 850°C in air.

Table 2. Summary of uncensored dynamic fatigue exponents of Kyocera silicon nitride materials as a function of test temperature

Material	Machining Orientation	Temperature (°C)	Fatigue Exponent
SN235	Transverse	850	164
SN235P	Transverse	850	140
SN237	Transverse	850	26
SN235	Transverse	1000	14
SN235P	Transverse	1000	13
SN237	Transverse	1000	30
SN235	Transverse	1200	14
SN235P	Transverse	1200	9

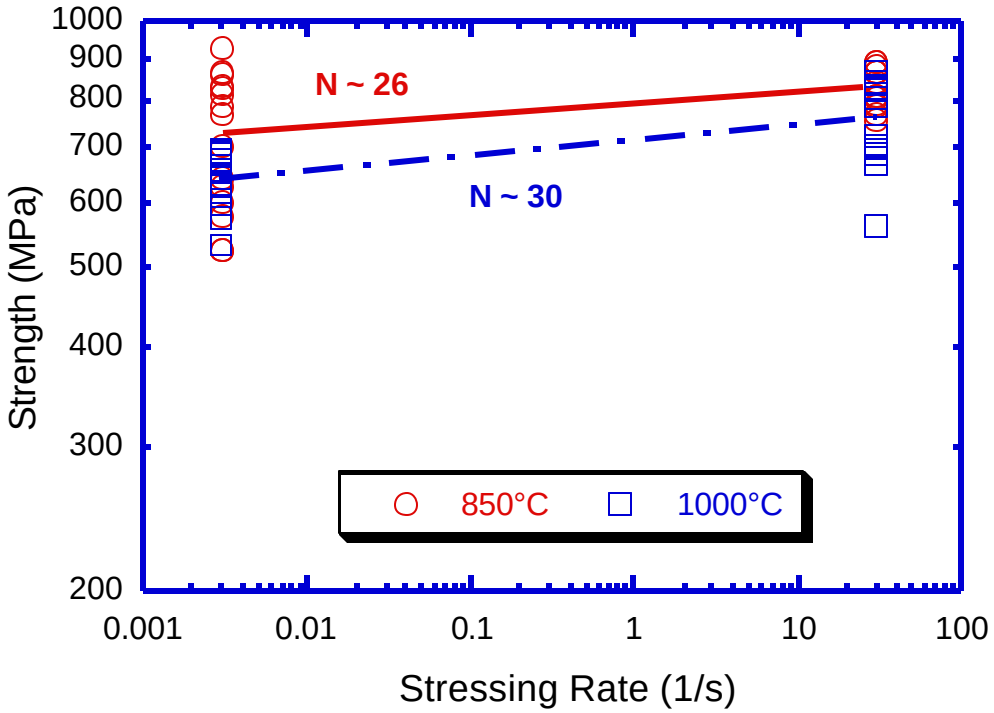

Figure 1. Strength versus stressing rate results of Kyocera SN237 silicon nitride tested at 850 and 1000°C.

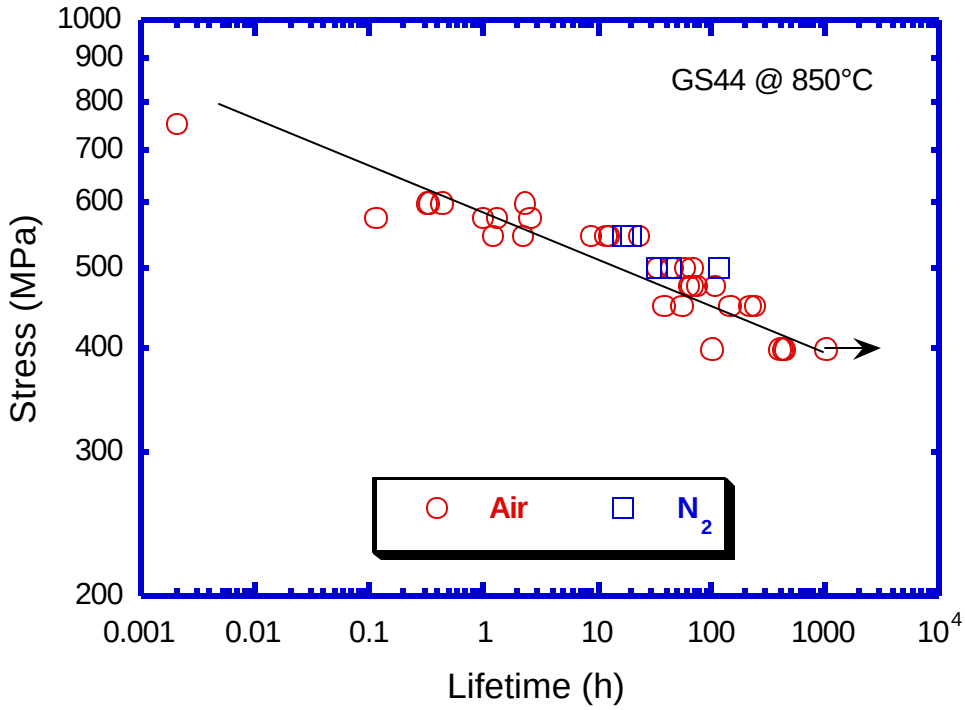

Figure 2. Stress versus lifetime curves of GS44 silicon nitride tested at 850°C in air and nitrogen environment.

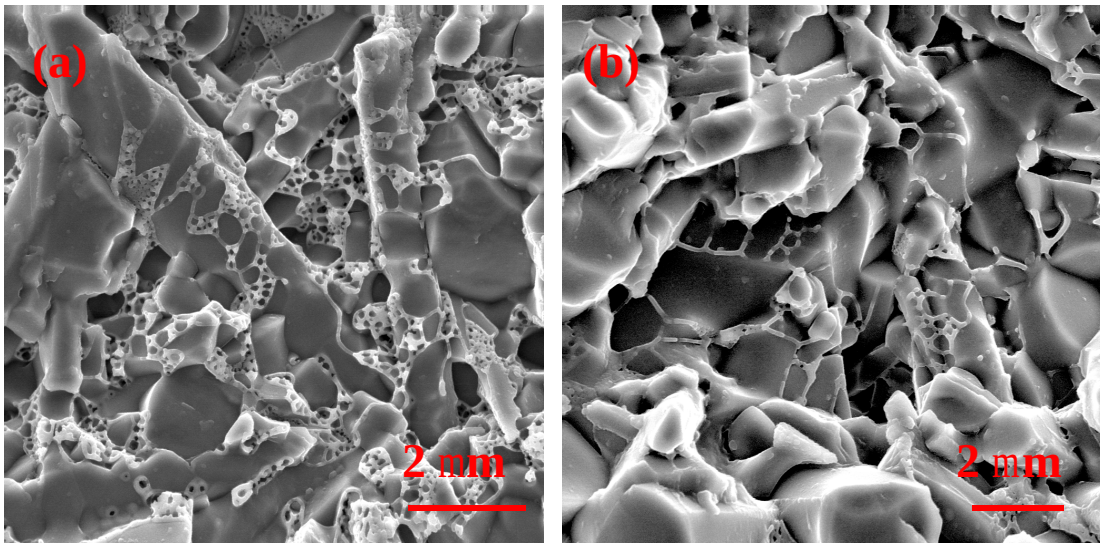

Figure 3. SEM microphotographs of Honeywell GS44 silicon nitride tested at 850°C in (a) air (400 MPa) and (b) nitrogen (500 MPa).

Durability of Diesel Engine Component Materials

Peter J. Blau and Ronald D. Ott
Oak Ridge National Laboratory

Objective/Scope

The objective of this effort is to enable the development of more durable, low-friction moving parts in diesel engines for heavy vehicle propulsion systems by conducting friction, lubrication, and wear analyses of advanced materials, surface treatments, and coatings. The scope of materials and coatings is broad and includes any metallic alloy, intermetallic compound, ceramic, or composite material which is likely to be best-suited for the given application. Parts of current interest include scuffing-critical components, like fuel injector plungers and EGR waste gate components. Hot scuffing is a primary surface damage mode of interest. Bench-scale simulations of the rubbing conditions in diesel engine environments are used to study the accumulation of surface damage, and to correlate this behavior with the properties and compositions of the surface species. The effects of mechanical, thermal, and chemical factors on scuffing and reciprocating sliding wear are being determined. Results will be used to refine material selection strategies and suggest materials for durability-critical engine components.

Technical Highlights

Baseline Testing of the High-Temperature Scuffing Apparatus. As indicated in the previous quarterly report, construction of the high-temperature, oscillating scuffing test system was completed, and it was calibrated to measure frictional torque. The basic geometric configuration consists of a horizontal, cylindrical specimen pivoting on a square, flat specimen with a central hole to avoid the center singularity. The shape of the oscillating contact is suggestive of a bowtie, and thus, we decided to call this test method the "bowtie scuffing test." A poster describing this test arrangement will be presented at the International Conference on Wear of Materials in Vancouver, Canada in April 2001.

A first series of unlubricated tests was performed using Type 304 stainless steel flat specimens and cylindrical specimens of Type 303 stainless steel, Stellite 6B, and GallTough™ a specialty stainless steel. The next set of tests was performed under liquid and solid lubricated conditions to determine the sensitivity of the apparatus to frictional torque. Results of these experiments are summarized in Table 1. The average friction coefficients for these tests were calculated from the device-compensated torque, applied normal force, and the distance of the contact from the center of oscillation. Friction coefficients ranged from 0.12, for the liquid lubricated case, to 0.97 for the non-lubricated Stellite 6B on 304 stainless steel. These values are reasonable, based on the principle investigator's experience.

A third series of experiments was run at room temperature and 600° C to evaluate the elevated temperature performance of the apparatus on baseline materials. This temperature was chosen to represent the conditions typical of diesel engine EGR system components, like components near the tubrocharger wastegate. Two replicate tests of the combination Type 303 stainless steel cylinder on Type 304 stainless steel flat specimens were performed. The load was 10.05 N, and the oscillation rate was 1.00+/-0.2 cyc/s. The flat specimens were finished by hand grinding on a glass plate on wet SiC 600 grit papers in distilled water.

Table 1.
Torque and Friction Coefficient Data from the First Set of Scuffing Tests
(The lower flat specimen was Type 304 stainless steel, 12.54 N load, 0.98 cyc/s, room temperature)

Cylinder Specimen Material	Lubricant	Test length (cycles)	Average Torque* (N-mm)	Friction Coefficient**
303 stainless steel	15W40 oil	30	12.35	0.12
303 stainless steel	graphite	30	36.19	0.18
303 stainless steel	none	20	39.72	0.40
GallTough stainless steel	none	100	78.75***	0.79
Stellite 6B	none	100	96.56***	0.97

* compensated for the zero-friction contact torque – average of two tests under these conditions
** calculated from the average torque and the location of the arcs of contact from the center pivot point
*** longer test length increased the level of damage and resulted in higher average torque readings

Room temperature tests were conducted for 3600 cycles. The first elevated temperature test was terminated after 480 cycles because of excessive grinding noise and specimen vibration. The second test was stopped after the same period of time so that replicate data could be compared. As with the previous tests, frictional torque was computed. As shown in Figure 1, the starting torque was much higher for elevated temperature tests of this material combination.

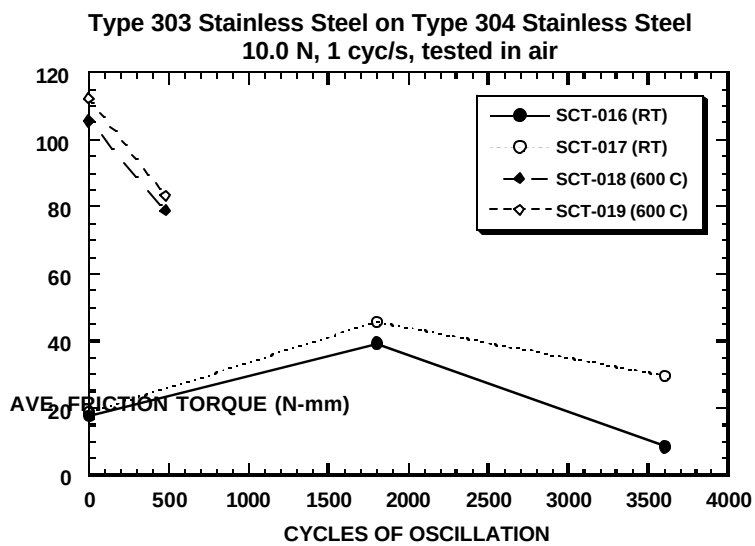

Figure 1. Comparison of replicate elevated temperature and room temperature tests.

A selection of candidate materials has been purchased, or otherwise obtained, and sent for machining to use in the cylinder-on-flat test configuration. The selection of rubbing couples was based on background literature research on materials compatibility for elevated temperature wear and on ORNL's experience with advanced ceramics. Some of the alloys will require heat treatment for optical performance, and this will be completed prior to elevated temperature testing.

Fuel Injector Wear Test Development. Work has begun on re-designing an existing ORNL test system to evaluate the durability of fuel injector plunger materials. Discussions have begun with a diesel engine manufacturer to work cooperatively in this area and more details will be presented in the following quarterly report.

Future Plans

1. Complete elevated temperature scuffing tests of selected material couples and prepare report.

2. Continue work on the redesign of a current ORNL wear testing system to evaluate the durability of fuel injector plungers.

Travel

None this period.

Status of Milestones

The following milestones were developed for FY 2001.

1) Complete baseline scuffing tests at room and elevated temperature. Submit report. (February 28, 2001 – report completed and submitted for clearance for publication and distribution as an ORNL Technical Report.)

2) Complete elevated temperature scuffing tests of leading candidate materials. Submit report. (March 31, 2001 – extension to June 30 is requested due to the late receipt of machined test specimens of the specimen materials.)

3) Complete design and construction of a computer-controlled fuel injector materials testing system capable of studying the effects of varying injector motions and loading cycles on material response. (September 30, 2001)

Publications and Presentations

(1) P. J. Blau and R. D. Ott, "Development of a High-Temperature, Bowtie Scuffing Test for Diesel Engine Applications," poster accepted for presentation at the International Conference on Wear of Materials, Vancouver, BC, Canada, April 23-26, 2001.

(2) P. J. Blau and R. D. Ott, "Development of a High-Temperature Scuffing Test for Evaluating Diesel Engine Component Materials - Construction, Calibration, and Baseline Data," ORNL Technical Report in process of review, printing, and distribution.

Implementing Agreement for A Programme of Research and Development on Advanced Materials for Transportation Applications

M. K. Ferber
Oak Ridge National Laboratory

Objective/Scope

The International Energy Agency (IEA) was formed via an international treaty of oil consuming countries in response to the energy crisis of the 1970s. A major objective of the IEA is to promote secure energy supplies on reasonable and equitable terms. The governing board of the IEA, which is composed of energy officials from each member country, regularly reviews the world energy situation. To facilitate this activity, each member country provides energy experts who serve temporary staff assignments at IEA headquarters. These staff or secretariat support the governing board by collecting and analyzing energy data, making projections in energy usage, and undertaking studies on specialized energy topics. The governing board is also assisted by several standing groups; one being the committee on energy research and technology (CERT), which encourages international cooperation on energy technology. Implementing agreements (IAs) are the legal instruments used to define the general scope of the collaborative projects. There are currently 40 active implementing agreements covering research topics such as advanced fuel cells, coal combustion science, district heating and cooling, enhanced oil recovery, fluidised bed conversion, fusion materials, solar heating and cooling, pulp and paper, hydropower, heat pumping technologies, hybrid and electric vehicles, high temperature super conductivity, wind turbines, and high temperature materials. A complete listing can be found at the IEA website, **http://www.iea.org**.

This progress report summarizes recent activities in the implementing agreement entitled, "Implementing Agreement For A Programme Of Research And Development On Advanced Materials For Transportation Applications." This implementing agreement currently consists of one active annex entitled," Annex II: Co-Operative Program on Ceramics for Advanced Engines and Other Conservation Applications". The motivation for this IA is the development of new and improved ceramic materials, brittle material design methods, and life prediction methodology. The objective of Annex II is coordinated R&D on advanced ceramics leading to standardized methods for testing and characterization.

The Executive Committee for the IA on Advanced Materials is also exploring the possibility of adding a new effort (Annex III) focusing on the characterization of materials for diesel engines. Possible topics include characterization of contact damage (fatigue) and novel methods for the assessment of the mechanical reliability of coatings.

Technical Highlights

General

During the Executive Committee Meeting in Malmo, Sweden, on June 22, 2000, a number of changes were proposed for both the implementing agreement and Annex II. In order to address these and other issues more quickly, the EC agreed to voting by fax (faxvote). During this reporting period, the following issue was addressed by this faxvote procedure:

Decision to change the language of Article 10 of our Implementing Agreement. Attachment 1 illustrates the proposed changes, which have been requested by the IEA Secretariat to facilitate participation by Non-Member Countries (all Contracting Parties to vote; unanimous decision needed).

The request was approved.

Annex II

Annex II currently consists of one active effort, Subtask 11. In this subtask, techniques for the measurement of thermal and mechanical fatigue of silicon nitride ceramics are being examined. National efforts in Japan and the United States focus on the development of procedures for evaluating the mechanical fatigue behavior of silicon nitride ceramics using either uniaxial flexure or biaxial test specimens. The national effort in Germany consists of the development of thermal fatigue procedures using the laser thermal shock equipment evaluated in Subtask 9. The national effort in Sweden will focus on the evaluation of the fracture surfaces of specimens tested in Japan, the United States, and Germany.

Subtask 11 will also include an international effort in which the thermal fatigue behavior of a single silicon nitride will be compared with the mechanical fatigue data generated at a temperature which is the same as that at the fracture point in thermal fatigue test. Germany will be responsible for the thermal fatigue testing while both Japan and the United States will conduct mechanical fatigue testing. Sweden will perform fractographic analysis of the specimens.

In the United States, specimens of GS44 silicon nitride (manufactured by Honeywell Ceramics Components) were machined. The elevated-temperature cyclic fatigue behavior of these specimens will be evaluated using the rotary bend fatigue (RBF) shown in Figure 1. Note that the dead weight loading apparatus for the RBF has been replaced by a computer-controlled pneumatic loading system, which allows the load to be varied as a function of time.

Annex III

To promote pre-competitive standard testing and characterization methods for diesel engine materials, DOE is proposing to start an international collaborative effort under the umbrella of the International Energy Agency. This effort, which would be in the form of a new annex under an existing Implementing Agreement (Advanced Materials For Transportation Applications), would focus on development and verification of advanced characterization techniques for diesel engine materials.

To better define the needs in this area, a subcontract was initiated with Gateway Materials Technology. The goals of this effort are as follows:

a) Develop a contact list for the diesel engine and ceramic coating community (engine manufacturers, coating suppliers, testing, government and academic research agencies).

b) Draft a survey to determine the needs and priorities for test standards for ceramic coatings in the diesel engine community. Submit the survey to Matt Ferber for review and comment.

c) Conduct the ceramic coatings survey by e-mail, sending the survey to the contact list names. Actively collect the survey replies. Analyze the results and draft a report on the method, results, and conclusions of the survey.

d) Make contact with and visit selected diesel engine manufacturers, coating suppliers, and research laboratories to discuss and refine the results of the ceramic coatings survey.

e) Analyze the results and complete the final report on the method, results, and conclusions of the survey and site visits.

f) Research and identify test standards (published and in draft) for ceramic coatings from US, EC, ISO, and Japanese standard organizations. Report on the identified standards.

Status of Milestones

All milestones are on track.

Communications/Visits/Travel

None

Publications

None

References

None

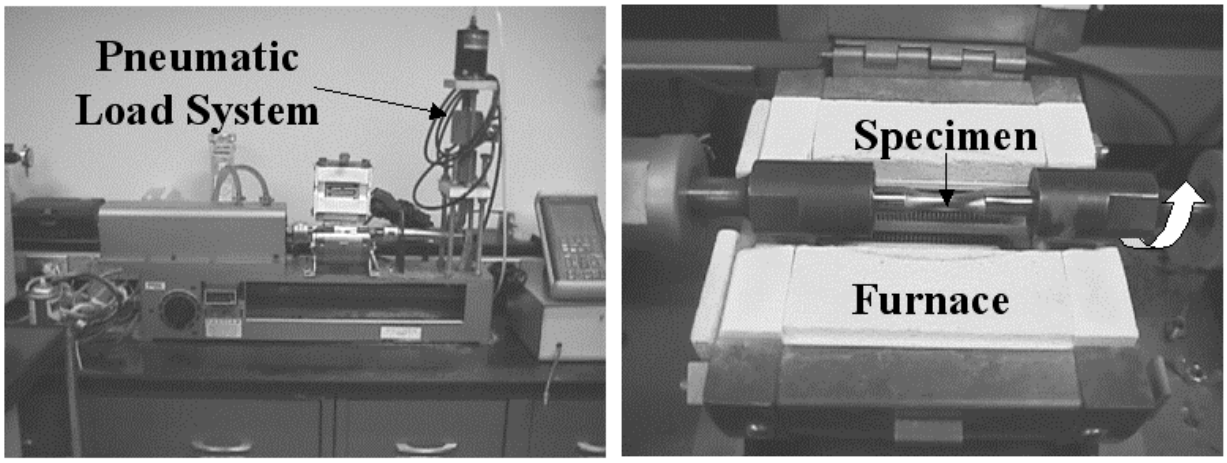

Figure 1: Overview of the RBF with Pneumatic Load System (left) and expanded view of specimen and furnace (right).

Standards For Reliability Testing Of Heavy Vehicle Propulsion Materials

Said Jahanmir, James F. Kelly, and William Luecke
National Institute of Standards and Technology

Objective/Scope

The objective of this project is to develop international standard test methods for assessing the reliability of ceramic components used in diesel engines and other heavy vehicle propulsion systems. Advanced ceramics such as silicon nitrides offer unique combination of properties that include light-weight, high-temperature strength, and resistance to wear and corrosion. These properties make them particularly attractive for diesel engines where their use as key engine components will allow the higher operating temperatures that lead to higher thermal efficiencies and environmentally cleaner propulsion systems. Reliability and cost-effectiveness are critical issues in implementing ceramics in the valve train of diesel engines. Ceramic valve train components are subjected to demanding conditions that include high contact loading, elevated temperatures, and corrosive environments. To ensure a reliable service life, standard test methods are needed to evaluate the performance of potential ceramics in highly loaded rolling and sliding contacts. This project will develop test methods for evaluating the contact damage behavior of ceramics under rolling and sliding conditions that simulate the cam roller followers, valves and valve seats. In support of this goal we will pursue four research thrusts. We will evaluate the effect of machining damage on contact reliability as well as the interactions between machining and contact damage that may lead to premature failure. The project will also consider fundamental issues in the relation between ceramic microstructure and performance reliability. Finally, we will investigate the basic mechanisms that lead to formation and propagation of contact damage and the effect on reliability of residual stresses developed during machining and by contact.

Technical Highlights

Although our plans are to investigate three basic types of contact damage in ceramics (Rolling Contact Fatigue, RCF, sliding wear and fretting, and Hertzian contact) we have focused this period on Rolling Contact Fatigue.

Standards for Rolling Contact Fatigue

During this reporting period we have begun refurbishing the four-head NTN Rolling Contact Fatigue test machine. In addition we are completing a detailed review of the literature on rolling contact fatigue and wear of silicon nitride to establish research areas. Although there are reports of a great number of RCF and RCW tests on silicon nitride over the past 25 years there are a great many unanswered questions. There are apparently no standards, US or foreign that address RCF or RCW in any geometry (3 balls on rod, ball on 3 (or 4) balls, or cylinder on cylinder). Our literature review has revealed a number of areas in the test technique that should be clarified as part of standards-related research:

- *Definition of Failure*. The NTN RCF test technique prescribes a fixed, rather high, vibration level for the definition of a spallation failure. Conversations with industrial users of the

tester lead us to believe that this definition may be too severe, in that by the time the vibration has reached this level, all information about the source of the spall is lost.

- *Ball spall/rod spall differences*. Although the 3-ball-on-rod test has been used for silicon nitride for many years, many of the research reports note that the failure that halted an individual test occurred in the metal ball, rather than the silicon nitride test rod. Methods must be developed and understood to drive the failures back to the rod.
- *Fractography*. Most existing research has very little to say about the fractographic nature of the spalls.
- *Interlaboratory comparisons*. There are no data that compare the results of the same test in different laboratories, or between different RCF techniques on the same material.
- *Lubricant/surface finish.* The NTN test protocol specifies a special roughened ball (originally developed for testing metal bearing materials) that causes the test to be run under conditions of asperity contact. The suitability of this procedure for ceramics has not been addressed. There is also no consensus in the literature on the lubricant used during the test. There is little beyond anecdotal evidence on the effect of different finishing methods for the rods on the RCF lifetime.
- *Wear effects.* Anecdotal evidence suggests that heavy wear of the silicon nitride rod hastens failure when wear debris is not adequately flushed from the contact area.

We intend to discuss all of these issues at our workshop at NIST on May 3. Table I lists the participants we have invited. Most have already committed to attend. We stressed in our invitation that although the primary goal is to develop standards and standard test methods, there are numerous issues that the project might address, including formation and propagation of rolling and sliding damage, assessment of contact fatigue under rolling and sliding, the influence of contact damage and machining induced damage on performance reliability, and the role of microstructure and operating conditions on damage formation and performance in rolling and/or sliding. We have stressed that we eagerly desire their input on research directions.

Moisture and Binder Content of Alumina

A work plan for IEA Subtask 12 was agreed to for the study of moisture and binder content of alumina granules provided by Japan. The spray-dried alumina granules and the testing protocols were distributed to the participating laboratories in the U.S. and the Germany, Japan, Belgium and Sweden for interlaboratory testing. The U.S., German, and Japanese laboratories have completed the measurements of moisture and binder content. The Swedish and Belgian laboratories chose not to participate in this activity.

Measurement of moisture content of a spray dried alumina powder

For determining moisture content in ceramic powders, the study participants agreed to use the same procedure that had been successfully used in IEA Subtask 10 (detailed in the previous quarterly report). The test assumes that the mass lost by a ceramic powder when it is heated to 105 °C is due to moisture loss and that all the moisture will be removed by holding the powder at that temperature for 2 hours. Eleven laboratories participated in this study and completed three measurements each on moisture content. They reported no reported difficulties with the procedures or the samples. Figure 1 and Table II show the results of the testing.

Precision Statement
From the results of the testing it is possible to make a precision statement for the determination of moisture in spray-dried powder using this method, following the practice of ASTM E691:

Repeatability standard deviation for moisture (within lab variability)	0.007 %
Reproducibility standard deviation for moisture (between lab variability)	0.018 %
95 % repeatability limit	0.020 %
95 % reproducibility limit	0.049 %

Measurement of binder content of a spray dried alumina powder
For determining the binder content, the study participants also agreed to use the same procedure that had been successfully used in IEA Subtask 10 (detailed in the previous quarterly report). This test assumes that the mass lost by a spray dried ceramic powder when it is heated to 500 °C is due to binder loss and that all the binder will be removed by holding the powder at 500 °C for 1 hour. Eleven laboratories participated in this study and completed three measurements each on binder content. They reported no difficulties with the procedures or the samples. Figure 2 and Table III show the results of the testing.

Precision Statement
From the results shown in Table III, it is possible to make a precision statement for the measurement of binder content using this procedure to measure binder content, following the method of ASTM E691:

Repeatability standard deviation for binder (within lab variability)	0.012 %
Reproducibility standard deviation for binder (between lab variability)	0.096 %
95 % repeatability limit	0.033 %
95 % reproducibility limit	0.268 %

Status of Milestones

1. Complete final report for the first year effort on Subtask 12 (December 30, 2000) – Expected completion date June 1, 2001.
2. Initiate a new project direction and develop collaboration with diesel engine companies in the U.S. and IEA countries (February 28, 2001) completed
3. Evaluate the feasibility of possible test methods for standardization (September 30, 2001) – on schedule

Communication/Visits/Travel

Luecke visited the NTN Technical Center (Ann Arbor, MI) on March 27th, 2001, to discuss test techniques for Rolling Contact Fatigue of silicon nitride with NTN engineers. NTN manufactures of the Rolling Contact Fatigue testing machine available at NIST.

Publications

None

References

None

Table I. Invited participants at the planned May 3 Workshop at NIST.

Participant	Company
Thomas Yonushonis	Cummins Engine Co.
Biljana Mikijelj	Ceradyne, Inc.
Ronald Chand	Chand Associates Inc.
Richard Allor	Ford Motor Co.
Nabil Hakim	Detroit Diesel Corporation
M. Lou Balmer-Millar	Caterpillar Inc. Technology Center
Hyung Yoon	Caterpillar Inc. Technical Center
Matt Ferber	Oak Ridge National Laboratory
D. Ray Johnson	Oak Ridge National Laboratory
Andrew McQueen	Kyocera Industrial Ceramics
Paul Wilbur	Colorado State U. Mechanical Eng.
Sidney Diamond	USDOE

Table II. Measured loss in mass fraction (%) from moisture.

Laboratory	Lab1	Lab2	Lab3	Lab4	Lab5	Lab6	Lab7	Lab8	Lab9	Lab10	Lab11
Test1	0.232	0.232	0.285	0.234	0.275	0.253	0.239	0.234	0.251	0.243	0.22
Test2	0.243	0.232	0.283	0.230	0.266	0.263	0.241	0.236	0.245	0.238	0.212
Test3	0.262	0.235	0.269	0.241	0.261	0.242	0.24	0.241	0.245	0.244	0.223
Mean	0.245	0.233	0.279	0.235	0.267	0.253	0.240	0.237	0.247	0.242	0.218

Table III. Measured loss in mass fraction (%) from binder.

Laboratory	Lab1	Lab2	Lab3	Lab4	Lab5	Lab6	Lab7	Lab8	Lab9	Lab10	Lab11
Test1	0.860	0.897	1.007	0.869	1.085	1.145	1.066	1.034	1.045	0.976	0.970
Test2	0.823	0.890	1.023	0.847	1.064	1.152	1.075	1.031	1.015	0.952	0.973
Test3	0.859	0.882	1.013	0.846	1.046	1.144	1.072	1.035	1.023	0.957	0.966
Mean	0.847	0.890	1.014	0.854	1.065	1.147	1.071	1.033	1.028	0.962	0.970

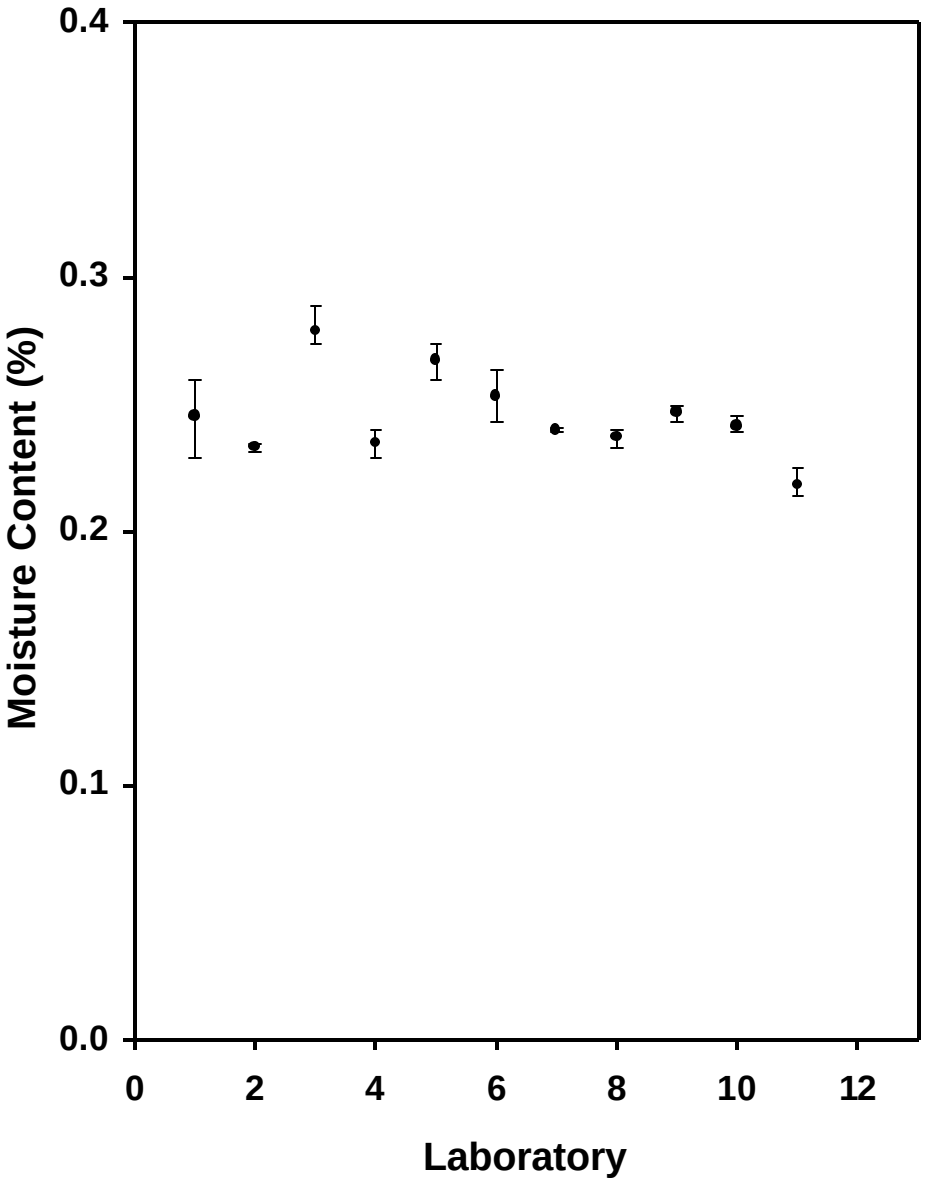

Figure 1. Results of moisture content measurements on alumina powder samples. The graph shows the maximum, minimum, and average values from each of the eleven laboratories.

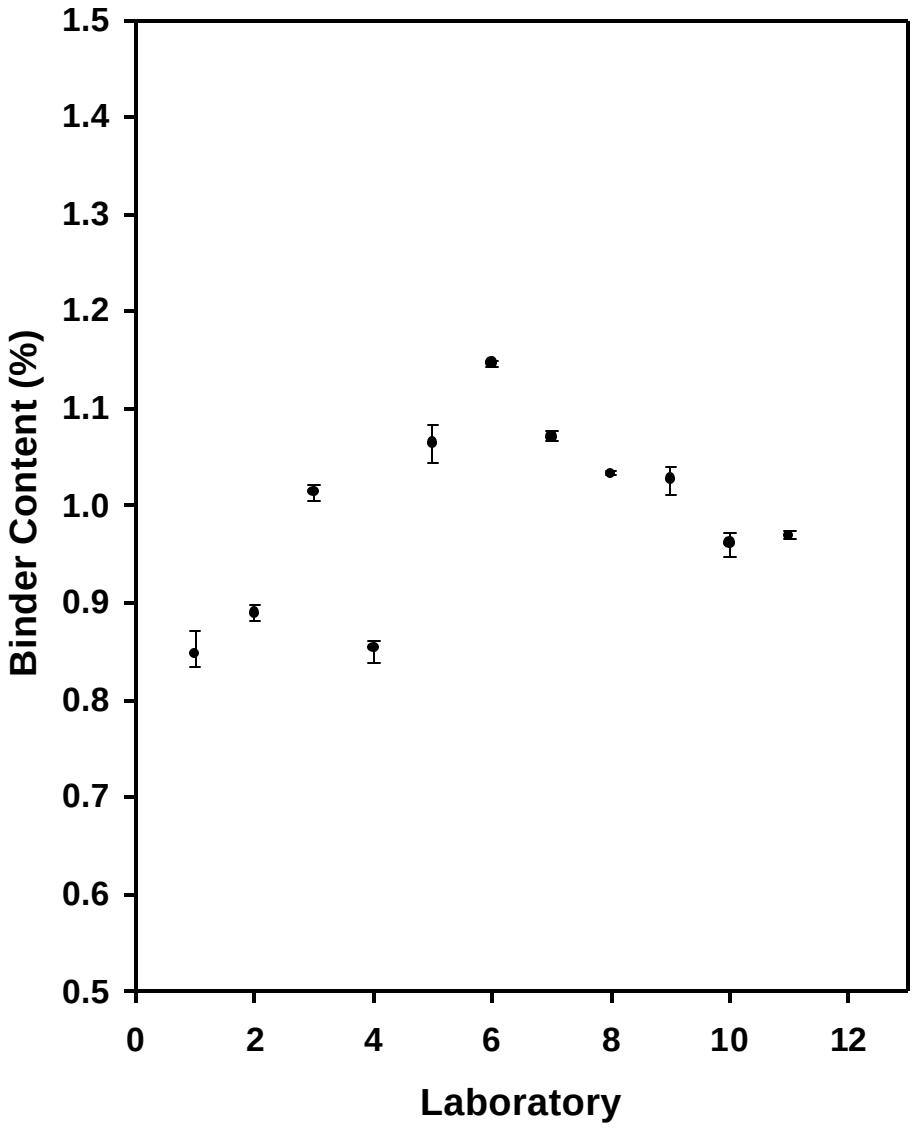

Figure 2. Results of binder content measurements on alumina powder samples. The graph shows the maximum, minimum, and average values from each of the eleven laboratories.

Mechanical Property Testing and Standards Development

George Quinn
National Institute of Standards and Technology

Objective/Scope

This task is to develop mechanical test method standards in support of the Propulsion Systems Materials Program. Test method development should meet the needs of the DOE engine community but should also consider the general USA structural ceramics community as well as foreign laboratories and companies. Draft recommendations for practices or procedures shall be developed based upon the needs identified above and circulated within the DOE engine community for review and modification. Round robins will be conducted as necessary. Procedures will be standardized by ASTM and/or ISO.

Technical Highlights

1. General

In this quarterly period, attention was focused on refinements to fracture toughness testing. Although this work seems to be dragging along, an end is in sight. The ASTM standard is being refined and corrected, and an ISO standard is being prepared for ballot. We also are tying this work into our extensive project on machining damage analysis. Experiments with the surface crack in flexure method on sintered silicon carbide confirmed that slightly (5%-10%) erroneous results could be obtained if vestigial lateral cracks remained in the specimen after polishing. This finding opened our eyes to a heretofore-unrealized source of error in the SCF method. A simple remedy for the problem was devised and results are now in agreement (within a few percent) with chevron notch and single-edged precrack beam data.

Other revisions to the fracture toughness standard C 1421 are in a formal ASTM ballot. The International Organization for Standards (ISO) draft fracture toughness SCF standard was extensively revised.

2. Fracture Toughness

a. ASTM standard C 1421 New SCF Experiments, Sintered Alpha Silicon Carbide

In the course of preparing ASTM C 1421, we compared fracture toughness outcomes from the surface crack in flexure (SCF), single-edged precracked beam (SEPB), and chevron notch in bending (CNB) to verify that consistent results could be obtained. Indeed, virtually identical results were obtained by these three methods for the hot-pressed silicon nitride NC 132 that comprised the reference material SRM 2100. Good correlations also were noted for alternative

materials, but we were puzzled by minor 5-10% discrepancies in the fracture toughness outcomes reported for Carborundum's sintered alpha silicon carbide (Hexoloy SA). A 10% difference may not sound like very much, but it disturbed us nonetheless. One should be concerned about a 10% error since one should be able to know whether a fracture toughness outcome of 2.7 MPa√m is genuinely different than an outcome of 3.0 MPa√m.

In this quarterly period, the discrepancy was traced to the presence of vestigial lateral cracks in the vicinity of the primary median crack. Figure 1 shows a schematic of the crack patterns that occur under a Knoop indentation. The goal of the SCF method is to produce a nice, primary, semi elliptical median type crack without interference of residual stresses or any other artifacts. Even after hand grinding or polishing off the requisite 4.5 to 5 times the indentation depth to remove the residual stresses, fragments of the lateral cracks may still be present and may shield the main crack during subsequent loading to fracture. This has not been appreciated up until now. One consequence of the shielding effect is that a greater load must be applied to the test piece to fracture it, than would otherwise be the case if the median crack were unshielded. Hence, the calculated fracture toughness by the SCF method overestimates the true fracture toughness. This could explain why the silicon carbide SCF results are often a little (5%-10%) greater than comparable SEPB or CNB outcomes.

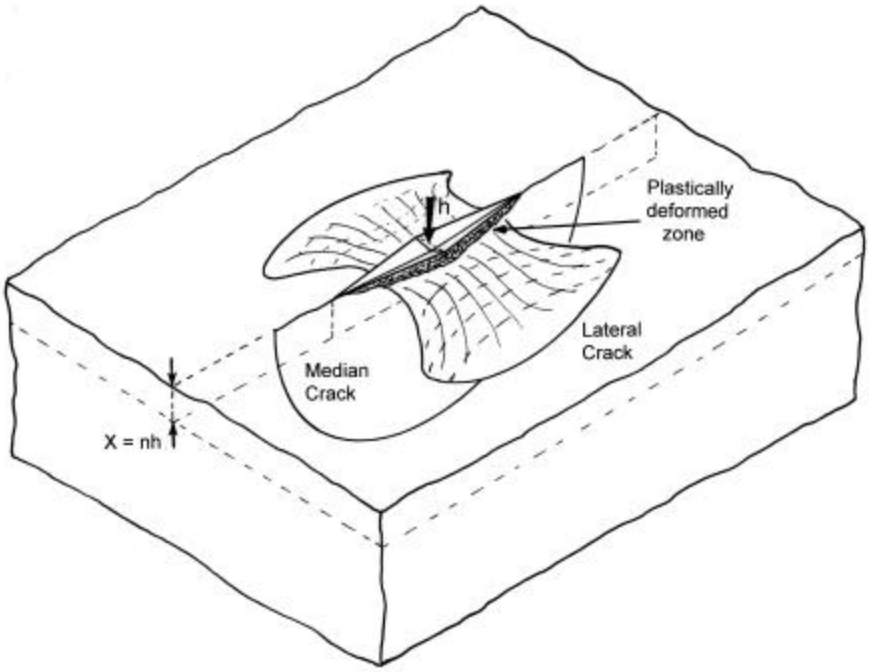

Figure 1 Knoop indentation creates a controlled median crack, but may also introduce lateral cracks that may not necessarily be removed during the customary grinding-polishing step.

We tested some NASA-Glenn chevron notch specimen fragments by the SCF method at NIST in order to obtain a direct comparison of fracture toughness. Specimens were Knoop precracked at NIST using a 49 N (5 kgf) load as prescribed in C1421. The indentation and residual stress damage zone were hand ground away in accordance with C 1421 with two important exceptions. During the hand polishing, the specimens were carefully monitored to detect whether lateral cracks were present. Some specimens also had much greater than the normal amounts removed by polishing. The results are shown in Figures 2 and 3 as a function of material removed normalized by the depth of the initial Knoop hardness impression. These figures show a little hump in the data, just at the point of material removal (X= 4.5 to 5.) that is prescribed in the ASTM standard. The hump is about 5-10% higher than the plateau value of fracture toughness for larger amounts removed.

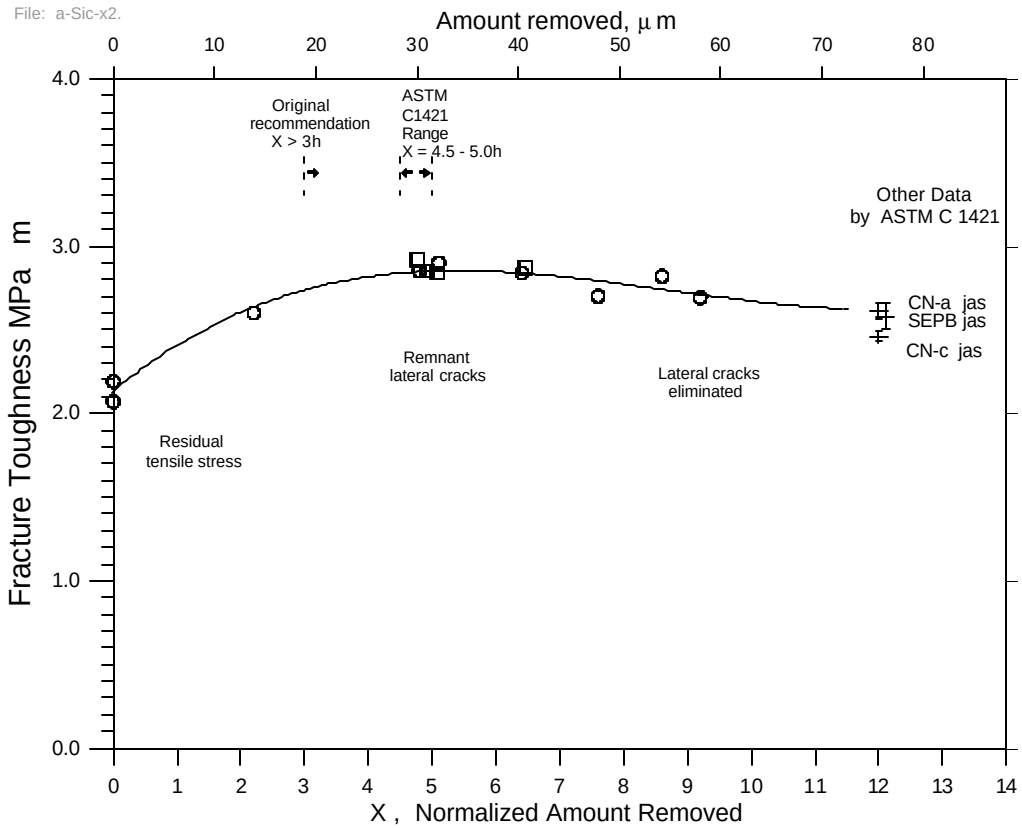

Figure 2 Fracture toughness data by the SCF method for sintered silicon carbide . The abscissa is the amount of material removed by hand grinding or polishing after an indentation and precrack are implanted. With no removal (X=0), residual stresses from the indentation plastic zone lower the apparent fracture toughness, and hence, it is necessary to polish the indentation zone away. The customary and standardized amount is 4.5 to 5.0. Unfortunately, lateral crack remnants partially shield the main crack and cause a slight overestimate of fracture toughness. Once sufficient material is removed, the SCF outcomes concur with chevron notch and single edged precracked beam data on the same batch of material (data on right hand side of graph.)

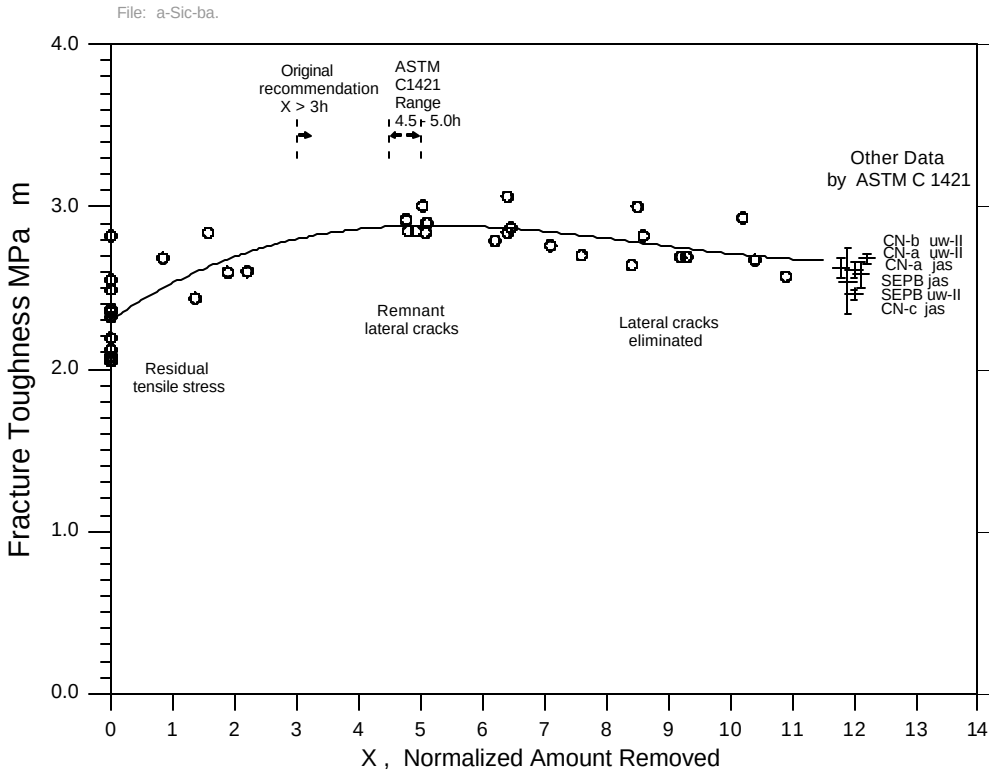

Figure 3 SCF silicon carbide data compared to other fracture toughness data for several data sets and batches of material.

The last traces of laterals were eliminated only after 7 to 10 times the indentation depth of material was removed.

Thus, we have detected a small glitch in the SCF test method. Consequently, we went back and reexamined <u>hundreds of previously tested</u> SCF specimens for evidence of vestigial laterals. These specimens from a very wide range of ceramic materials had been tested over the course of 15 years. The inspection procedure was very simple. The tensile surfaces of the fractured test pieces were examined for tell tale pullouts or chip outs in the vicinity of the Knoop precrack as shown in Figure 4. Hand polishing or grinding tends to create pullouts from the lateral cracks. Remnants of lateral cracks were only detected in a handful of materials that had a fracture toughness less than 3.0 MPa√m.

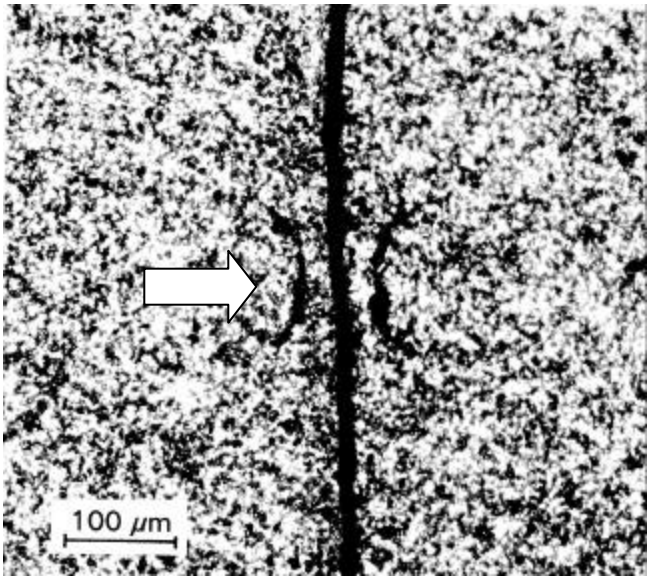

Figure 4 The tensile surface of a SCF silicon carbide test specimen after fracture, showing traces of lateral cracks. The lateral crack remnants protrude down into the interior and interfere with the stress field in the vicinity of the primary median crack that lies on the fractured plane. The tensile stress was applied horizontally in this figure.

These results were written up in a paper that was submitted to the Journal of the American Ceramic Society. Recommendations on how to detect and eliminate interfering lateral cracks were written into the new ISO draft standard based on this method, just in time for it's planned ballot in the summer of 2001. We also will propose that the SCF method be revised slightly in C 1421. The remedy for the problem is quite simple: after hand polishing 4.5 to 5.0 times the indentation depth away to remove the residual stresses, examine the tensile surface with a low power optical microscope at 20X to 100X. If vestigial laterals are present, then hand grind a little deeper prior to fracturing the specimen.

b. Green dye trick to highlight SCF precracks

While reexamining these hundreds of specimens, we also checked whether a new trick that we had contrived could help highlight the main median cracks. Detecting the precracks on the fracture surface has always been a problem with some materials. Ideally, one could find the precrack with an optical microscope, but often a scanning electron microscope must be used. Recently, we had tried the simple expedient of applying green ink from a common felt tip pen onto the fracture surfaces while looking through an optical microscope. While checking the hundreds of formerly tested specimens, we learned that the green dye trick was very effective in

highlighting the precrack, especially in white, gray, or translucent material. This is a simple trick that anyone can do and words to recommend this were immediately added to the list of revisions for the ASTM and ISO standards.

c. ASTM standard C 1421 and ISO standard, New SCF Experiments, Ceradyne 147-31N SRBSN

A new series of experiments were performed on Ceradyne's sintered reaction bonded silicon nitride (SRBSN), grade 147. We are eager to compare the tiny Knoop controlled cracks to the machining damage cracks from grinding damage. We have already (last quarterly report) conducted an extensive fractographic analysis of rods and bend bars ground by various treatments and then fractured in flexure. We intend to study the nature and character of the machining cracks a bit further. How deep are cracks formed by 320 grit grinding wheels compared to 600 grit wheels? How deep are the orthogonal or parallel machining cracks? How do the machining cracks behave in this material, with a microstructure composed of elongated beta silicon nitride crystals intended to enhance the fracture toughness and fracture resistance and R-curve behavior?

Our fracture toughness testing confirms the fracture toughness of this material is about 5.6 MPa√m. whether measured by chevron notch, single edged precracked beam, or surface cracks in flexure. This is surprising. We decided to explore this further by testing a larger number of surface crack specimens but varying the indentation loads and amounts of material removed. The results are shown in Figure 5. We will save a discussion of these results for the next quarterly report and a research paper. For the moment, we point out that precrack size could be controlled to small sizes via the SCF method and that there again seems to be a rather small effect of crack size upon fracture toughness. This suggests than any R-curve behavior in this material is slight.

d. Revisions to C 1421

The over 40 revisions to the ASTM fracture toughness standards are balloting in ASTM. Details on the proposed revisions are in the last quarterly progress report.

3. Flexure Testing of Cylindrical Ceramic Specimens

There was no work on cylindrical rod testing this period, other than to perform the fracture toughness experiments on the Ceradyne silicon nitride described above. The controlled flaw fracture toughness results were compared directly to the apparent fracture toughness outcomes and crack sizes observed in machined rods and bars. These results are being analyzed further as this is being written.

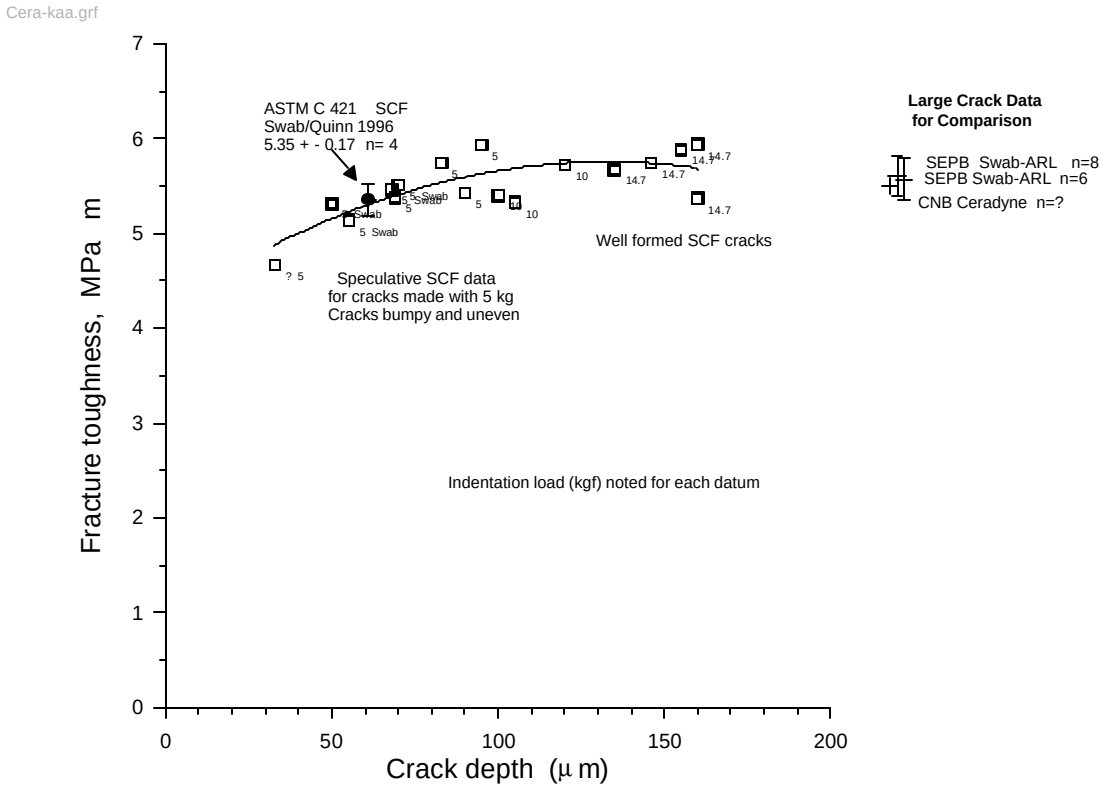

Figure 5 Fracture toughness by the SCF method compared to data generated by chevron notch (courtesy Ceradyne) and single-edged precracked beam (courtesy J. Swab, US ARL.) . An earlier set of SCF data produced by Swab and Quinn in 1997 is shown for comparison. There is little variation in fracture toughness with method or crack size.

4. Revision to ASTM Standard C 1161, Flexural Strength of Advanced Ceramics

The substantial amount of work that has been done at ORNL and NIST and elsewhere in the last few years on the topic of machining ceramics has been very timely. We have learned that there is a trend to finer grit wheels in preparation of both components and laboratory test pieces. Therefore we will begin to revise the basic or "standard" machining specification in the master bend bar standard, ASTM C 1161. A visit to Chand, Norton-Higgins, and Bomas in Massachusetts was made to get the latest information and perspectives of three of the leading shops in the United States on this matter. A proposal for a revision to C 1161 will be prepared in the last weeks of April 2001, and presented at the ASTM meeting in Indianapolis. More on this topic will be in the next quarterly report.

5. Other

a. Design of new Semi articulating flexure fixtures for rectangular specimens

No activity this period

b. ISO TC 206, Working Group 16, Fracture Toughness by SCF method

The draft standard was extensively rewritten in light of the new research results discussed above. In particular, warnings about possible influence of lateral cracks were added. Many editorial changes were made in response to inputs received from United Kingdom, Japan and Canada. Over 100 changes in all were made.

c. ISO TC 206, Working Group 2, Flexure Strength at Room Temperature

The document has been approved an ISO standard.

d. ISO TC 206, Working Group 8, Flexure Strength at Elevated Temperature

No activity this period.

e. Modify ASTM Standards C 1198 and C 1259 for Elastic Modulus by Resonance

Revisions to standard C 1198 and C 1259 were balloted in ASTM. The revisions to the two standards are an appendix that includes a simple correction factor for elastic modulus if the beam specimens have chamfered edges such as in a flexural strength bar.

Status of Milestones

Milestones will be revised after consultations with R. Johnson and S. Diamond. Diametral compression testing is on hold pending completion of other tasks.

Communications/Visits/Travel

Data was exchanged with Jon Salem at NASA-Glenn on evaluating the fracture toughness of sintered silicon carbide and refining ASTM C 1421.

G. Quinn contacted Ceradyne to review new findings on fracture toughness of Ceradyne's SRBSN grade 147-31N.

G. Quinn visited Chand Associates and the Norton Higgins Grinding Center as well as Bomas Machine Specialties in April in order to review the machining specifications in ASTM C 1161 and MIL STD 1942.

Publications

1. G. D. Quinn and J. A. Salem, "Effect of Lateral Cracks Upon Fracture Toughness Determined by the Surface Crack in Flexure Method," subm. to J. Am. Ceram. Soc. March, 2001.